POLITÉCNICA

ESCUELA TÉCNICA SUPERIOR DE INGENIEROS INDUSTRIALES
UNIVERSIDAD POLITÉCNICA DE MADRID

José Gutiérrez Abascal, 2. 28006 Madrid
Tel.: 91 336 3060
info.industriales@upm.es

www.industriales.upm.es

Beatriz Láinez Muñiz

05 TRABAJO FIN DE MASTER

INDUSTRIALES

TRABAJO FIN DE MASTER

ESTRATEGIAS DE GESTION TÉRMICA DEL AIRE INTERNO PARA CONVERTIDORES FERROVIARIOS DE ALTO RENDIMIENTO

TRABAJO FIN DE MASTER
PARA LA OBTENCIÓN DEL
TÍTULO DE **MASTER EN INGENIERÍA INDUSTRIAL**

MAYO **2024**

Beatriz Láinez Muñiz

DIRECTOR DEL TRABAJO FIN DE MASTER:
Oficina de Relaciones Internacionales
Stefan Östlund (KTH)

INDUSTRIALES
ETSII | UPM

POLITÉCNICA

KTH ROYAL INSTITUTE
OF TECHNOLOGY

Degree Project in the Field of Technology Electric Power Engineering (KTH, Sweden) and the Main Field of Study Industrial Engineering (UPM, Spain)

Second cycle, 30 credits

Internal air thermal management strategies for high performance railway converters

BEATRIZ LAINEZ MUÑIZ

Stockholm, Sweden, 2024

Internal air thermal management strategies for high performance railway converters

BEATRIZ LAINEZ MUÑIZ

Date: May 15, 2024

Supervisor: Xiongfei Wang
Examiner: Stefan Östlund
School of Electrical Engineering and Computer Science
Host company: Alstom
Swedish title: Strategier för intern luftvärmehantering för järnvägsomvandlare med hög prestanda

Abstract

In the current climate crisis situation, the development and wide operating range of electric mobility is of great importance, with electric rail traction being the main form of electric transport over medium-long distances. In this sense, electric traction converters are undergoing a deep modification, moving towards more powerful, more compact converters with a wider operating range.

This project addresses the problem of overheating of the internal air of a railway electric traction converter when it operates in extreme environments with high temperatures, around 50ºC or 60ºC. In these cases, the existing cooling system, which uses external air at ambient temperature as the coolant fluid, is not enough to ensure safe operation of the converter.

This limits the operating range of electric trains with high power density converters, which cannot operate in hot climates. Furthermore, it poses a risk for other operating ranges in the near future, where the development of converters with higher current levels and thus higher power losses will again challenge conventional cooling systems.

This project uses the MITRAC/TC1500™ traction converter developed by Alstom as a basis for proposing different additional cooling systems that complement the conventional one, with the use of different cooling technologies, including forced air convection, heat pipes, liquid-cooled cold plates and Peltier cells, also called thermoelectric coolers.

The implementation of the different technologies is evaluated based on mathematical models developed in MATLAB® and computational fluid dynamics simulations in StarCCM+®.

The results obtained allow to conclude that the use of heat pipes and Peltier cells is the most recommendable for the development of thermal management systems for electric traction converters, provided that they are implemented with a good external heat dissipation medium, preferably ambient temperature air flows already that already exist in the converter. Furthermore, it is shown that the same cooling technology can provide very different results depending on its implementation.

Keywords

Cold Plate, Electric Cooling, Electric Traction Converter, Forced Air Convection, Heat Pipes, Internal Air, Peltier Cells, Railway, Thermoelectric Cooler.

Sammanfattning

I den rådande klimatkrisen är det mycket viktigt att utveckla elektrisk mobilitet och att ha ett brett användningsområde, där elektrisk järnvägsdrift är den viktigaste formen av elektrisk transport över medellånga avstånd. Omvandlarna för elektrisk traktion genomgår därför en genomgripande förändring, mot kraftfullare och mer kompakta omvandlare med ett bredare driftsområde.

Detta projekt behandlar problemet med överhettning av den inre luften i en elektrisk traktionsomvandlare för tåg när den används i extrema miljöer med höga temperaturer, runt 50°C eller 60°C. I dessa fall är det befintliga kylsystemet, som använder extern luft vid omgivningstemperatur som kylmedel, inte tillräckligt för att garantera en säker drift av omvandlaren.

Detta begränsar användningsområdet för elektriska tåg med omvandlare med hög effektdensitet, som inte kan användas i varma klimat. Dessutom utgör det en risk för andra driftområden inom den närmaste framtiden, där utvecklingen av omvandlare med högre strömnivåer och därmed högre effektförluster återigen kommer att utmana konventionella kylsystem.

I projektet används MITRAC/TC1500™, en traktionsomvandlare som utvecklats av Alstom, som grund för att föreslå olika ytterligare kylsystem som kompletterar det konventionella, med användning av olika kyltekniker, inklusive luftkonvektion, värmerör, vätskekylda kylplattor och Peltierceller, även kallade termoelektriska kylare.

Implementeringen av de olika teknikerna utvärderas baserat på matematiska modeller som utvecklats i MATLAB® och beräkningsflödesdynamiska simuleringar i StarCCM+®.

De erhållna resultaten gör det möjligt att dra slutsatsen att användningen av värmerör och Peltier-celler är det mest rekommenderade för utvecklingen av termiska styrsystem för elektriska traktionsomvandlare, förutsatt att de implementeras med ett bra externt värmeavledningsmedium, helst luftflöden vid omgivningstemperatur som redan finns i omvandlaren. Dessutom visas att samma kylteknik kan ge mycket olika resultat beroende på hur den implementeras.

Resumen

En la situación de crisis climática acutal, el desarrollo y la amplitud de rango de operaión de la movilidad eléctrica adquiere gran importancia, siendo la tracción eléctrica ferroviaria la principal forma de transporte eléctrico en las medias-largas distancias. En este sentido, los convertidores de tracción eléctrica están surfiendo una profunda modificación, yendo hacia convertidores más potentes, más compactos y con mayor rango de operación.

Este proyecto aborda el problema de sobrecalentamiento del aire interno de un convertidor de tracción eléctrica ferroviario cuando éste opera en ambientes extremos con altas temperaturas, en torno a 50ºC o 60ºC. En estos casos, el sistema de refrigeración existente, que utiliza aire externo a temperatura ambiente como fluido refrigerante, no es suficiente para garantizar una operación segura del mismo.

Esto limita el rango de operación de los trenes eléctricos con convertidores de alta densidad de potencia, que no pueden operar en climas cálidos. Además, supone un riesgo para otros rangos de operación en un futuro próximo, donde el desarrollo de convertidores con mayores niveles de corriente y, por tanto, mayores pérdidas de potencia, rete de nuevo a los sistemas de refrigeración convencionales.

En este proyecto se utiliza el convertidor de tracción MITRAC/TC1500™ desarrollado por Alstom como base para proponer diferentes sistemas de refrigeración adicionales que complementan al convencional y emplean distintas tecnologías de refrigeración, entre las que se incluyen convección forzada de aire, tubos de calor, placas frías de refrigeración líquida y células de Peltier, también denominadas refrigeradores termoeléctrictos.

La implementacion de las diferentes tecnologías se evalúa en base a modelos matemáticos desarrollados en el *software* MATLAB® y a simulaciones de dinámica de fluidos computacional en StarCCM+®.

Los resultados obtenidos permiten concluir que el uso de los tubos de calor y las células de Peltier es el más recomendable para el desarrollo de los sistemas de gestión térmica de los convertidores de tracción eléctrica, siempre que se implementen con un buen medio de disipación de calor externo, preferiblemente flujos de aire a temperatura ambiente ya existentes en el convertidor. Además, se demuestra que una misma tecnología de refrigeración puede aportar resultados muy diferentes dependiendo de su implementación.

Acknowledgments

To the managers of Alstom Sweden, for giving me the opportunity to carry out this project. To the supervisors and colleagues of Alstom Sweden who have worked with me, for their attention and dedication during all this time.

To the team of professors in the Department of Electric Mobility at the Royal Institute of Technology of Stockholm, for awakening my interest in research in this area and providing me with access to the documentation and support necessary for the development of the project.

To my supervisor and examiner, professors at the Royal Institute of Technology of Stockholm, for their quick response to any doubts or questions and for their dedication in reviewing and correcting the project.

To the International Relations Office of the School of Industrial Engineering of the Polytechnic University of Madrid, for giving me all the facilities for the development of the project.

To my friends, colleagues and family for their advice, patience and support.

And, in short, to all the people who have surrounded me during my Master's years, who in one way or another have contributed to the development of this project.

Stockholm, May 2024
Beatriz Lainez Muñiz

Contents

List of Figures

List of Tables

List of acronyms and abbreviations

AC	Alternating Current
CFD	Computational Fluid Dynamic
DC	Direct Current
EOS	MITRAC^{TM} EOS - Control platform product name
GDU	Gate Drive Unit
HVAC	High Voltage Alternating Current
IGBT	Insulated Gate Bipolar Transistor
MITRAC	MITRAC Propulsion System - Product name
NASA	National Aeronautics and Space Administration of United States
RC	Resistor Capacitor
Ref.	Reference
s.t.	subject to

Chapter 1

Introduction

This thesis addresses the problem of thermal management for high-performance railway converters, particularly the indirectly cooled components from internal air circulation. The increased performance density in railway traction results in highly compact converter designs that use the last generation of power semiconductors with high converter currents. These factors, coupled with a trend towards increasing ambient temperatures in various applications, point to the need for new cooling system designs to ensure the reliable operation of the converters.

1.1 Electric Railway Traction

The critic climatic situation of recent years, together with the possibility of obtaining electric energy from renewable sources, leads to the electrification of the economy and, consequently, to the electrification of the transport.

Railway is the most powerful sector concerning electric mobility, and its development and importance is expected to continue growing in the coming years. Compared with diesel fueled locomotives, electric trains have better energy efficiency, lower emissions and lower operating cost. Moreover, most electric trains use regenerative braking, getting the train's kinetic energy back during braking periods and converting it into electricity to power other trains connected to the same overhead line. In general, electric trains are also more responsive and reliable than diesel locomotives.

This section uses one of the Alstom's electric train system desgins to explain the basis of railway electric traction. In the chosen system, 50% of the axles in each train car are driving axles. The whole system overview can

be seen in Figure 1.1.

Several steps are required in order to convert the electric power drawn from the high voltage alternating current (HVAC) overhead line into the mechanical energy in the driving axles. First, the AC voltage from the line is stepped down to a suitable voltage level for the propulsion system. Thereafter, this AC voltage is converted into controllable DC link voltage, which is then transformed into the three-phase voltage with controllable magnitude and frequency that is fed into the electric motors. Finally, electric motors convert electric power into mechanical power which is transferred to the axles.

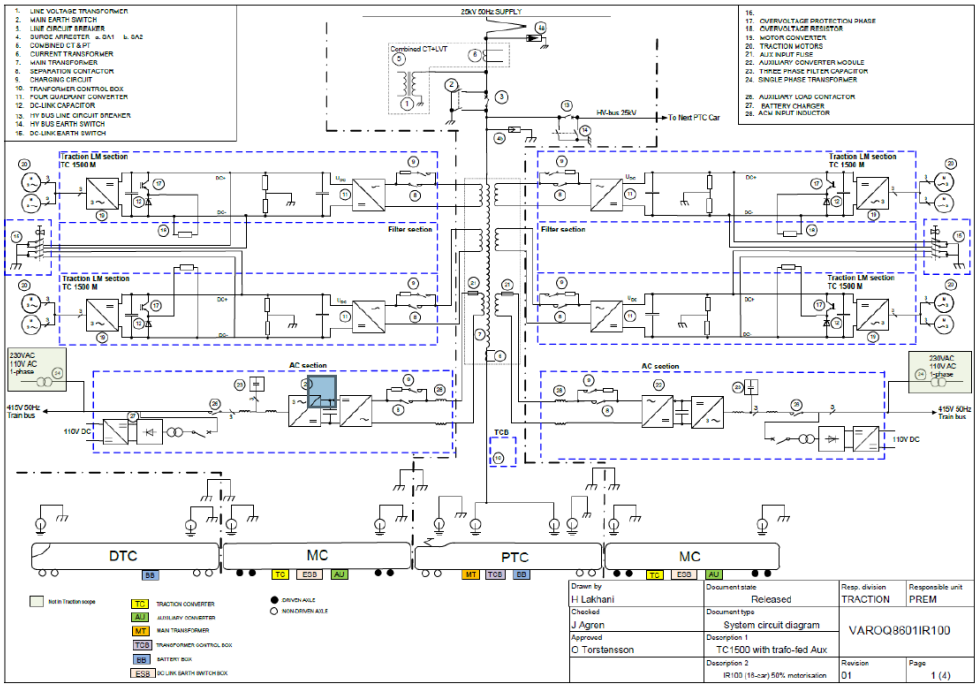

Figure 1.1: Main circuit overview of one Four Car Unit for 50% motorization. **Source:** [1].

The complete system complies with a high voltage system, a propulsion system, and an auxiliary system.

The high voltage system is roof mounted. It connects the overhead line (25 kV AC, 50 Hz) with the train through the pantograph and powers the main transformer, where the voltage level is reduced from high voltage to medium voltage. The line voltage is then distributed to both the propulsion and auxiliary systems which are connected to the secondary side of the main transformer. Propulsion control and protection are also part of the high voltage system.

The propulsion system is based on the MITRAC™ propulsion traction converter. The objective of the propulsion system is to convert the AC voltage coming from the secondary side of the main transformer into controlled voltage to power the traction motors for driving or braking the train via the mechanical drive system.

This process complies with two steps. First, the AC medium voltage is converted into a controlled DC voltage link in the so-called line converter; then the DC voltage is transformed into three-phase voltage with variable amplitude and frequency in the motor converter.

The propulsion system feeds the mechanical drive system which is composed of three-phase squirrel cage asynchronous, four poles, open and self-ventilated machines, and two-stages, half-suspended gearboxes that transmit the power from the motors to the axles, adapting torque and speed as required.

Apart from traction converter unit, a DC link earth switch box and propulsion control are part of the propulsion system.

Finally, the auxiliary system powers auxiliary loads and batteries chargers. It is mainly composed of the auxiliary converter and the battery charger. The three-phase voltage is supplied to a synchronized AC bus by the converter, whereas the DC voltage is achieved by means of an integrated battery charger of 110 VDC connected to the three-phase auxiliary bus.

The converter is connected to the secondary side of the main transformer and converts the feeding voltage into three-phase AC voltage which is supplied to a synchronized AC bus. It also includes measurement and control devices to ensure proper and safe operation of the auxiliary systems.

The chargers are connected to the three-phase auxiliary bus. The AC voltage is rectified and the output voltage is regulated according to the battery requirements. A filter is added to ensure smooth DC battery voltage. In case of necessity, the charger can also be supplied via the external 415 VAC.

1.2 Problem Formulation

The thesis addresses the thermal management of a high-density railway converter, in particular the front section of the MITRAC/TC1500™ converter developed by Alstom. The structure of the converter is shown in Figure 1.2.

The converter complies with three different sections: Two converter sections or front sections and one middle section. The two front sections are sealed with IP65 enclosures and, therefore, air exchange with the environment is not possible. In contrast, the middle section has ventilation fans that use

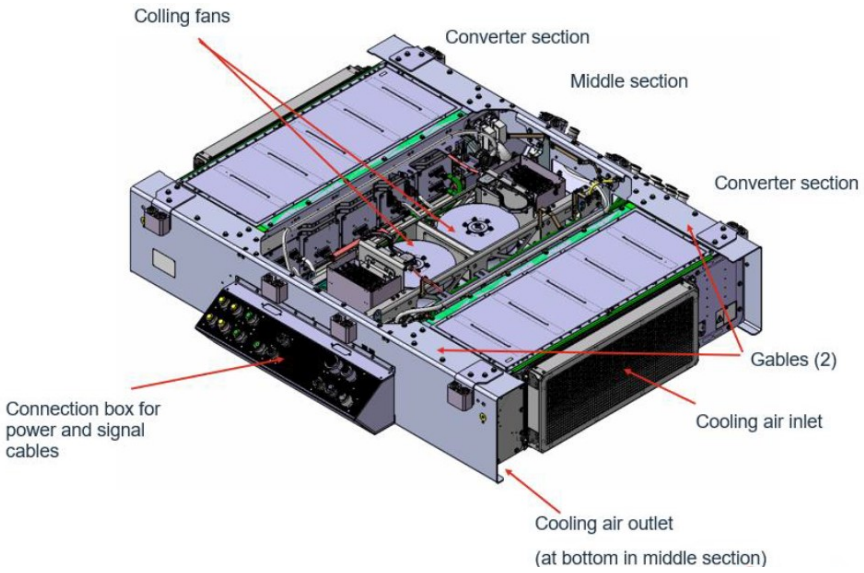

Figure 1.2: Model of traction converter MITRAC/TC1500^{TM}. **Source:** [2].

external air. This external air is also used as the coolant fluid for the front section by using heat exchangers.

The temperature inside the front sections is limited to 70^{o}C as most components cannot withstand higher temperatures. The inner temperature is likely to be increased due to the development of a new generation of power semiconductors which carry higher currents. This imply that the current flowing through the busbars and other electrical equipment is also higher and thus dissipate more heat power as losses, which need to be dissipated by a smaller volume of air as converters tends to be more compact. Moreover, the atmosphere temperature can be quite high in some working conditions, for instance up to more than 50^{o}C for train operation in India. Atmosphere temperature is also expected to increase due to climate change.

Furthermore, as the converter is situated in the under-frame of the train, some other heat power coming from the train's mechanical system, such as brakes, contributes to an increase in the temperature of the incoming air flow.

Similar problem occurs with metro trains inside the tunnels. The air volume around the train inside the tunnels is not enough to dissipate the heat coming from the braking system and, thus, the air temperature around the converter is high with disregard of the external temperature.

All of this means that the temperature of the incoming air is increased while more heat power needs to be dissipated in the front sections. That challenges the current cooling system design and states the need for new heat

dissipating strategies that can ensure converter's reliability.

1.3 Purpose

The purpose of this thesis is to support the development of electric traction aiming for more compact and high-density power traction converters and to surpass one of the technical barriers when it comes to electrification of the transportation sector: The thermal management of electric converters.

If achieved, this would not only make electric traction feasible for more applications, allowing higher penetration of electric motors in the transportation sector when it comes to long and medium distances, but also would allow to increase the power density and efficiency of traction converters leading to higher quality services and reduced cost operations in the railway industry.

The main beneficiaries of the successful outcome of this project are directly related to rail transport services in hot climate areas, such as India or the Middle East. On the one hand, users would enjoy a more reliable service in the case of already electrified lines as well as the possibility of using electric transport with all the advantages associated with it on lines that until now have not been possible to electrify due to problems related to heat dissipation in the electrical components. On the other hand, train manufacturers would see their market niche broadened, being able to offer products with a wider operating temperature range and greater durability. Finally, rail system operators in these locations would benefit from lower operating costs due to more compact and efficient systems.

Other indirect beneficiaries relate to other sectors of industry that face similar problems with regard to the thermal management of electric drive equipment, an example of which is the automotive industry.

From environmental, ethical and social points of view, further development of electric traction converters would especially benefit the population in hot climate areas where diesel transport could be replaced by electric transport with comparable reliability. This would reduce local emissions, directly related to health problems, air quality and resource depletion. In addition, in the case of using electricity from zero or low-emission sources to feed the locomotives would contribute to the fight against the greenhouse effect and global warming.

1.4 Goals

The goals of this project are to analyze potential improvements of the cooling system for air-cooled railway traction converters based on a variety of selected technologies, and to state which of these technologies or combination of them is best suited to the needs of the MITRAC/TC1500^{TM} traction converter, ensuring that the inner temperature is below 70^{o}C in all operating conditions.

1.5 Research Methodology

To achieve the goals stated in Section 1.4, the main research method that is used is simulation. Two different types of simulations are carried out for this thesis. On the one hand, mathematical models based on analytical expressions are developed in the software MATLAB®. On the other hand, CFD simulations are run for mechanical-thermal models using the software StarCCM+®. Experiments are disregarded as a possible method to be used owing to the lack of resources and the limited timeframe for the development of the project.

With regards to data collection, it is based on internal documentation facilitated by Alstom, and results of simulations and lab experiments previously carried out.

The evaluation of different technologies is based on both quantitative features obtained from the models and simulation results, and qualitative features grounded in the knowledge acquired during the research stage. The quantitative features that are taken into account are *(i)* Heat Power, *(ii)* Volume, *(iii)* Weight, *(iv)* Coefficient of Performance, and *(v)* Heat Power Density, whereas the qualitative ones are *(vi)* Reliability of Design, *(vii)* Feasibility, *(viii)* Robustness, *(ix)* Cost, and *(x)* Maintenance. To analyse the results and compare the different proposed designs, the weighted average method is used based on these features. For future comparisons with other projects, the thermal resistance of the implementation of each technology is calculated.

Finally, the validation of the results is mainly based on the comparison between the outputs of the two types of simulations used and in discussions with experts from Alstom Sweden to adjust the input parameters and check reliability of simulations and results.

1.6 Delimitations

Although the MITRAC/TC1500™ traction converter is used to exemplify the work done, the aim of this thesis is not to design a definitive cooling system applied exclusively to this specific converter, but to carry out a broader analysis of possible improvements and advances in the internal air cooling systems of traction converters that can be used as inputs to improve cooling performance in different models according to the specific requirements of each project. Therefore, the definition of a final and well-specified model design and all the tests and verifications necessary for its implementation in commercial trains are outside the scope of the project.

When it comes to research, two main limitations can be identified. On the one hand, the available time to conduct each task is reduced so papers and documentation to be read are selected based on their relevance to the project. Thus, some interesting reports not directly related to the topic itself, but that, if considered, could give an extra approach to the study might be left out of the reading material. On the other hand, the possibility of getting in contact with people working in similar areas in other industries is limited mainly due to accessibility.

Few limitations are found regarding the availability of information and data used to conduct the thermal and mechanical studies of the front section for the MITRAC/TC1500™ converter. Assumptions are only made with regards to how much power from the IGBTs' and discharge resistors' heat losses go directly to the heat sink and how much is transferred to the internal air. The actual value changes with the operating temperature, however it is considered constant for this project.

Most of the limitations of the project are related to the mathematical models and CFD simulations developed for the different refrigeration technologies. First, simplified models both for the technologies themselves and for the front section are used since complete simulations are too heavy to be run on ordinary computers. These simplifications include the following:

1. Electrical components inside the front section are modeled as black boxes and configured as heat sources.

2. Generic fan curves are used to model fan as boundary conditions.

3. Convection coefficients are calculated using analytical expressions, this might introduce some deviations from the results obtained in a lab, for instance.

4. Heat pipes are modeled as solid materials with very high thermal conductivity, based on the calculation provided in Appendix D.

5. The effect of gravity is only considered for natural convection simulations and disregarded for forced convection cases.

6. Peltier cells are modeled as two plates kept at constant temperature with an adiabatic medium in between, based on the information provided in Appendix E.

Moreover, some assumptions are taken when setting simulations parameters:

1. Steady state is assumed.

2. External air is assumed to have a constant temperature of 60°C.

3. The temperature in compartment six is assumed to be 70°C, considered as the worst case scenario.

4. Air velocity in the under-frame of the train is assumed to be 20% of the train speed.

Finally, in the analysis and evaluation stage, it is important to note that no lab experiments are carried out. This would influence the validation of the results, improving their reliability. Also, many of the features used to compare different technologies are based on a qualitative analysis. On the contrary, if a quantitative or mixed analysis were to be carried out for some of these features, the conclusions drawn from the results could be affected. A good example to this is, for example, if an exhaustive cost analysis would be carried out.

1.7 Structure of the thesis

Chapter 2 presents a brief description of the MITRAC/TC1500™ developed by Alstom, including its cooling system, and describes and discusses the state-of-the-art of a variety of cooling technologies used in different sectors of industry that could be applied to internal cooling of traction converters. Chapter 3 provides the methodology used through out this project, and Chapter 4 develops mathematical models and Computational Fluid Dynamics (CFD) simulations to evaluate the performance of some of these technologies applied to the MITRAC/TC1500™, and exposes the obtained results. This chapter is completed with a critical analysis and discussion of the results. Finally,

Chapter 5 summarises the main conclusions, where recommendations or steps to be followed to improve the thermal cooling of the internal air of the front section of the MITRAC/TC1500^{TM} are presented, together with possible trends for future work.

Chapter 2

Background

In order to address the problem of internal cooling of the converter section of an electric traction converter, it is necessary not only to be familiar with the mechanical and thermal characteristics of the converter to be studied, but also to know the different cooling technologies existing in the industrial market, both conventional and non-conventional, as well as their main advantages, disadvantages and areas of application.

2.1 MITRAC/TC1500^{TM} Traction Converter

The MITRAC/TC1500^{TM} is one of the MITRAC Power^{TM} traction converters developed by Alstom. This technology is characterized by its flexibility and scalability thanks to its modular structure, and is implemented in commercial trains in Europe and Asia.

The MITRAC/TC1500^{TM} traction converter unit consists of three distinct parts: Two front sections or converter sections, where the main components are located, and one middle section in between, as can be seen in Figure 1.2. In some cases an auxiliary section can also be added, but in this document the general case with only three sections is used. The traction converter unit is located in the under-frame of the motorized cars of the train.

As already mentioned, this is a scalable technology, so the traction converters can be of different sizes, called S (small), M (medium) or L (large), depending on the number of modules in the front section. In addition, there are different configurations inside the converter depending on how many motors need to be driven and whether each has an individual converter or not. Therefore the number of required IGBTs and other components changes from model to model.

In this document, a M size converter with the so-called "LMM" configuration is considered. The schematic of the front section for this configuration is shown in Figure 2.1. In this way, each front section has one line converter and one motor converter which feeds two motors. Therefore, each traction converter unit drives four motors in total.

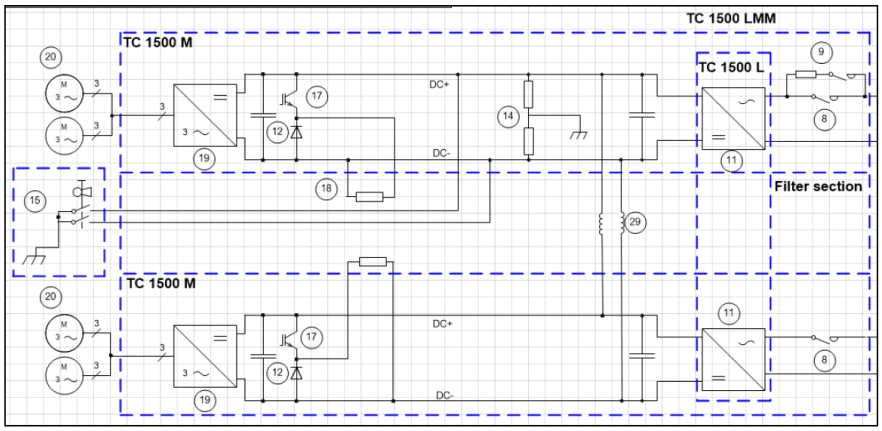

Figure 2.1: Electrical scheme for LMM configuration in TC1500. **Source:** [2].

The main functions of the front section, and the traction converter itself, are the following:

- Line converter: Medium voltage AC is converted into traction DC link. It is a four quadrant type and the line voltage power factor is kept close to one both for traction and braking.
- Motor converter: Traction DC link is converted into three-phase variable voltage to power the traction motors. When braking traction motors act as generators, mechanical energy is converted into electrical energy that is fed back to the network to power other trains.
- Overvoltage protection.
- Charging circuit: Manage the connection between the secondary side of the main transformer and the line converter to charge the DC link.
- Earth fault detection.
- Cooling: Cooling system is described in detail in Section 2.1.1.

Power electronic equipments such as IGBTs, gate drive units, busbars and DC-link capacitors are packed together and located inside the front or converter section. In the considered configuration, there are in total sixteen IGBT modules, each of which consists of two transistors, so that in total a front section has thirty-two IGBTs. Six of the modules correspond to the motor converter, eight to the line converter and two to the overvoltage protection.

When it comes to the physical distribution of the equipment, for the M size converter, the front section is composed of six different modules, denominated compartment zero, one, two, three, four, and six. Compartment zero includes the control system and the cooling fan. Compartments one to four contain the power electronics and active components for the line and motor converters and the overvoltage protection. Finally, compartment six houses other required equipment such as contactors.

In order to avoid dust pollution, the front section is sealed with IP65 enclosure.

Table 2.1: Technical data of the traction converter. **Source:** [2].

Description	**Technical Data**
System Data	
Ambient Temperature	-10°C to +50°C
Input AC voltage	870 V
Passive discharge time $<$ 50 V	10 min
IP Class front section	IP65
IP Class middle section	IP20
Line Converter	
Input Current, cont.	2 x 450 Arms
Input Current, max	2 x 1100 Arms
Motor Converter	
Nominal DC link voltage	1500 - 1800 V
Maximum DC link voltage, shut down	2100 V
Output Phase Current, cont.	2 x 280 Arms
Output Phase Current, max	2 x 585 Arms
Preliminary weights (Without bathtub)	915 +/- 1% kg
Preliminary dimensions (Without bathtub)	2440 x 2314 x 554 mm

Regarding power supplies, there are three different available power supplies in the converter that are used to power different components:

- 750 VDC or 1500 VDC which is the supply for the traction system.
- Three-phase 400 VAC, *i.e.,* 230 VAC (50 / 60 Hz) used to power the fans.

- 110 VDC used to power the control equipment.

Moreover, air pressure from the pneumatic system (*e.g.,* braking system) could also be used as a power supply. This would be an option for short time though. In the long time perspective, the pneumatic brake system will be phased out to other solutions.

Finally, general technical data of the traction converter can be seen in Table 2.1.

2.1.1 Cooling System

Currently, the thermal management in the converter is done as shown in the schematic of Figure 2.2. There are three air circuits in the converter. Two closed air circuits inside each of the front sections (red arrows in Figure 2.2) and one open circuit in which the air is drawn from the environment (blue arrows in Figure 2.2).

The external air is drawn through heat exchangers that are used to cool down the closed air flows in the front sections. Then, the air flow goes below the IGBTs through the main heat sink and, lastly, it arrives to the middle section to cool down the components located there. Finally, it is ejected back into the environment. In all of the air circuits, fans are used to create the air flows.

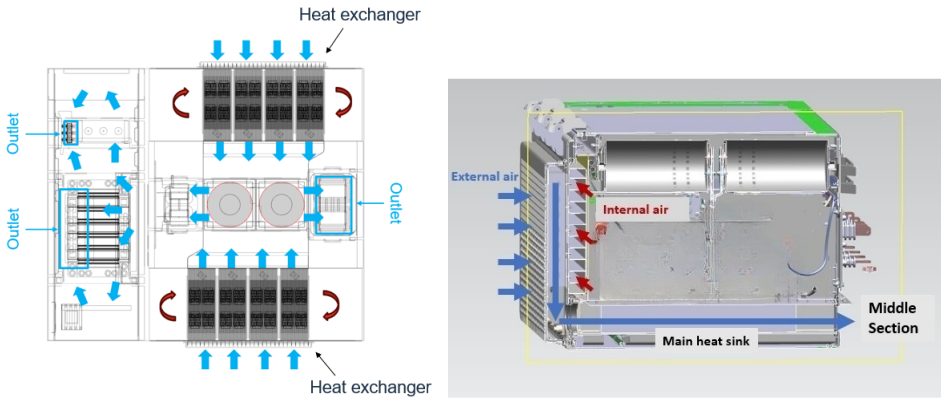

(a) Upper view (b) Side view

Figure 2.2: Schematics of the cooling system in MITRAC/TC1500™. **Source:** Adapted from Alstom's internal documentation.

Cooling inside the front section is done by means of an internal fan located in compartment zero and the heat absorbed by the internal air is

dissipated through the enclosure walls and by the external air going through the front cover, which is designed as heat exchanger. Therefore, the internal air flows from compartment zero to compartment six absorbing heat and returns through the front cover heat exchanger transferring the heat to the external air flow.

It is worth mentioning that apart from the heat exchanger in the front cover, part of the heat from the internal air is dissipated by free convection through the outer casing of the converter.

2.1.2 Heat Losses in the Front Section

Under normal operating conditions, the various components inside the front section dissipate heat to the internal air flow which needs to be removed to keep the internal temperature below 70°C and ensure reliable operation of the traction converter.

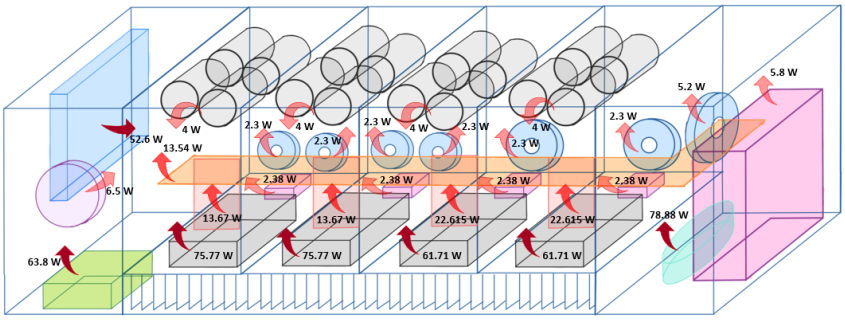

Figure 2.3: Heat dissipation distribution inside the front section.

Figure 2.3 shows a "box model" of the front section, where all major components are represented as boxes. The red arrows represent the heat dissipation of the individual components. The darker they are, the higher the heat value.

Heat values represented in Figure 2.3 are summarized in Table 2.2. The total heat transferred to the internal air flow by all the components amounts to 613.1 W. It is assumed that 3% of the heat dissipated by the IGBTs and 5% of the heat losses from the discharge resistors is transferred to the internal air flow. The rest is considered to be dissipated directly in the main heat sink localted below them.

Table 2.2: Heat losses inside the front section.

Component	Heat dissipation (W)	Heat dissipation (%)	Number of "boxes"	Heat dissipation per "box" (W)
EOS	52.6	8,58	1	52.6
Fan	6.5	1,06	1	6.5
Power Supply	63.8	10,41	1	63.8
IGBTs + GDUs	274.96	44,85	4	75. 77 (x2) & 61.71 (x2)
Busbars	72.57	11,82	4	13.67 (x2) & 22.615 (x2)
Discharge resistors	9.52	1,55	4	2.38
DC Feeder	13.54	2.21	1	13.54
Current sensors	19	3.10	7	2.3 (x6) & 5.2 (x1)
Capacitors	16	2.60	4	4
DC Voltage sensor + contactor	78.88	12,87	1	78.88
RC Circuit	5.8	0.95	1	5.8
TOTAL	**613.1**	**100**	-	-

2.1.3 Mechanical and Physical Constraints and Possibilities in the Front Section

The front section is composed of a large number of components and equipment with different functionalities and characteristics and the positioning of each of them is carefully thought to obtain the best operating conditions, trying to maximise the performance, efficiency, reliability and robustness of the converter. Therefore, whenever any modification is made it is important to minimize the relocation of any component.

Also, it is crucial to try to add as minimum weight as possible in the front cover, where the heat exchanger is located, as this wall is used as door for maintenance and needs to be taken out easily. Another relevant constraint for the front cover is the pressure drop in the external air flow. The pressure drop has to be limited to ensure high speed of the air while going through the main heat sink. Moreover, the speed of the incoming air is also a limited to avoid filter clogging.

Finally, another important constraint is to keep the front section sealed to avoid component failure and deterioration due to impurities.

In order to design or add new elements to the front section to improve its cooling system, there are certain surfaces and spaces that can be used.

On the one hand, the bottom walls and the side wall of compartment six have space for placing devices if necessary. In addition, there is a 29 mm height gap under the converter, between the main heat sink and the bottom plate, which could be used if desired.

Finally, outside the converter there is a gable which can be used as a heat sink, as it is a metal plate with a large surface area, approximately 1 m^2, and located only 4 mm away from the external wall of the converter. The disadvantage is that the gable is not in the speed direction, so the air flow besides it depends on the train's direction.

2.2 Review of the State-of-the-Art of Electronic Cooling

According to the US Air Force Avionics Integrity Program, high temperature is the cause of up to 55% of electronic device failures (Ref. [3]). Therefore, thermal management is a key factor in most industries nowadays, including automotive, robotics, telecommunications, nuclear, and electronics.

Thermal management of electric and electronic equipment aims to decrease working temperature and to improve the durability of the devices, while fulfilling physical and mechanical constraints derived from their specific applications, such as mass and volume limitations, robustness against vibrations, and noise reduction requirements, among others.

The fast development of high technology and the increase of power density in new electronic devices make it crucial for electric cooling to be improved in order to face the greater density of heat flux generated by higher currents flowing through the equipment and to avoid thermal runaway in power semiconductors, where silicon remains the workhorse material.

As it can be seen in Figure 2.4, the heat generated during the operation of the component is transferred through conduction to the external case of the component and then it is transferred to the external air through convection and radiation. The heat flux that can be transferred to the air is limited by the air temperature around the component and the heat exchange area that is available. This is the simplest way of heat dissipation, the so-called natural convection, and it can be done with or without a heat sink, *i.e.,* a coupled surface with fins, generally made of aluminum or any other material with high thermal conductivity, meant to increase the exchange area and thus the heat flux.

However, the dissipation of heat generated during the operation of an electronic component can be enhanced by using different methods and heat transfer technologies.

A summary of the available heat transfer and electric or electronic cooling technologies is assessed below. Both conventional and emerging technologies are included. It is important to note that they are commonly found in the literature as heat transfer technologies rather than electric cooling since their principle of operation is to move heat away from the components, it is, to transfer heat from one medium to another.

Most of the heat transfer methods that are used or under study nowadays and that can somehow be applied to traction converters are shown in Figure

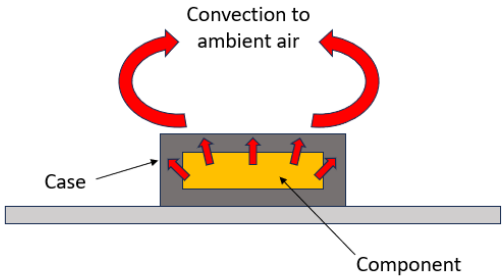

Figure 2.4: Schematic of natural convection cooling in an electronic component.

2.5, where they are also classified attending to two different criteria. On the one hand, they can be either active or passive. The former are those that need to be supplied with external power to work whereas the latter do not require any external power to operate. On the other hand, they can be classified regarding whether the cooling medium, generally a fluid, is or not in contact with the device that requires cooling, in this case, they are categorized as direct and indirect contact technologies, respectively.

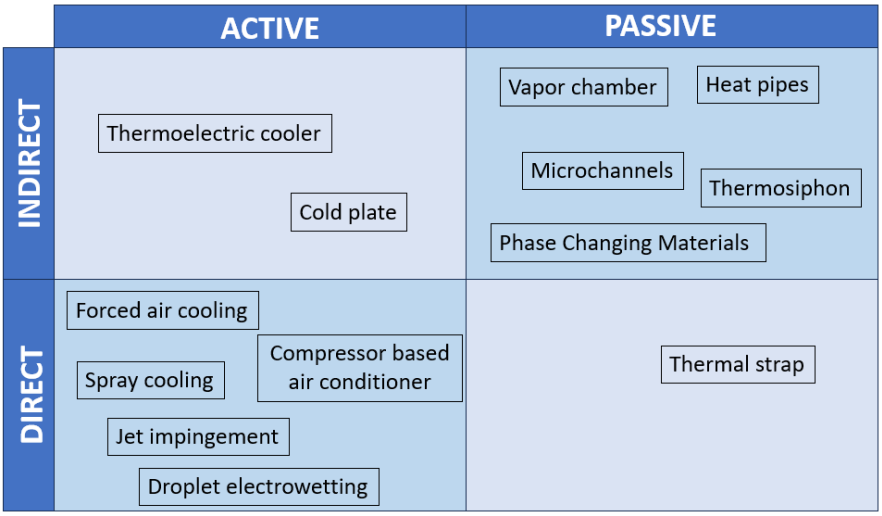

Figure 2.5: Classification of heat transfer technologies.

2.2.1 Active Cooling Technologies

2.2.1.1 Forced Air Cooling

Forced air cooling is an active cooling method in which air is forced by means of one or several fans to flow around the component to be cooled down or through a heat sink coupled to it so that the heat generated in the electric device is absorbed by the air and move away from the area around it.

Heat transfer capability is increased compared to natural convection owing to a larger flow rate. In comparison with liquid cooling systems, it has less power heat transfer capability and lower cost. In general terms, it is also more compact since air is the ultimate medium for all heat rejection, no matter which cooling system is used.

Forced air cooling is trending now in advanced traction inverters with wide-bandgap semiconductors that are able to operate at higher temperatures. However, it presents some drawbacks, mainly that air flow rates are limited by the pressure drop and that the heat transfer coefficient is lower for gases than for liquids.

2.2.1.2 Compressor-based Air Conditioner

A small-scale traditional refrigerating cycle can be used to cool down the air in the heat sink around the electronic component. A compressor-based air conditioner cycle consists of a coolant fluid that flows through an evaporator, a compressor, an expansion valve, and a condenser in a closed circuit. The heat from the area that wants to be cooled down is absorbed and used to evaporate the coolant liquid, later the coolant vapor flows through the compressor where its temperature is increased by means of pressure increase and it goes straight to the condenser where all the heat is rejected, and the coolant becomes liquid again. Finally, it is pumped back to the expansion valve and the evaporator to repeat the cycle. The expansion valve is used to regulate the fluid entering the evaporator and guarantees the continuous operation of the system.

It is a safe option as it is already a mature technology with relatively high efficiency that has been used for countless applications since the beginning of the 19^{th} century. Moreover, its power requirements are much lower than those for new upcoming technologies such as thermoelectric coolers. Nevertheless, it also presents some drawbacks such as the large volume that it occupies, even the small-scale ones, which make them unsuitable for new trends in electronic equipment where compactness is a prerequisite. In addition, maintenance is

needed approximately twice a year.

2.2.1.3 Spray Cooling

This cooling strategy consists of ejecting a coolant liquid as separated tiny droplets that evaporate when they touch the hot surface of the electronic component case, absorbing heat and thus reducing its temperature. The bubble nucleation process, which requires a great amount of energy to overcome the energy barrier, together with liquid film agitation due to the droplets' impact, allows to obtain heat dissipation values around 140 - 200 W/cm^2 (Ref. [3]). This heat transfer capacity depends on the nozzle size and location as well as on the physical properties of the coolant fluid.

The main disadvantage of this cooling strategy is its high-pressure operating conditions and the easy clogging of the nozzle. Moreover, it is still under development and there is a big need for research on heat transfer in film nucleate boiling to further improve efficiency and reliability.

2.2.1.4 Jet Impingement

Similarly to spray cooling, jet impingement cooling is an active cooling strategy that implies direct contact between the component and the cooling fluid, which is a liquid. The main difference is that in this case the liquid is ejected as a stream instead of as separated droplets. Its cooling capacity is almost as high as for spray cooling, around 115 - 150 W/cm^2 (Ref. [4]) and it benefits from a low thermal resistance. However, it suffers from stability in the temperature of the component's surface due to the single-phase fluid. In addition, jet stream leads to a high pressure drop.

Although it has not been implemented in electric transport applications yet, it is widely used in power electronic cooling applications owing to its low thermal resistance, and, as stated in Ref. [5], current studies go towards designing a closed cycle jet impingement system for hybrid electric vehicles. Other research is oriented towards optimizing the configuration of the nozzle and the number of jet streams as they play a key role in the heat transfer capacity of the system. Lastly, phase changing nanoparticles are considered a promising cooling fluid for this technology.

2.2.1.5 Droplet Electrowetting

Droplet electrowetting is a novel and developing cooling strategy thought to cool down hot spots. As the name suggests, it is based on the electrowetting effect which changes the contact angle of the droplet with the surface as a response to an applied voltage level on the interface between the solid and the liquid. Therefore, the droplets move automatically toward the hot spots as a result of a combination of the electro- and thermo-capillary effects.

As of now, the documented heat dissipation capacity is 30 - 40 W/cm^2 (Ref. [6]). However, there are plenty of researches aiming to increase this figure. They are mainly based on changing wettability, controlling the fluid's movement, and enhancing phase change heat transfer. All in all, according to Zhihao Zhang *et al.,* in Ref. [3], droplet electrowetting seems to be a promising cooling technology that offers a quick response to hot spot cooling with no energy consumption nor pressure drop.

2.2.1.6 Cold Plate

Cold plates are metal plates with very low thermal resistance through which pipes with a cooling fluid, usually a mix of water and glycol, circulate. They form part of closed-circuit liquid cooling circuits in such a way that the liquid absorbs the heat from the component as it passes through the cold plate and then transports it to another heat exchanger in contact with the outside air where the heat is transferred from the liquid to the environment. The cooled liquid is then pumped back to the cold plate to repeat the cycle, as can be seen in Figure 2.6.

When compared to air, liquid cooling allows to transfer higher heat flux resulting in a more efficient and compact technology. Moreover, forced liquid cooling is generally quieter than forced air. Its main drawback is the risk of leakage which can cause short circuits and electric faults.

Heat dissipation density in a cold plate is over 5 W/cm^2 for the most simple ones (Ref. [8]). This figure is enlarged if pin fins are added.

According to Ref. [5], cold plate liquid cooling is one of the most used methods historically. When implementing it, the plate can be in direct contact with the component to be cooled or attached to it using a thermal interface material and heat spreaders, which is called an indirect contact cold plate. While direct contact leads to a better heat transfer efficiency and up to 50% lower thermal resistance, indirect contact cold plates perform better in terms of stability and are, therefore, more commonly used.

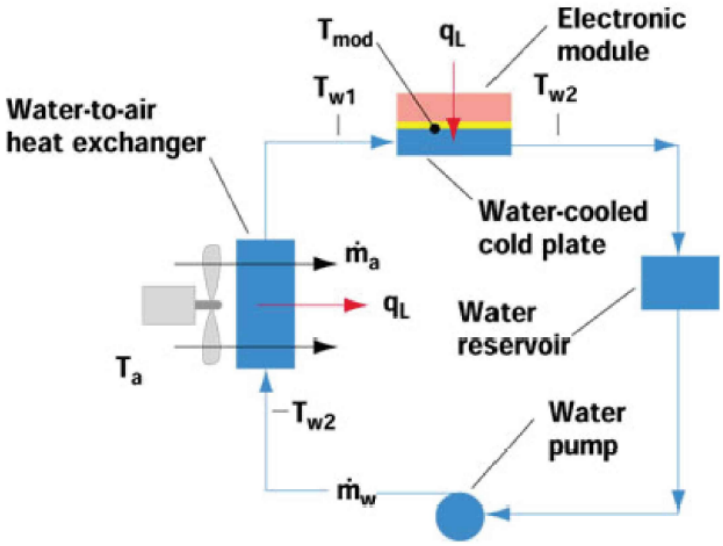

Figure 2.6: Scheme of liquid cooling using a cold plate (T_a stands for the air temperature, q_L for the heat flux, T_{mod} for the controlled temperature in the component, T_{w1} and T_{w2} for the temperature of the water in the inlet and outlet of the cold plate, respectively. And $\dot{m}_a$ and $\dot{m}_w$ represents the air and water mass flows, respectively). **Source:** Adapted from Ref. [7].

Most used cold plates nowadays are single-phase, *i.e.,* the liquid fluid is always in the liquid state. However, current research goes towards improving two-phase cold plates. These are likely to have higher heat flux and more uniform temperature distribution owing to the latent heat. Moreover, lower pump power would be needed for low flow rates compared to single-phase cold plates. Poly-carbonated cold plates are also under study as they seem to achieve better results than copper ones for similar operating conditions.

2.2.1.7 Thermoelectric Cooler

Thermoelectric coolers, also known as Peltier cells, are composed of two different metal plates joined through N and P-type semiconductors. These semiconductors are connected electrically in series and thermically in parallel. A voltage difference is applied to the system so that an electrical current flows through the metals and semiconductors and a temperature difference between the two sides is induced due to the Peltier effect. In other words, when an electric current is flowing through the Peltier cell it acts as a heat pump and

transfers heat from one side to the other depending on the direction of the current. Figure 2.7 shows the operating principle of a thermoelectric element.

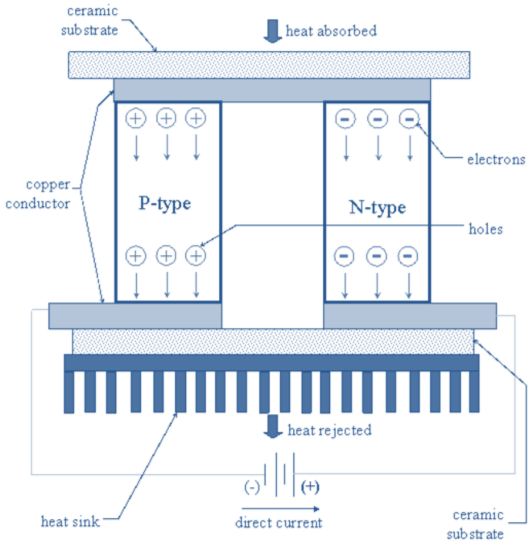

Figure 2.7: Peltier effect scheme. **Source:** Adapted from Ref. [9].

Despite their relatively low efficiency and heat flux (approximately 5 W/cm^2, according to Ref. [10]), thermoelectric coolers present some advantages against traditional cooling systems such as vapor compressors. The main reasons for their use are their small size and compactness since volume limitations are common in electronic cooling as well as in many other applications. Moreover, they have no moving parts which makes them maintenance-free. Finally, they can also be used when a precise temperature is desired on one of the sides since they can be easily controlled by applying different DC voltage levels.

2.2.2 Passive Cooling Technologies

2.2.2.1 Thermal Straps

Thermal straps are a straightforward and simple technology to transfer heat from one point to another. The straps are made of materials with very high thermal conductivity and are coupled to a chip or hot spot so that the heat generated in the component is transported to larger surfaces or to external walls, where it is easier to dissipate.

Their main advantage, apart from their simplicity, is that they allow vibration isolation thanks to the material's flexibility. This is the reason why they are commonly used in aerospace applications, where vibrations are an important constraint. Despite its simplicity, there are still researchers aiming to find new materials with better characteristics.

2.2.2.2 Heat Pipes

A heat pipe is a very efficient thermal conductor which transfers heat at almost constant temperature. It consists of a sealed metal tube with a wick structure on its inner surface. Inside there is a small amount of working fluid, generally water, at its saturation point. On one side of the pipe – the so-called evaporator – heat is absorbed which causes the evaporation of the fluid. This results in an increase of pressure that pushes the vapor towards the other side of the pipe – the condenser. This side can be coupled with a heat sink so that the heat is transferred to the external environment and the fluid condensates. The liquid is then absorbed by the wick surface which pumps it back to the evaporator side by capillary pressure. The result is a continuous operation. A schematic of the process is shown in Figure 2.8.

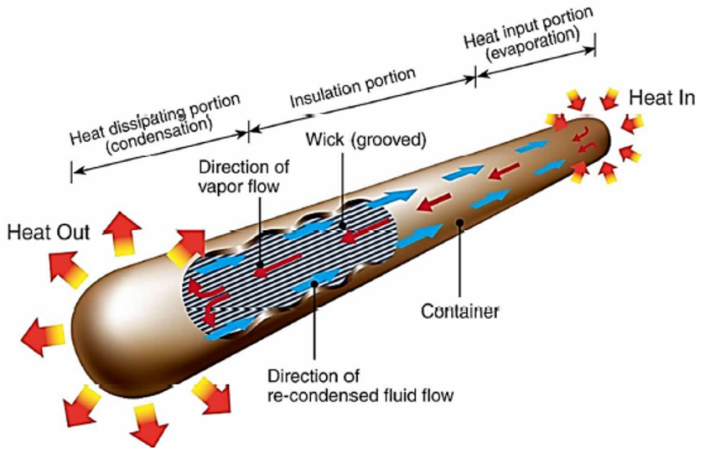

Figure 2.8: Scheme of a heat pipe. **Source:** Adapted from Ref. [11].

High thermal conductivity together with isothermal performance allows heat pipes to be used as an efficient method for cooling electronic components, being able to dissipate 10 - 300 W/cm^2 (Ref. [12]). Higher heat flux is achieved if the pipe is located vertically with the condenser side above the

evaporator since capillarity is assisted by gravity to transport liquid back to the evaporator.

Moreover, heat pipes present other advantages such as no need for an external power source since fluid is pushed by capillary force. This also allows the pipe to work in both directions so that either end can work as an evaporator or condenser indistinctly. Finally, they are very light, they have no moving parts or any other sensible components so their life expectancy can be up to twenty years with no need for maintenance (Ref. [13]), and the spillage risk is very small due to the small amount of liquid that they contain.

2.2.2.3 Thermosiphon

A thermosiphon is similar to a heat pipe in the sense that is a passive method to remove heat which consists of a two-phase coolant fluid flowing inside a sealed pipe that transports heat from one location - the evaporator - to another - the condenser. The main difference with a heat pipe is that in thermosiphons the driving force is gravity, *i.e.,* it is based on natural convection and, therefore, they cannot operate horizontally or against gravity, as heat pipes do.

Furthermore, unlike heat pipes, thermosiphons do not necessarily operate under vacuum conditions, which increases the risk of failure due to bubble formation inside the loop.

Thermosiphons are simpler and cheaper than heat pipes since there is no need for a wick structure. As they are two-phase system they keep constant temperature which makes them useful in applications where stable temperature is required.

2.2.2.4 Vapor Chamber

Vapor chambers are flat metal plates with vacuum conditions inside them which operate based on the same principle as heat pipes. Unlike heat pipes, vapor chambers are flat which makes it easier to couple them with electronic components that need to be cooled down. Moreover, they are able to transfer up to 500 W/cm^2 in all different directions instead of only along the pipe, making the heat dissipation more efficient (Ref. [14]).

The main drawback and the reason why they are not replacing heat pipes in most applications is their high cost. Thus, they are only used in high-class products nowadays.

2.2.2.5 Phase Changing Materials

These are materials with high heat of fusion which can store and release thermal energy by changing from solid to liquid phase and vice-versa. Their application in electric cooling is based on the fact that the heat generation in an electric component is not constant so during peak heat release the material would melt storing energy and cooling down the component and later this thermal energy is dissipated through a heat sink coupled to it so that the phase changing material solidifies again, resulting in a passive cooling technology.

As their operation principle is based on phase change, they have a uniform temperature distribution on the surface which ensures a longer lifetime of the electronic devices. Phase changing materials can be used on their own to act as thermal storage as explained above, or can be used to enhance already existing heat exchangers if used as an envelope to cool down a coolant fluid that flows through a heat exchanger. The latter implementation is still being tested in an experiment carried out by NASA (Ref. [15]).

The most commonly used materials for high temperatures are organic materials such as paraffin waxes. However, the range of temperature is limited depending on the selected material, and the thermal properties of the material degrade with a high number of thermal cycles. Thus, it is beneficial to select the phase change temperature close to the limit temperature so that it only melts when extra cooling is necessary.

The main drawback of using phase changing material as cooling technology for electronic devices is their relatively high volume, as their absorption capacity is around 0.05 Wh/cm^3 (Ref. [16]). In addition, there is a need for research regarding their physical and chemical properties as well as looking for eco-friendly phase changing materials.

2.2.2.6 Microchannels

Microchannels are thought of as a modification of the traditional heat sink. The coolant fluid flows through differently shaped narrow channels to improve heat transfer properties due to the increase of disturbances in the boundary layer. The height of the channels can be only 0.5 mm (Ref. [17]) and the distance between tubes can vary with the temperature gradient to aim for an isothermal surface.

They can be implemented combined with some of the already exposed technologies, such as cold plates or phase changing materials, to enhance heat transfer. Their main drawback is that they suffer from a huge pressure drop

and that they make the system much more complex and, sometimes, heavy.

2.2.3 Discussion on Heat Transfer Technologies

From the review of the state-of-the-art of cooling technologies, it can be established that there are several trade-offs that might arise when designing a thermal management system for electric and electronic components. In general terms, while liquid cooling is more efficient and adaptable than air cooling, the risk of leakage and increased system complexity must be carefully considered. Similarly, while two-phase heat absorption methods offer greater efficiency thanks to the use of latent heat, issues such as pressure drop and fluid channel oscillations must be addressed.

Furthermore, it should not be forgotten that the design of the structure and the surface properties, such as roughness and wettability, play a fundamental role in the efficiency of the system, regardless of the type of cooling technology used.

With regards to the ongoing project, a primary selection of promising technologies to be used is assessed below.

Among all the explained technologies, spray cooling, jet impingement cooling and droplet electrowetting are discarded and will not be considered in the further evaluation for the cooling system of the traction converter because they imply direct contact with a liquid coolant which can bring in impurities inside the converter section and cause failure or deterioration of the components. On the contrary, thermoelectric coolers, cold plates, heat pipes, phase changing materials and compressor-based air conditioner could be promising technologies and will be considered in further evaluations. Forced air cooling is also considered as it is the one that is currently implemented in the MITRAC/TC1500™.

Vapor chambers and thermosiphons have a similar principle of operation to heat pipes. However, in the thermosiphon the risk of leakage is higher as it contains more liquid and the vapour chambers are still under development and are very expensive. Therefore, although they are not considered along this project, the evaluation carried out for heat pipes can be easily scalable to these technologies. In addition, the implementation of thermal straps is very similar to that of heat pipes, but they have lower thermal conductivity. Thus, they are also not seen as a primary technology to be used.

Lastly, microchannels are normally used combined with one or more of the rest of the technologies, so they are not considered on their own.

To conclude, the thermal management system is frequently made up of

several components, and optimization and innovative approaches to lowering total thermal resistance and energy consumption are still needed. Moreover, the problem of being eco-friendly and recyclable must also be taken into account when designing a thermal management system.

Chapter 3

Methodology

The evaluation of the different models provided in Chapter 4 is based on the heat transfer achieved by each of them. Heat transfer capacity of each design is calculated by using mathematical and fluid dynamic models. This chapter covers the methodology relating to both forms of modelling. It also explains the procedure followed for the post-processing of the results.

3.1 Heat Convection Coefficient

The heat convection coefficients are used as input parameters for both mathematical and thermal models. They are calculated for each air flow involved in heat transfer in all the different designs. Its calculation is based on analytical expressions for the Nusselt number, that represents the increase in heat transfer due to convection of a fluid on a surface as compared to heat transfer by conduction alone, according to the specific conditions of each case.

The methodology applied individually to each flow is the following.

1. Set the properties of the flow: Density, specific heat, dynamic viscosity and thermal conductivity. All of these depend on the temperature of the fluid.

   The values used for the hot and cold air streams are shown in Table 3.1.

	Temperature (T)	**Density** (ρ)	**Specific Heat** (c_p)	**Viscosity** (μ)	**Thermal conductivity** (k)
Cold air	60ºC	1.093 kg/m^3	1008 J/kgºC	1.963·10^{-5} kg/ms	0.027 W/mºC
Hot air	70ºC or 68.5ºC	1.029 kg/m^3	1009 J/kgºC	2.052·10^{-5} kg/ms	0.029 W/mºC

Table 3.1: Properties for hot and cold air flows.

2. Establish the volume flow rate and derive the average speed of the flow. This is done by simulating the model in Star CCM+® by means of CFD to obtain the speed. In some specific cases the average speed is chosen as an input parameter.

   The selection of the air volume flow rate or average speed for each case is provided and justified in Appendix A.

3. Among all the possible convection options in Ref. [18], select the model that best suits the air flow to be analysed, and set the characteristic length of the convective surface. In general terms, the different options that are used in this project are the following:

   - Forced convection inside tubes. This model is used when the fluid is enclosed in tubes and flows along its longest length, as shown in Figure 3.1.

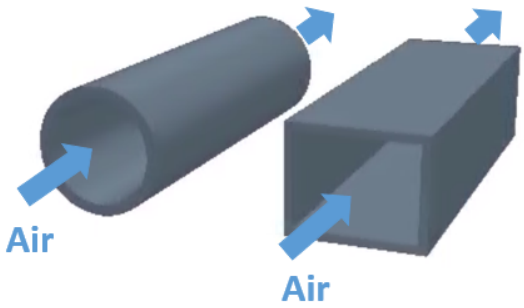

Figure 3.1: Flow inside tubes.

This model is also used to model flows that travel parallel to a flat finned surface and the distance between the end of the fins and the next wall, parallel to the plate and enclosing the fluid, is less than 5 mm. In this case, a tube is made up of two consecutive fins and the two flat walls perpendicular to it, the plate to which the fins are coupled, and the one close to the opposite end of the fins (see Figure 3.2).

In this convection model, the characteristic length is the diameter of the tubes or, in the case of non-circular tubes, the so-called hydraulic diameter, calculated as

$$D_h = 4\frac{A_c}{P} \tag{3.1}$$

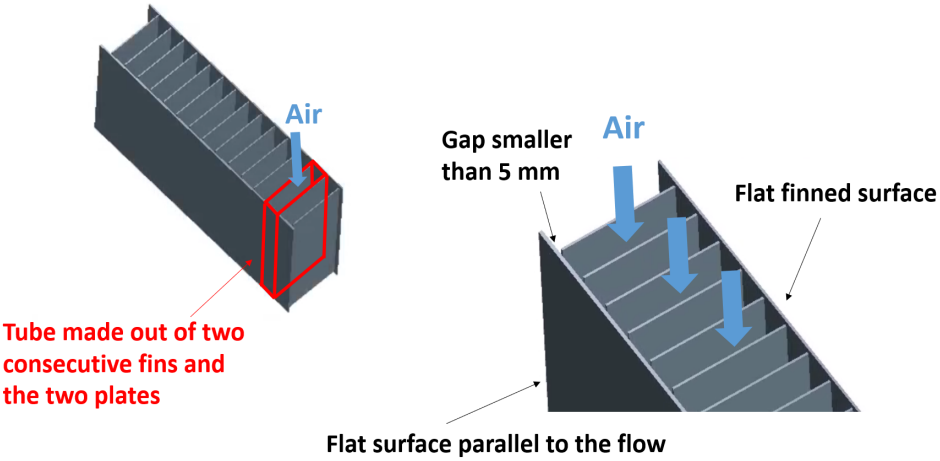

Figure 3.2: Flow between two consecutive fins and two parallel flat plates.

where A_c is the cross-sectional area of the tube and P the perimeter.

- Forced convection on a flat surface. This is used for flows that move parallel to a flat plate, with or without fins, where the the opposite wall is 5 mm away or further, as shown in Figure 3.3. The characteristic length in this case is the length of the plate in the direction of the speed of he flow.

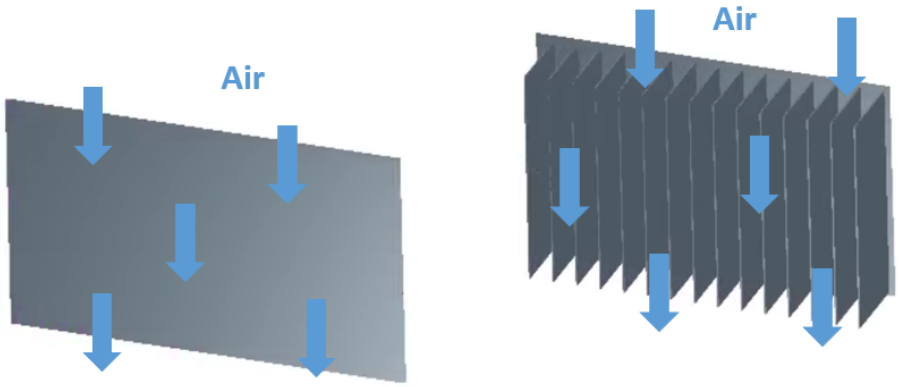

Figure 3.3: Flow parallel to a flat plate, without and with fins.

- Forced convection around tubes. This is used when there is an external flow perpendicular to closed tubes (see Figure 3.4), where the heat-exchanging surface is the external surface of the tubes. In this case, the characteristic length to model the flow is the diameter of the tubes, or the hydraulic diameter according to Equation (3.1).

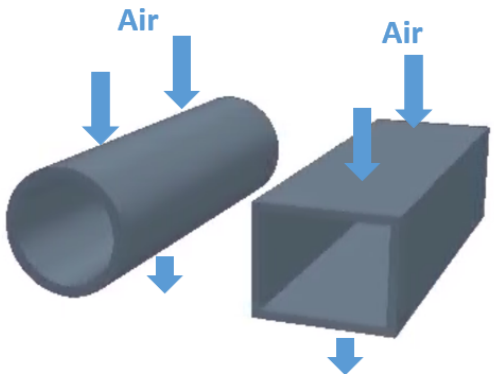

Figure 3.4: Flow perpendicular to closed tubes.

The selection for each air flow is provided and justified in Appendix A.

4. Calculate the Reynolds (Re) and Prandtl (Pr) numbers. The Reynolds number represents the ratio between the inertia forces and viscous forces in the fluid and is used to characterize the flow as laminar or turbulent. The Prandtl number, on the other hand, shows the relationship between the rate of diffusion of the momentum quantity and the thermal diffusivity. They are defined as follows

$$Re = \frac{L_c v \rho}{\mu} \tag{3.2}$$

$$Pr = \frac{c_p \mu}{k} \tag{3.3}$$

where L_c is the characteristic length of the convective surface, the diameter in the case of pipes, and the length parallel to the flow in the case of flat surfaces. v is the speed of the flow, either average or local depending on the application. And ρ, μ, c_p, k are the density, dynamic viscosity, specific heat and thermal conductivity of the fluid.

5. Calculate the Nusselt (Nu) number according to the selected model chosen in step 3 and the dimensionless numbers obtained in step 4. The analytical expressions used in each case can be found in Appendix A.

6. Calculate the heat convection coefficient (h) from the definition of the Nusselt (Nu) number as

$$Nu = \frac{hL_c}{k} \quad \rightarrow \quad h = \frac{Nu \cdot k}{L_c} \tag{3.4}$$

3.2 Mathematical Modelling

The mathematical model uses the equivalent thermal resistance model to calculate the convective heat transfer.

The purpose of the mathematical models, beyond validating the results by comparison, is to make a feasibility analysis prior to the CFD simulations and to check what is the heat transfer capacity of each of the flows separately.

Therefore, the complete heat transfer from the internal sinus of the hot air flow to the cold air flow, passing through the aluminum plate by conduction, is not modeled as such. Instead, the convection of the hot flow and the convection of the cold flow on the plate are modeled separately.

Figure 3.5 shows the equivalent convection resistance diagram for the convection of a fluid on a surface, where the heat travels from the higher temperature end to the lower temperature end.

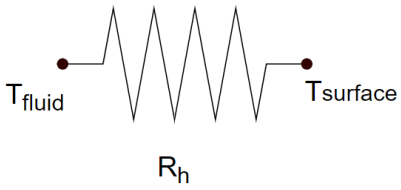

Figure 3.5: Equivalent convection resistance. T_{fluid} is the temperature of the fluid and $T_{surface}$ is the temperature of the surface. R_h is the thermal resistance.

The convective thermal resistance, R_h, is provided in Equation (3.5).

$$R_h = \frac{1}{hA} \tag{3.5}$$

where h is the heat convection coefficient calculated according to Section 3.1, and A is the area of the convection surface.

The heat transferred by convection, Q, is calculated according to Equation (3.6).

$$\Delta T = R_h Q \quad \rightarrow \quad Q = \frac{\Delta T}{R_h} = hA\Delta T \tag{3.6}$$

where ΔT is the temperature difference between the hot and cold elements, either $T_{fluid} - T_{surface}$ or vice-versa depending on the direction of the heat flow.

Equation (3.6) is applicable to both hot and cold flows in the different designs proposed in Chapter 4. For the calculation of the results with the mathematical models, the limiting flow is used in each case.

The choice of the limiting flow, the heat exchange area and the temperature difference for each of the proposed designs are exposed in Appendix B.

It is important to remember that in case of modification of the heat exchanger, the heat that would be transferred by the heat exchanger if it were not modified must be subtracted to the calculated heat value, to avoid computing it twice. In all other cases, the effect of the modifications on the heat transfer through the front cover should be studied and taken into account if necessary.

3.3 CFD Modelling

Once the CFD model is run in StarCCM+®, the heat transfer in each case is calculated by applying the first law of thermodynamics, so that by conservation of energy, Equation (3.7) can be applied, where the left-hand term represents the heat output and the right-hand term the change in internal energy, kinetic and thermal, experienced by the flow of hot air.

$$Q = \dot{m} c_p \Delta T \tag{3.7}$$

Q represents the heat power, c_p the specific heat of the fluid, in this case, the internal air, $\dot{m}$ the internal air mass flow, whose value varies depending on the design, and is defined as $\dot{m} = \dot{v}\rho$, with $\dot{v}$ being the volume flow rate and ρ the density of the fluid. ΔT is the temperature difference in the internal air before and after going through the considered technology, predicted in the simulation software.

The inputs for the simulation software are the following:

- All plates are made out of aluminum alloy UNSA92014, with a thermal conductivity of 193 W/mK.
- The inlet temperature for all cold air flows is 60°C.
- The inlet temperature for all hot air flows in compartment six is 70°C.
- The inlet temperature for all hot air flows in compartment zero is 68.5°C.
- The volume flow rate (or airspeed in some cases) for each air flow varies for the different cases. The used values are provided in Appendix A.
- The heat transfer coefficient for each air flow is calculated analytically as explained in Section 3.1.

As in the mathematical calculation, the effect of the added components on the heat flow in the heat exchanger of the front cover must be taken into account and subtracted if necessary.

3.4 Evaluation of the Results

The proposed designs are evaluated according to the following characteristics:

i. Heat Power (W): Amount of heat removed from the internal air flow by the add-on cooling system.

ii. Volume (cm^3): Volume occupied in the front section by the add-on cooling system. In the case of external add-on components volume added to the front section.

iii. Weight (kg): Added weight to the front section due to the add-on cooling system.

iv. Coefficient of Performance (CoP): Relation between the heat power removed from the internal air by the add-on cooling system, and the power supplied to that cooling system.

v. Heat Power Density (W/cm^3): Relation between the heat power removed from the internal air, and the volume occupied by the add-on cooling system in the front section.

vi. Reliability of Design: How realistic the behavior of the model is, that is, how close would be the real behavior of the new cooling system and the air flows involved to the predictions, expectations, and assumptions used to create the design.

vii. Feasibility: How easily can it be implemented and how well the design fits the MITRAC/TC1500^{TM} converter based on the constraints considered in the Section 2.1.3.

viii. Robustness: Ability to operate continuously without failure of the various components of the add-on cooling system or the rest of the converter. Vibration and collision resistance are also included.

ix. Cost: How expensive, in economic terms, would it be to implement the add-on cooling system.

x. Maintenance: How often are the components in the add-on cooling system required to be checked out. How complex would that checking be in comparison with the current maintenance procedures.

The features *i*-*v* are quantitative and are measured in the units indicated, with the exception of the Coefficient of Performance, which is dimensionless. The rest, *v*-*x*, are qualitative and are evaluated as *very good*, *good*, *neutral*, *bad* and *very bad*, according to the criteria shown in Table 3.4.

Once each of these features is evaluated for all the proposed designs, A to G in Chapter 4, the weighted average method is applied in order to have a common scale and compare the facilitate comparisons.

The weighting coefficient (w_n) given to each of the features is shown in Figure 3.6, and the criteria for this assignment is exposed in Table 3.5.

The scale to be used is 1 to 5, 1 being the worst case and 5 being the best one. This scale is applied individually to each of the quantitative and qualitative features considered in the study, according to the criteria shown in Tables 3.2 and 3.3.

Finally, the overall score for each design is calculated as shown in Equation (3.8).

$$Score = \sum_{n=1}^{10} w_n S_n \tag{3.8}$$

Where n denotes the features *i* to *x*, w_n the weighting coefficient for feature n and S_n the individual score for the feature n in the evaluated design.

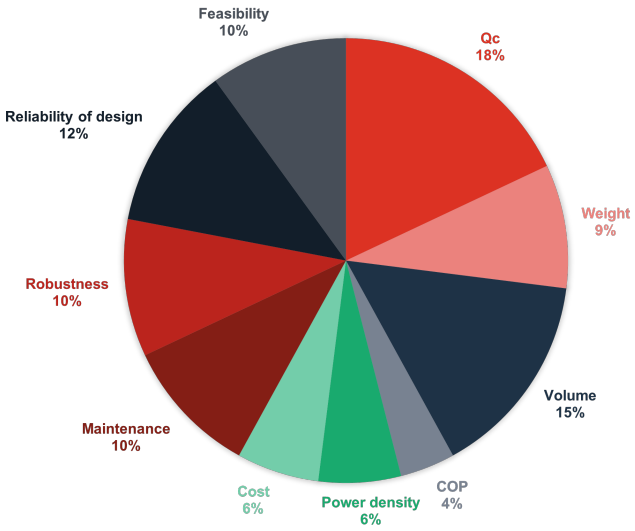

Figure 3.6: Weight factor distribution for weighted average evaluation.

Table 3.2: Criteria for weighted average evaluation. Quantitative features.

Score	Heat Power (W)	Weight (kg)	Volume (cm^3)	CoP	Heat Power Density (W/cm^3)
1	< 100	> 2.2	> 1500	< 60	< 0.4
2	[100, 160]	[1.65, 2.2]	[1000, 1500]	[60, 120]	[0.4, 0.8]
3	[160, 220]	[1.1, 1.65]	[500, 1000]	[120, 180]	[0.8, 1.2]
4	[220, 300]	[0.55, 1.1]	(0, 500]	[180, 240]	[1.2, 1.6]
5	> 300	< 0.55	0	> 240	> 1.6

Table 3.3: Criteria for weighted average evaluation. Quantitative features.

Score	Cathegory
1	*Very bad*
2	*Bad*
3	*Neutral*
4	*Good*
5	*Very good*

On the other hand, to facilitate the comparison of results with the results of other similar projects, the thermal resistance of each of the proposed designs is calculated.

The thermal resistance is given by the quotient between the heat transferred, Q, and the temperature difference between the medium to be cooled (internal air in the front section) and the cooling medium (external air

at ambient temperature), $T_{hot} - T_{cold}$ (see Equation (3.9)).

$$R_{th} = \frac{Q}{T_{hot} - T_{cold}} \tag{3.9}$$

In this project the temperature difference is always 10°C, based on the assumptions stated in the Section 3.3, therefore comparisons within the limits of this project can be made only in terms of heat output.

Table 3.4: Criteria for evaluation of qualitative features.

	Cost	**Maintenance**	**Robustness**	**Feasibility**	**Reliability of Design**
Very good	The extra costs in the new design are small enough to positively influence a potential user's decision to purchase the converter, even if high-temperature operation is not necessary.	The new design requires no extra maintenance.	The failure rate of the components involved is very low, regardless of their maintenance. There are no moving parts outside the converter case. It is not necessary to consider the leakage of liquids.	The design can be easily implemented without affecting any of the constraints in Section 2.1.3, nor making substantial modifications to the converter.	All design components and air flows are expected to work as predicted.
Good	The extra costs in the new design are small enough to positively influence a potential user's decision to purchase the converter, even if high-temperature operation is not a priority requirement.	The new design requires simple or easily accessible maintenance.	The failure rate of the components involved is very low if properly maintained. There are no moving parts or elements external to the converter box. No need to consider the leakage of liquids.	The design can be easily implemented, but affects some of the constraints in Section 2.1.3. No substantial modifications are made to the converter.	Some of the components of the design may work slightly differently than predicted without noticeably affecting the result. All air flows are expected to work as predicted.
Neutral	The extra costs in the new design do not influence a potential user's decision to purchase the converter if high-temperature operation is a requirement.	The new design requires internal maintenance similar to the existing one.	The failure rate of the components involved is low if properly maintained. It has moving parts, but not external to the converter case. It is not necessary to consider the leakage of liquids.	The design can be easily implemented, but affects some of the constraints in Section 2.1.3, and involves some substantial modification to the converter.	Some of the components of the design may perform slightly differently than predicted, as well as some of the air flows, but this would not critically affect the result.
Bad	The extra costs in the new design are high enough to influence, but not decisively, a potential user's decision to purchase the converter even though high-temperature operation is necessary.	The new design requires the addition of new and different procedures to the existing maintenance.	The failure rate of the components involved is medium to low if properly maintained. It has movable elements and/or external to the converter case. No need to consider the leakage of liquids.	The implementation of the design is complex, it affects some of the constraints in Section 2.1.3, but involves some substantial modification to the converter.	Some of the components of the design may perform significantly differently than predicted, as well as some of the air flows, slightly affecting the result.
Very bad	The extra costs in the new design are high enough to have a decisive influence on a potential user's decision to purchase the converter, even though high-temperature operation is necessary.	The new design involves changing the frequency of maintenance of the converter and the procedures used.	The failure rate of the components involved is medium. It has movable elements and/or external to the converter case. Liquid leakage must be considered as a risk.	The implementation of the design is complex, affects some of the constraints in Section **??** and involves some substantial modification to the converter.	Some of the components of the design may perform significantly differently than predicted, as well as some of the air flows, significantly affecting the result.

Factor	w_n	**Justification**
CoP	0.04	There are electric power supplies in the traction converter that can be used to supply the different technologies considered. Moreover, even if the CoP is low, it does not have a big influence on the total power consumption of the traction converter as the add-on cooling system is thought to be used with extremely high ambient temperatures, being turned off the rest of the time.
Heat Power Density	0.06	The low value in this feature is due to its redundancy. Both heat power and volume are already considered as separate features with higher weighting coefficients.
Cost	0.06	Operation in extremely high ambient temperature is a specific necessity, only required on certain trains. Therefore, it can be paid for as an extra service and does not need to be implemented in the main line of traction converters.
Weight	0.09	An excessive increase in weight inside the front cover could necessitate the modification of the mechanical connection between the traction converter box and the train under-frame, otherwise weight gain is not a major problem. However, the weight plays a critical role in the case of an increase in the weight on the front cover, as it hinders maintenance work.
Maintenance	0.1	The need for more frequent or complex maintenance tasks, requiring more time, may affect the quality of service and the availability of trains to run. It also indirectly increases costs.
Robustness	0.1	This is an essential feature to ensure the provision of high-quality train services, avoiding service interruptions due to traction system failures.
Feasibility	0.1	This is an essential feature to ensure the provision of high-quality train services, avoiding service interruptions due to traction system failures.
Reliability of design	0.12	This is an essential characteristic to validate the design in question, if this value is too low the value of the rest of the factors is subordinated to it, decreasing their reliability.
Volume	0.15	When working with high power density converters, the volume of the converter should be kept as small as possible, as the trend is towards more and more compact converters.
Heat power	0.18	It is the objective of the design, therefore it gets the highest value.

Table 3.5: Weighting coefficients for weighted average calculation.

Chapter 4

Cooling Technologies Applied to MITRAC/TC1500^{TM}

This chapter presents seven different approaches to increase the heat transfer capacity between the internal air in the traction converter MITRAC/TC1500^{TM} developed by Alstom and the external ambient considering some of the cooling technologies studied in Section 2.2.

It is important to note that each of the designs includes only one isolated modification to the current cooling system. This is because the objective of this chapter is not to find the ultimate definitive cooling system for the MITRAC/TC1500^{TM}, but to analyze the performance of each of the approaches or technologies individually so that the finding of this thesis can be extrapolated to other models of traction converters, and be used as a starter point to future modifications of the thermal management systems for other products.

The suggested approaches include three models with pure air forced convection, two with heat pipes, one with a cold plate, and two with Peltier cells, also known as thermoelectric coolers. Designs with phase changing materials and compressor-based air conditioner systems are disregarded due to the high volume required to remove the same amount of heat power.

As specified in Chapter 3, the results exposed here are valid for an internal temperature of 70°C, and an ambient temperature of 60°C. It is worth mentioning that this ambient temperature is very high and could jeopardize the safe operation of other components of the train propulsion system. It is a matter of looking for a challenging scenario with a future perspective.

4.1 Evaluation of Selected Technologies

4.1.1 Forced Air Cooling

4.1.1.1 Design A. Modified Front Cover Heat Exchanger

As explained in Section 2.1.1, the main way of removing heat from the internal air is through the front cover, that is modelled as a heat exchanger. This design consists on modifying the physical layout and the mechanical structure of that heat exchanger to increase the contact surface between hot and cold air streams and enhance heat transfer between both mediums. The proposed layout is shown in Figure 4.1, and it consists of alternating hot tubes so that they are in contact with cold air through most of their walls. A first layer of cold air

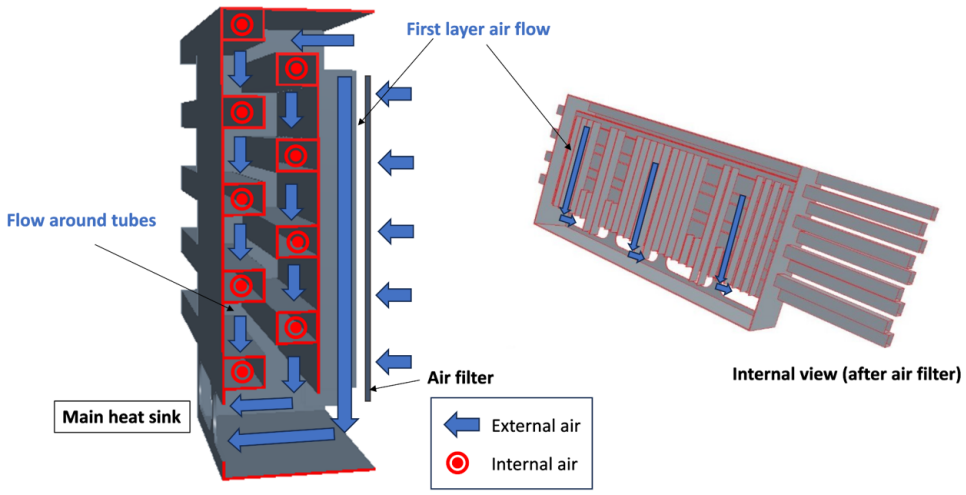

Figure 4.1: Design A. Modified front cover heat exchanger.

is added just beside the entrance of the external air through the filter, keeping the finned channels of the current layout, to avoid a large pressure drop in the external air flow. If the pressure drop in the external air flow is too big the air speed in the main heat sink would be smaller and, therefore, its cooling capacity would be reduced.

Table 4.1 shows the fluid mechanics models applied to each of the air flows: Internal air through the tubes, external air around the tubes, and external air in the first layer (see Figure 4.1), together with the heat convection coefficients

for each of them. More detailed information regarding how each air flow is modeled can be found in Appendix A.

Table 4.1: Air flow modelling for Design A.

Air flow	**Fluid modelling**	**Heat convection coefficient** (h)
Internal air	Forced convection inside tube	41.92 W/m^{2}K
External air around tubes	Forced convection around staggered tube bundles	28.85 W/m^{2}K
External air first layer	Forced convection inside tubes	18.05 W/m^{2}K

The results predicted by the simulation show that the total heat power in the front cover increases by 237 W when compared to the original layout. Moreover, the pressure drop in the external air flow is only 4 Pa smaller than in the original layout. According to the mathematical model, the heat power extracted from internal air flow is 299 W more if this layout is used.

The evaluation of the rest of the studied features is shown in Table 4.2. First, this modification of the front cover implies an increase in weight of 2.4 kg owing to the extra amount of aluminum needed. Furthermore, when it comes to volume, the new layout is 40 mm thicker than the original one, which leads to an increase of 1 559 cm^3 in the front cover. Therefore, the heat power density for this option is 0.15 W/cm^3, while the coefficient of performance does not apply since it is a passive solution.

It is important to note that the increase of volume and weight in this design are especially critical as they refer to the front cover, a moving part that must be easily removed for maintenance. In addition, its widening causes a change in the external dimensions of the converter box that may make the coupling of the traction converter to the train more difficult.

Table 4.2: Evaluation of Design A.

Heat Power (Q)	**Weight**	**Volume**	**CoP**	**Heat Power Density**
237 W	2.4 kg	1 559 cm^3	*Passive*	0.15 W/cm^3

Reliability of design	**Feasibility**	**Robustness**	**Cost**	**Maintenance**
Very good	*Neutral*	*Very good*	*Bad*	*Very good*

In the qualitative analysis, robustness and maintenance are categorized as *very good* because neither moving parts, nor new components are added to the system. Feasibility is set as *neutral* since there is no need to modify anything inside the front section, but a whole new front cover needs to be designed, tested, and manufactured. The latter is also the reason why the cost of this option is considered as *bad* since the new manufacturing process results in a significant increase in cost. Finally, the operating principle is the same as in

the current cooling system, therefore there is no risk for the model not to work as described. Thus, the reliability of the design is evaluated as *very good*.

4.1.1.2 Design B. Heat Exchanger in the Bottom Gap

There is an empty space below the main heat sink that is meant to be used as a heat exchanger in this option by forcing part of the internal air to flow through this new channel. Both the upper and lower surfaces of the channel are in contact with external (cold) air, the upper one with the air flowing through the main heat sink and the lower one with the external ambient, as can be seen in Figure 4.2.

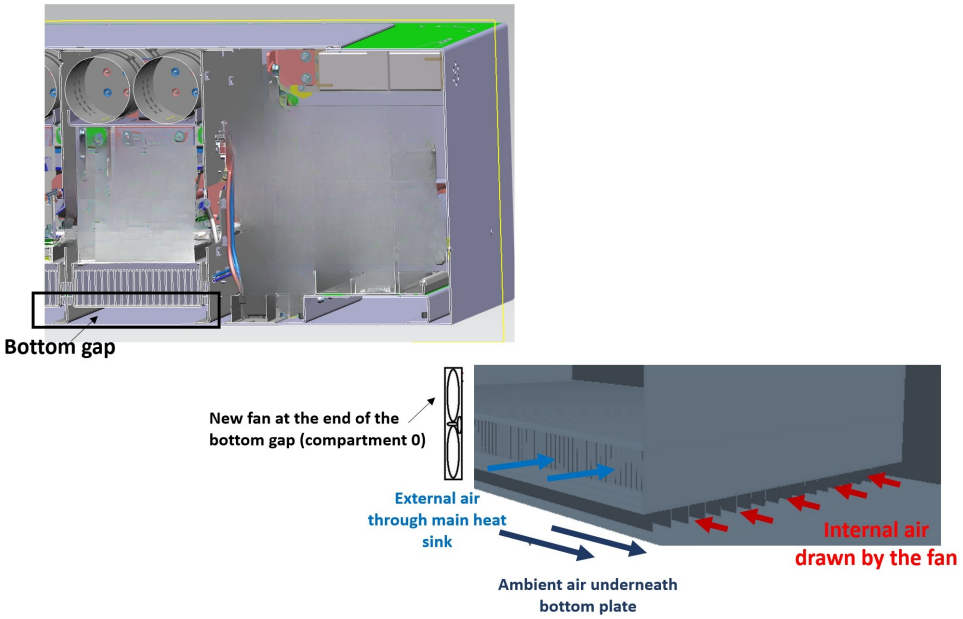

Figure 4.2: Design B. Heat exchanger implemetned in the bottom gap.

This option is divided into two possible designs:

- One in which no extra fan is considered, *i.e.,* only the already existing fan is sitting in compartment zero. It is assumed that either the pressure drop between compartments six and zero is enough to move the air naturally, or that the current fan can be relocated so that it draws both air flows: The one in the front cover and the one in the bottom gap.
- Another one where an extra fan is considered, *i.e.,* compartment zero is modified to host two fans. The added fan forces the air to flow

through the bottom channel. This increases the mass flow compared to the previous design.

Apart from the internal air, ambient air underneath the bottom plate and the air flowing through the heat sink play a role in the heat transfer capacity of this design (see Figure 4.2). The fluid mechanic model of each of them and the obtained heat transfer coefficients for each of them are shown in Table 4.3.

Table 4.3: Air flow modelling for Design B.

Air flow	**Fluid modelling**	**Heat convection coefficient** (h)
Internal air without extra fan	Forced convection inside tubes	10.83 W/m^{2}K
Internal air with an extra fan	Forced convection inside tubes	16.50 W/m^{2}K
External air in heat sink	Forced convection inside tubes	47.67 W/m^{2}K
Ambient air underneath bottom plate	Forced convection on flat plate	5.50 W/m^{2}K

The heat transfer for these designs obtained in the thermal simulations is 79 W if only one fan is considered and 136.4 W with the added fan. In both cases, the main limitation of the heat power is the small mass flow going through the gap. According to the mathematical model, the heat transfer capacity is 94 W for the first design and 143 W for the design that includes two fans. For both methodologies, the added heat losses owing to the extra fan are taken into account when computing the overall improvement in cooling capacity.

The add-on system in this case is fins and, in the second design, a new fan, which pushes part of the hot air flow through this new channel. The weight of the system depends on the number of fins added, the unitary weight being 0.11 kg/fin. The weight of the fan is estimated to be 0.3 kg, based on Ref. [19]. The total weight of the proposed models, with and without the new fan, are 1.9 and 2.2 kg respectively. The only computed volume is the volume occupied by the fan inside compartment zero, and it is estimated to be 160 cm^3, using Ref. [19] as a reference too. Thus, the power density as well as the coefficient of performance can only be calculated for the second model, as it is shown in Table 4.4. The power supply for the fan is 1.5 W (Ref. [19]).

Table 4.4: Evaluation of Design B.

	Heat Power (Q)	**Weight**	**Volume**	**CoP**	**Heat Power Density**
No extra fan	79 W	1.9 kg	0 cm^3	*Passive*	-
Extra fan	136 W	2.1 kg	160 cm^3	90.93	0.85 W/cm^3

	Reliability of design	**Feasibility**	**Robustness**	**Cost**	**Maintenance**
No extra fan	*Very bad*	*Very good*	*Very good*	*Very good*	*Very good*
Extra fan	*Very good*	*Very good*	*Neutral*	*Good*	*Neutral*

In the approach without the new fan, feasibility, maintenance, robustness, and cost are evaluated as *very good* as the only modification to be done is to add fins in the bottom gap, which is easy to do, cheap and does not imply parts that may fail or require maintenance. On the contrary, the reliability of the design is set to be *very bad* because it is very unlikely that the air flow would flow naturally through the channel in the desired direction if an extra fan were not added. This means that the design would not work as predicted.

On the other hand, in the model with the new fan, feasibility keeps the same value, it is still an easy solution to implement, but robustness and maintenance are categorized as *neutral* because a fan or any rotating machine increases the rate of failures sensibly and needs to be checked out periodically. The price of the solution is also slightly more expensive, so the cost is set to *good*. The reliability of design, unlike in the previous model, is considered *very good* because the operation principle is the same as in the original cooling system: Forced air cooling with a fan forcing the internal air to flow as desired.

4.1.2 Heat Pipes

4.1.2.1 Design C. Heat Pipes Coupled to the Gable

Design C consists of using heat pipes to transfer heat from the internal air in compartment six, where the internal air temperature is maximum, to an external gable which is a large aluminum plate located along the side of the converter (see Figure 4.3).

The dissipation of heat from the gable to the environment cannot be done by natural convection, since the gable is perpendicular to the speed of the train, which means that, in the best case, if the gable faces the front of the train, the external airflow impinges perpendicular to the plate and, in the worst, when the gable is facing the rear of the train, the incident flow is very small because it is protected from the incoming air due to the speed by the converter box. In either case, the convection heat dissipation, assuming a train speed of 120 km/h, and an ambient temperature of 60°C, does not exceed 25 W (see Appendix B).

Therefore, two different options are considered in this Design to dissipate the heat from the gable. It can be done either by redirecting the exhausting air coming from the air conditioner system from the passenger cars or by an additional external fan placed outside the converter box. In both cases, force convection is used by forcing the air flow parallel to the gable.

For the analysis in this document, it is assumed that the external cooling is based on an external fan. The option of redirecting the passenger's air-conditioning output and making it flow parallel to the gable is more

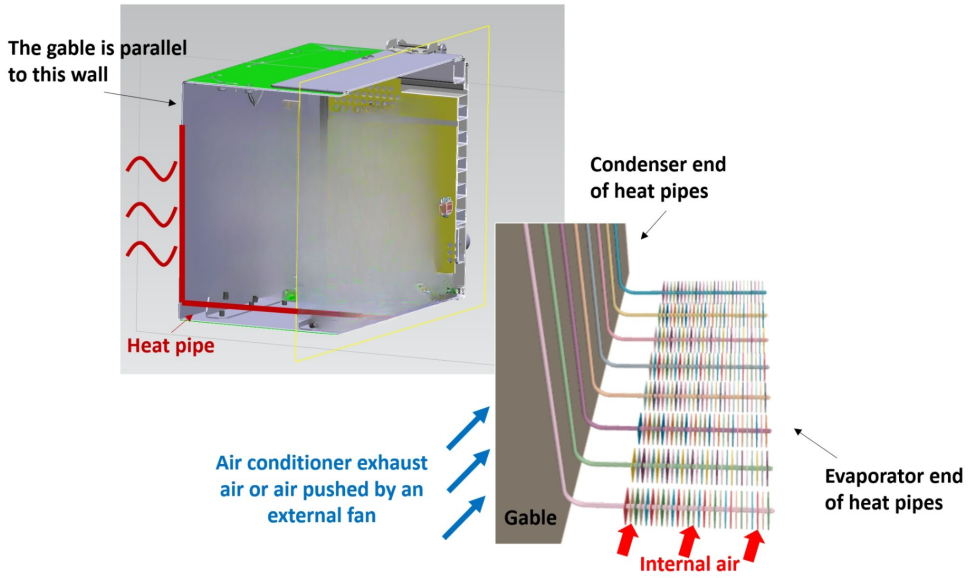

Figure 4.3: Design C. Heat pipes coupled to the gable with external heat dissipator system.

advantageous due to the lower air temperature, but it is less realistic and for a good feasibility analysis it is necessary to know where and how the output of the air-conditioning system is produced, as well as under which conditions of temperature, pressure and humidity. In addition, these conditions can vary widely between different models of trains, so this is left for a deeper investigation is this design wants to be further developed and it is not addressed in this thesis.

The design of the heat pipes based on the available space and surfaces in compartment six leads to the use of heat pipes with a heat transfer capacity of 28 W each when the temperature difference between the evaporator and the condenser is at least 6.2°C. This capacity calculation takes into account the gravity effect, which is beneficial in this case as the condenser is above the evaporator. Moreover, the heat pipes are bent 90° and flattened to fit the space between the converter box and the gable, with a consequent decrease in heat transfer capacity. The dimensioning of heat pipes is exposed in Appendix D.

Based on the available space in compartment six, and on the heat transfer capacity, a total of eight heat pipes are considered in this design. Moreover, fins are added to the evaporator end to enhance heat transfer. However, this is a flexible design. In this sense, heat transfer capacity can be increased by

adding more heat pipes or by increasing the heat absorption surface in the fins, and, in the same way, it can be decreased if fewer heat pipes or fewer or smaller fins are used. All of this is subject to the heat dissipation capacity in the gable to avoid overheating.

Internal air in the low part of compartment six and the external air pushed by the fan are the air flows in this option (see Figure 4.3). The fluid mechanic model used to calculate their heat convection coefficient, together with the respective values can be seen in Table 4.5.

Table 4.5: Air flow modelling for Design C.

Air flow	**Fluid modelling**	**Heat convection coefficient** (h)
Internal air	Forced convection around tubes	46.56 W/m^{2}K
External air beside gable	Forced convection on a flat plate	22.10 W/m^{2}K

Approximately, 158 W are removed from the internal as shown in the CFD simulation. According to the mathematical model, the cold air stream is able to dissipate up to 409 W from the gable before the heat pipes start to work in the opposite direction, heating up the internal air to cool down the gable. Additional simulations were run to demonstrate that the natural convection in the gable is not able to dissipate more than 25 W in spite of its large area (see Appendix C).

With the considered number of heat pipes and fins, the total weight of this model is 0.7 kg and the occupied volume 112 cm^3. Both values would increase with a larger number of heat pipes or fins, and decrease in the opposite case. The external fan and any other equipment located outside the converter box are not considered for this computation, as it only concerns the front section. Moreover, the power supplied to the external fan is not computed, as it is not part of the design as such, that is the reason why this design is consider a passive design. The heat power density and is shown in Table 4.6.

Table 4.6: Evaluation of Design C.

Heat Power (Q)	**Weight**	**Volume**	**CoP**	**Heat Power Density**
158 W	0.7 kg	112 cm^3	*Passive*	1.41 W/cm^3

Reliability of design	**Feasibility**	**Robustness**	**Cost**	**Maintenance**
Bad	*Very Bad*	*Bad*	*Very bad*	*Good*

This design presents several technical difficulties that make it costly and challenge its robustness. On the one hand, the heat pipes need to be embedded both in the side wall of the converter and in the gable, this increases the

transmission of vibrations and mechanical stress between the two surfaces. Moreover, the holes through which the heat pipes are introduced in the side wall have to be properly sealed. On the other hand, the external heat dissipation system outside of the converter box must be built from scratch, including protection against vibration, collisions, and floods. All of this explains that both cost and feasibility are set as *very bad* for this model. When it comes to robustness, it is considered as *bad* and not *very bad* because the rate of failure of the heat pipes is extremely small. Maintenance is categorized as *good* because, even though it is required, the fan is outside of the converter box which make it easier to be checked out.

Finally, the reliability of the design takes into account both external and internal air modelling. For the internal air flow, the main risk is that the amount of air flowing around the heat pipes may be smaller than predicted in Appendix A, while for the external one, it is that, with the exception of the temperature, ambient conditions are not taken into account and may influence the properties of the air pushed by the fan. These are the reasons why it is evaluated as *bad*.

4.1.2.2 Design D. Heat Pipes in the Bottom Gap

The empty channel below the IGBTs' main heat sinks is meant to be used to cool down heat pipes in this design. The heat pipes are located as shown in Figure 4.4, with the evaporator ends towards the entrance of internal air flow in compartment six, so that internal air can be precooled before entering the heat exchanger in the front cover, and the condenser side in the bottom gap. In order to cool down the condenser ends, external (cold) air is used, therefore the bottom gap must be sealed to avoid mixing internal and external air flows.

There are two options for bringing cold air into the bottom gap, either holes are drilled in the bottom plate and the ambient air flowing underneath the plate is let in and out, or a portion of the air flowing through the heat sink is extracted through holes at the beginning of the heat sink. In this document, it is the latter option that is used and therefore shown in Figure 4.4. The reason is that the air flowing through the heat sink is already filtered and reduces the likelihood of deterioration of the heat pipes due to impurities or collisions.

It is important to note that in this case the evaporator end of the heat pipes is above the condenser, and, therefore, gravity plays the opposite role, reducing heat transfer capacity as water must flow against gravity. Moreover, the heat pipes are bent 70^{o}, which also reduces their capacity. The design of the heat pipes considering these capacity reductions and the physical constraints from compartment six leads to the use of heat pipes with a heat transfer capacity of

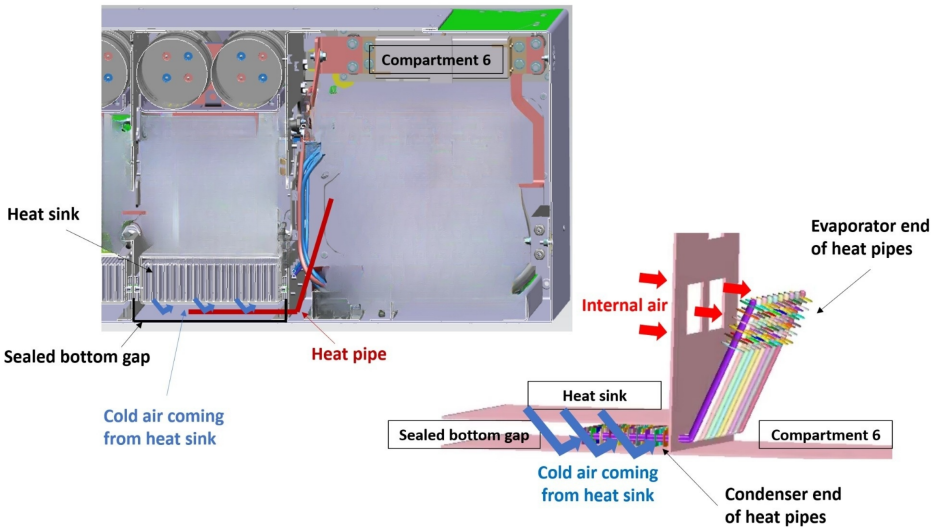

Figure 4.4: Design D. Heat pipes using the bottom gap as heat dissipator with air extracted from heat sink.

19 W each, when the temperature difference between both ends is at least 3°C (see Appendix D).

As for Design C (Section 4.1.2.1), the number of heat pipes and fins is determined according to the available space. In this case, ten heat pipes are considered, and fins are included at both ends of the heat pipes.

The modelling of the cold air flow in the bottom gap, considered as spillage from the heat sink, and the internal air entering compartment six and their corresponding heat convection coefficient can be seen in Table 4.7.

Table 4.7: Air flow modelling for Design D.

Air flow	**Fluid modelling**	**Heat convection coefficient** (h)
Internal air	Forced convection around tubes	58.65 W/m^{2}K
Cold air in bottom gap	Forced convection around tubes	94.93 W/m^{2}K

From the simulation, this option is able to remove up to 165 W from the internal air. The transfer is limited due to the small area of absorption of the heat pipes. According to the mathematical model, the cold air stream in the bottom gap is able to dissipate up to 208 W from the condenser side of the heat pipes, if required, before the air in the bottom gap is overheated and the heat pipes start to work in the opposite direction.

With regards to other features (see Table 4.8), this is a passive design,

where the add-on equipment is the heat pipes and the fins coupled to them at both ends. The weight, therefore, depends on the number of fins that are added, the more fins the higher the weight. For the layout proposed in this document, the estimated weight amounts to 0.8 kg and the occupied volume to 120 cm^3. This leads to a heat power density of 1.38 W/cm^3. Once again, these figures are linked to the chosen number of heat pipes, as weight and volume increase as more heat pipes are added.

The reliability of the design, in this case, is considered as *very good*, since, being based on the current model whose behavior is well known, there is no risk that the air flows do not flow around the heat pipes or remain still and, moreover, the temperature difference between the hot and cold ends of the heat pipes is much larger than necessary for their operation, so there is margin in case the actual value is higher than the theoretical one. Furthermore, heat pipes are very robust with an extremely low rate of failures while they require no maintenance, these are the reasons why robustness and maintenance are also set to *very good* in this design. Finally, feasibility and cost are categorized as *neutral* because they include, not only the purchase and implementation of heat pipes, but also the sealing of the whole bottom gap.

Table 4.8: Evaluation of Design D.

Heat Power (Q)	**Weight**	**Volume**	**CoP**	**Heat Power Density**
165 W	0.8 kg	120 cm^3	*Passive*	1.38 W/cm^3

Reliability of design	**Feasibility**	**Robustness**	**Cost**	**Maintenance**
Very good	*Neutral*	*Very good*	*Neutral*	*Very good*

4.1.3 Cold Plate

4.1.3.1 Design E. Cold Plate in Compartment Zero Using the Bottom Gap

This is a liquid cooling implementation. A mixture of water and 30% of glycol is circulated through a closed circuit of pipes from a cold plate in compartment zero, where heat is absorbed from the internal air and the water temperature increases, to the bottom gap, where a stream of cold air is used to dissipate the heat and reduce the water temperature again. The water is then pumped back to the cold plate to start a new cycle. A schematic of this design is provided in Figure 4.5.

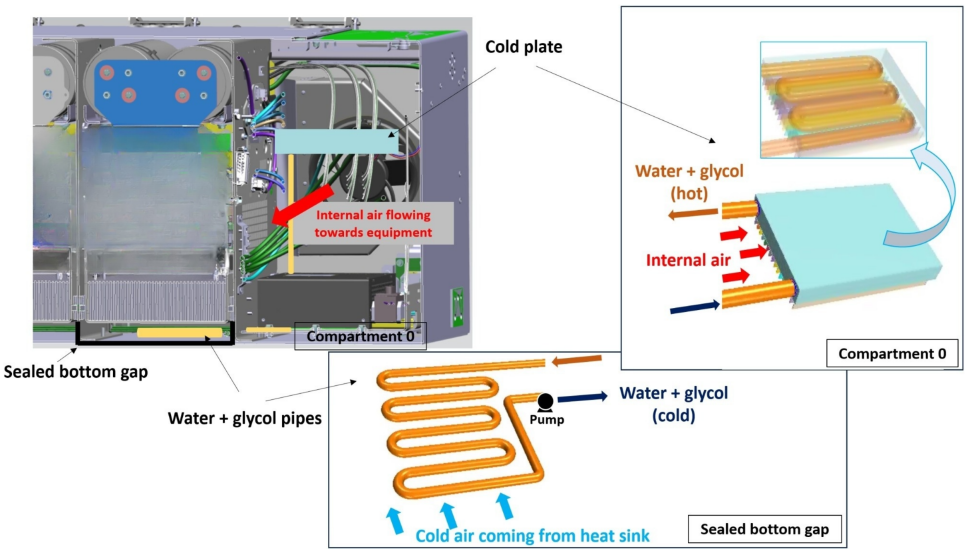

Figure 4.5: Design E. Cold plate in compartment zero using the bottom gap as heat dissipator.

In compartment zero, the internal fan pushes air towards the cold plate, which has fins to improve heat absorption, before it enters compartment one and begins its cooling work along the front section. Therefore, the internal air coming out of compartment zero has a lower temperature compared to the current design and, as a consequence, has a greater capacity to absorb heat when flowing around the busbars and other elements.

On the other hand, analogous to design D (Section 4.1.2.2), in the bottom gap the flow of air that cools the water mixture in the pipes can either come from the outside, entering through the bottom plate, or from the heat sink, entering through the top of the bottom gap as a small spillage of the air flow that cools the IGBTs.

This analysis, as in Design D (Section 4.1.2.2), uses the air from the heat sink as air to circulate through the bottom gap, for safety and filtering reasons. However, the results can be extrapolated from one option to another as long as the maximum power that each air flow is capable of dissipating is taken into account.

Adiabatic pipes connect the cold plate in compartment zero and the cooling loop in the bottom gap. The pipe circuit must include, apart from the pump, a small water reservoir and sensors and valves that ensure the reliable operation of the system. All of these components can be located either inside the front section or moved out to the middle section so that they are easier to access if

needed. In addition, the bottom gap must be sealed so that internal and external air flows are not mixed.

Table 4.9 shows the convection model used for each of the involved air flows, internal air in compartment zero and cold air in the bottom gap coming from the heat sink, and the liquid flow. The heat convection coefficient for each of the flows are also provided.

Table 4.9: Air flow modelling for Design E.

Flow	**Fluid modelling**	**Heat convection coefficient** (h)
Internal air	Forced convection on a flat plate	26.10 W/m^{2}K
Cold air in bottom gap	Forced convection around tubes	83.57 W/m^{2}K
Water + glycol	Forced convection inside tubes	853.43 W/m^{2}K

The output from the CFD simulation shows that this option removes approximately 216 W from the internal air. According to the mathematical model, the heat exchange between the water mixture and the cold air stream in the bottom gap can reach values up to 324 W if it is fully utilized, with higher heat power values the water temperature in the inlet of the cold plate could not be maintained.

If the power supply for the pump is 0.5 W (Ref. [20]), the coefficient of performance of this option becomes 237.8 W/cm^3. The whole system including the pump, cold plate, pipes, water reservoir and sensors and controllers accounts to 0.25 kg and 835 cm^3. Therefore, the heat power density is 0.14.

Apart from the already mentioned features, Table 4.10, summarizes the evaluation of the qualitative features for this design proposal. The liquid loop has to be implemented from scratch and the bottom gap has to be sealed, but there is no need to move any already existing equipment, thus the feasibility is set to *bad*. This, together with the high price of the equipment, also justifies the evaluation of the cost which is set to *very bad*. Robustness is also *very bad* in this case due to the high risk of water leakage and the large number of sensors that can fail, as well as the pump. Moreover, this kind of cooling loop requires maintenance at least once a year, therefore maintenance is *bad*. On the contrary, the reliability of the design is *very good* as it is a well-known technology used among different industries.

Table 4.10: Evaluation of Design E.

Heat Power (Q)	**Weight**	**Volume**	**CoP**	**Heat Power Density**
216 W	0.25 kg	835 cm^3	237.8	0.14 W/cm^3

Reliability of design	**Feasibility**	**Robustness**	**Cost**	**Maintenance**
Very good	*Bad*	*Very bad*	*Very bad*	*Bad*

4.1.4 Peltier Cell

4.1.4.1 Design F. Peltier Cells in Compartment Zero Coupled to the Gable

Peltier cells can be used as cooling elements as they keep a constant temperature on one of the sides, acting like a heat pump and transferring heat to the other side.

The idea is to place Peltier cells along an empty wall or surface in the front section, so that the wall temperature is kept at a constant temperature regardless of the ambient temperature, and the internal air is cooled down as it gets in contact with it.

This design proposes to attach Peltier cells to the side wall of compartment zero, and to add fins in the central area of the wall. The choice is due to the fact that the volumetric air flow is maximum in this region because of the internal fan. Figure 4.6 shows the implementation of the design.

As shown in Figure 4.6, the gable is used as a heat sink in this design. The configuration is exactly the same as explained in Section 4.1.2.1 for Design C.

However, as the area of the Peltier cells is very small, it is necessary to have a thin layer of heat spreader or thermal interface material in the coupling both between it and the gable and between it and the side wall of the compartment zero. This layer has a very high thermal conductivity, allowing the heat from the hot face of the Peltier plate to be distributed throughout the gable to prevent overheating of the gable and subsequent failure. In the cold side of the cell, the function of the heat spreader is to spread the effect of the low temperature of the controlled face of the cell along the whole wall, to cope with the heat transferred by the internal air flowing on the inner side of the wall.

The number of Peltier cells that are added may vary depending on boundary conditions, in this case, two cells are added aiming for a compromise between the input current, and therefore power, that decreases with the number of cells, and the complexity and cost of the system, which are higher as more cells are added. It is worth mentioning that the electrical feed of the cells

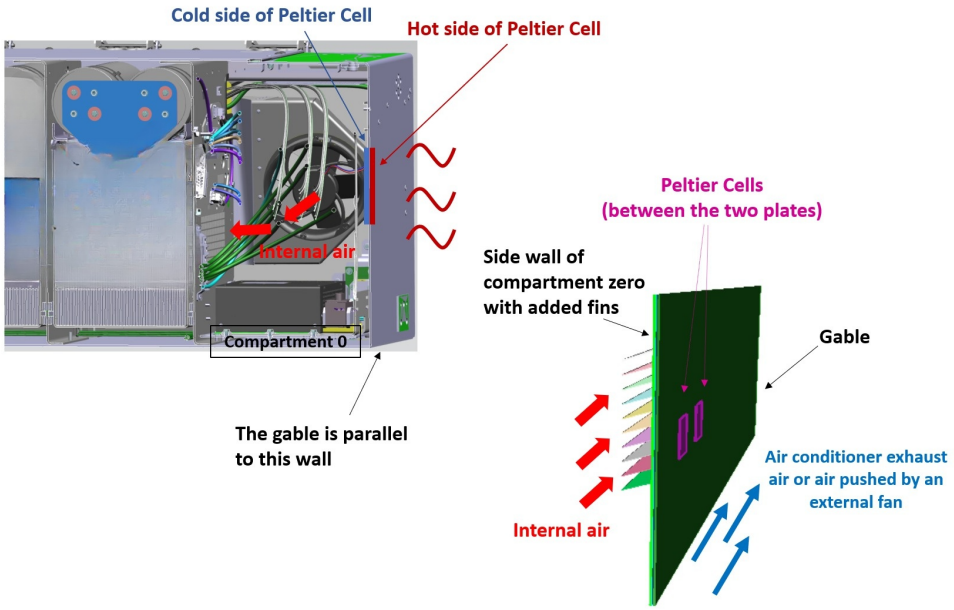

Figure 4.6: Design F. Peltier cells attached to the side wall of compartment zero and to the gable.

must be in parallel as they are controlled through the voltage level. More information regarding Peltier cells selection is provided in Appendix E.

Heat transfer occurs by means of convection of the external air flow and the internal air flow in compartment zero. The model used to study each of the air flows and the obtained heat transfer coefficient are shown in Table 4.11.

Table 4.11: Air flow modelling for Design F.

Air flow	**Fluid modelling**	**Heat convection coefficient** (h)
Internal air	Forced convection on a flat plate	21.05 W/m^{2}K
External air parallel to the gable	Forced convection on a flat plate	22.10 W/m^{2}K

The heat removal from the internal airflow predicted by the CFD simulation is 388 W. According to the mathematical model, the cold air stream is able to dissipate up to 511 W from the gable before its temperature becomes too high for the external air to be able to dissipate more heat. This would cause the overheating of the Peltier cells.

The evaluation of this design on the basis of the selected features is provided in Table 4.12. The considered Peltier cells weigh 0.047 kg and are 2 mm wide (see Appendix E). Therefore, computing them, together with the heat spreader, and the added fins, the total increase in weight and volume of the

design are 4.7 kg and 1 474 cm^3, respectively. The required power supply for the operating point of the Peltier cells is 66 W, therefore the total input power is 132 W, which leads to a coefficient of performance of 2.9. It is important to note that the power supply to the external fan is not considered, as it is not part of the design as such.

Table 4.12: Evaluation of Design F.

Heat Power (Q)	**Weight**	**Volume**	**CoP**	**Heat Power Density**
336 W	2.1 kg	1 390 cm^3	2.55	0.24 W/cm^3

Reliability of design	**Feasibility**	**Robustness**	**Cost**	**Maintenance**
Good	*Very bad*	*Bad*	*Very bad*	*Good*

The use of Peltier elements implies the use of an electric supply with controlled voltage. Therefore, controllers are required for the design to operate as expected. Even though these controllers may fail, their failure rate is not that high to justify the evaluation of the robustness as *bad* in this model. The reason is that a failure of the external heat dissipator, either the external fan or the exhausting air from the air conditioner, is much more probable due to their moving parts, and implies an overheat of the Peltier elements. Thus, the new cooling system stops working immediately. With regards to feasibility, it is set to *very bad* because of the difficulties in coupling the Peltier elements to the side wall and the gable, as it means a mechanical union between both surfaces with the consequent transmission of vibrations and other stresses. In addition, the manufacturing of the external heat dissipator is considered here too. This is closely related to the evaluation of the cost, which is also *very bad* as all the implementation, together with the purchase of the Peltier elements, controllers and the feeding system makes this option expensive. Maintenace is set to *good* because Peltier cells do not require any kind of maintenance as they have no moving parts, thus, only the maintenance for the external system, which is easier to access, is required. Lastly, the reliability of design is also *good*, the only component that may not behave as expected is the heat spreader if the thermal conductivity is lower than that of the simulation.

4.1.4.2 Design G. Front Cover Heat Exchanger Enhanced with Peltier Cells

This design aims to enhance heat transfer capacity in the heat exchanger in the front cover by increasing the temperature difference between the cold and hot mediums. In order to do so, three Peltier cells are added between the hot

and cold plates of the front cover. Similarly to Design F (Section 4.1.4.1), they are coupled through thermal interface materials, or heat spreaders, to the aluminum plates where heat exchange occurs.

The cold side of the Peltier cell is kept at constant temperature thanks to controllers and is used to reduce the temperature of the internal air. The heat in the hot side of the cells is dissipated by using the external air flow entering through the filter in the current front cover.

This model does not imply any change in the air behavior, nor in the hot side nor in the cold side of the current heat exchanger. The modeling and heat transfer coefficients of these air flows are as shown in Table 4.13, and a representatino of how the suggested design can be implemented is shown in Figure 4.7.

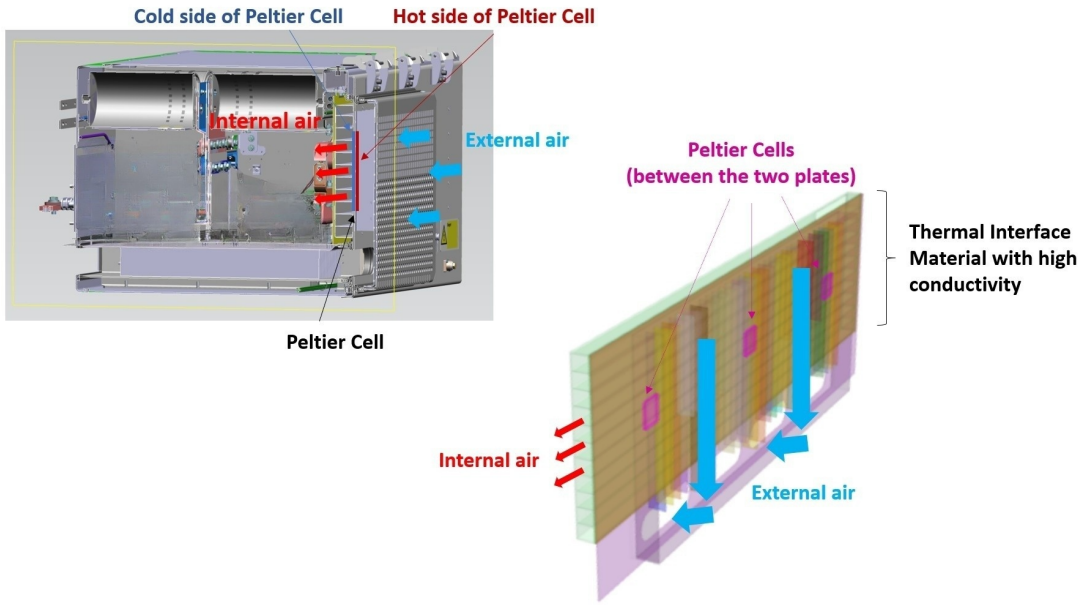

Figure 4.7: Design G. Front cover heat exchanger enhanced with Peltier cells.

Table 4.13: Air flow modeling for design G.

Air flow	**Fluid modelling**	**Heat convection coefficient** (h)
Internal air	Forced convection inside tubes	41.92 W/m^{2}K
External air	Forced convection inside tubes	20.02 W/m^{2}K

As in option F (Section 4.1.4.1), the number of Peltier cells may vary depending on the boundary conditions and constraints. It is always a trade off

between the input current, and therefore power, and the cost and complexity of the system. In this case, the input current plays an important role due to safety reasons. The front cover is removed for maintenance of the front section, thus all electrical connections between the converter and the front cover, *i.e.,* the cables feeding the Peltier cells, must be disconnected each time it is open. Even though, circuit breakers are added in the feeding system of the Peltier cells to guarantee the safety of the workers, if it is open by incident before cutting the power supply, a high current could cause an accident.

The heat transfer increase with this design is approximately 445 W more than that of the original heat exchanger when the temperature of the external air is 60°C, according to the thermal simulation. From the mathematical model, the heat transfer is predicted to be 457 W.

Similarly to all the previous cases, Table 4.14 summarizes the evaluation of the quantitative and qualitative features for this design. The weight computes both the Peltier cells and the thermal interface materials, and the volume the increase in width of the front cover, which is approximately 5 mm. This leads to a heat power density of 0.3 W/cm^3. The input power per cell is 65 W, therefore the total input power is 195 W, resulting in a coefficient of performance of 2.28.

Table 4.14: Evaluation of Design G.

Heat Power (Q)	**Weight**	**Volume**	**CoP**	**Heat Power Density**
445 W	2.35 kg	1 476 cm^3	2.28	0.3 W/cm^3

Reliability of design	**Feasibility**	**Robustness**	**Cost**	**Maintenance**
Good	*Good*	*Very good*	*Bad*	*Very good*

The reliability of the design is *good*, just like in Design F (Section 4.1.4.1), since the only difference that might be encountered is the thermal conductivity of the heat spreader. Moreover, the failure rate of electric controllers for the thermoelectric coolers is very low, and the air flows are kept as in the original design, therefore the robustness is evaluated as *very good*. For the same reason, there is no need for extra maintenance and it is categorized as *very good*. On the other hand, feasibility is set to *good* because this design implies the manufacture of a new front cover, slightly modified, where the electrical connection and the increase in weight act as bottlenecks, but it does not involve any modification in the rest of the front section. This new manufacture and the acquisition of the Peltier cells sets the cost to *bad*.

4.2 Analysis and Comments of the Results

This section analyses and discusses the results presented in Section 4.1, and states the advantages and disadvantages of each of the designs. Moreover, significant comparisons between different designs are carried out.

It is worth mentioning that the heat power shown in the results represents the amount of additional heat that is removed from the internal air flow of the front section and not the total heat that is extracted. For this it would be necessary to take into account the heat removed thanks to the original cooling system, especially the heat transfer through the heat exchanger in the front cover.

This value is only taken into account in Designs A and G, as the simulations calculate the total value of heat exchanged in the front cover, instead of the increase in heat transfer due to the modifications. Thus, to be able to compare these designs with the rest, the difference between the heat transfer with and without the new components under the same boundary conditions is determined and stated as the result.

For the rest of the designs, it can be established that the changes produced in the internal air flow due to the implementation of the new components for the cooling system (changes in temperature or mass flow rate of the internal air flow at the inlet of the heat exchanger) hardly affect the heat flow in a noticeable way. Several CFD simulations with varying conditions regarding the temperature and the mass flow rate of the internal air at the inlet of the front cover are simulated to ensure that this statement is applicable.

4.2.1 Thermal Simulations and Analytical Models

One of the most striking features of the results presented in Section 4.1 is the great difference between the values obtained in the mathematical model and those obtained from the simulations. The latter are the values used to carry out the analysis of the results, the outputs of the analytical or mathematical models being purely indicative with the aim of pre-studying the viability of the designs and, subsequently, validating the results.

In Designs A, B and G, the thermal power values predicted in both models represent the heat extracted from the internal air flow of the front section.

In these cases, the thermal power values extracted from the mathematical models are between 3% and 20% higher than those from their respective thermal simulations. These differences are due to the following factors:

- Air mass flow rates are assumed to be constant in the mathematical

model, whereas in the thermal model mass flow rates change along the flow as a result of the boundary conditions imposed. For instance, in Design A, the external air flow in the first layer enters along the entire length of the plate so that the mass flow rate is higher in the bottom part of the channels. Similarly, the internal air mass flow rate increases as it gets closer to the fan in Designs A and B.

- Directly related to the mass flow rate, in the mathematical model the air velocity is assumed constant and equal to the mean air flow velocity, while in the simulation software, the air velocity is different along the length of the flow.

- The temperature difference between hot and cold mediums is considered constant in the mathematical model, *i.e.,* temperature reduction along the internal air flow is not computed.

- Tubes are considered cylinders based on hydraulic diameter calculation.

- Heat power used to heat up the aluminum of the plates and tubes is not considered in the mathematical model, *i.e.,* aluminum is assumed to be a perfect thermal conductor in those models.

- In Design G, the thermal conductivity of the heat spreader is assumed to be infinitive in the analytical model.

In the other cases, the CFD simulations do measure this same value, and the mathematical model is designed to calculate the maximum capacity of the external or cold air flow to dissipate the absorbed heat. Therefore, in Designs C, D, E and F, the thermal power values obtained by the two methodologies are not expected to converge, as they represent different physical quantities, which explains why the difference between the values of the two types of models is so large.

Such cases are those using the gable and the bottom gap as heat sinks. The reason for calculating the heat dissipation capacity of the cold air flow instead of the heat absorption in the internal air flow is that the latter value varies easily with the number of heat pipes used in Designs C and D, or cold plates in Design E, as well as the area of the heat spreader or the temperature difference in the Peltier cell in Design F. However, in the previous cases (Designs A, B and G), the heat dissipation capacity of the internal air is limited by the mass flow rate of the internal air and is not as easily scalable as in these cases.

The proportional difference between the heat absorbed values according to CFD simulations and the dissipation capacity of the external air according to analytical models varies from 25% to almost 200% in the different designs.

These figures show the scope for increasing heat absorption. For example, in Design C, a margin of 195% can be interpreted as the possibility, if the physical space would allow it, to add a larger number of heat pipes, or heat pipes with larger diameters, without compromising the external heat dissipation capacity in the gable with the external flow conditions considered. Likewise, the smallest margin is obtained for Design F, which indicates that a greater reduction in the temperature of the side wall of compartment zero, linked to a greater need for heat dissipation in the gable, could lead to overheating of the gable and, consequently, the failure of the Peltier cells.

4.2.2 Discussion on the Designs

As explained in Chapter 3, the weighted average method is used to compare the different design proposals. For a more comprehensive analysis, design B is split into two designs in this analysis, one does not consider the extra fan (Design B.1) and the other one considers it (Design B.2).

Table 4.15: Weighted average evaluation.

Design	Heat Power	Weight	Volume	CoP	Heat Power Density	Cost	Maintenance	Robustness	Reliability of Design	Feasibility	WEIGHTED AVERAGE
A	4	1	1	5	1	2	5	5	5	3	**3.24**
B.1	1	2	5	5	5	5	5	5	1	5	**3.53**
B.2	2	2	4	2	3	4	3	3	5	5	**3.34**
C	2	4	4	5	4	1	4	2	2	1	**2.76**
D	3	4	4	5	4	3	5	5	5	3	**4.02**
E	3	5	3	4	3	1	2	1	5	2	**2.94**
F	5	2	2	1	1	1	4	2	3	1	**2.60**
G	5	1	3	1	1	2	5	5	4	4	**3.54**
w_n	0.18	0.09	0.15	0.04	0.06	0.06	0.1	0.1	0.12	0.1	

Table 4.15 shows an overview of the value given to each of the features for all the different designs, as well as the weighted average for each of them.

The weighted average value is out of 5, the higher it is, the better the design is from an overall perspective. It is worth remembering that the weighting coefficients (w_n) are distributed according to the specific requirements for the MITRAC/TC1500^{TM} traction converter.

The evaluation of each feature for each design is represented in Figure 4.8, which is used as a basis for conducting the analyses below.

Finally, the proposed designs, A to G, can be ranked on the basis of the obtained overall score as shown in Table 4.16.

It is easy to see that the worst designs are the ones using the gable as a heat sink, *i.e.,* Designs C and F. Their main features can be seen in Figure 4.9.

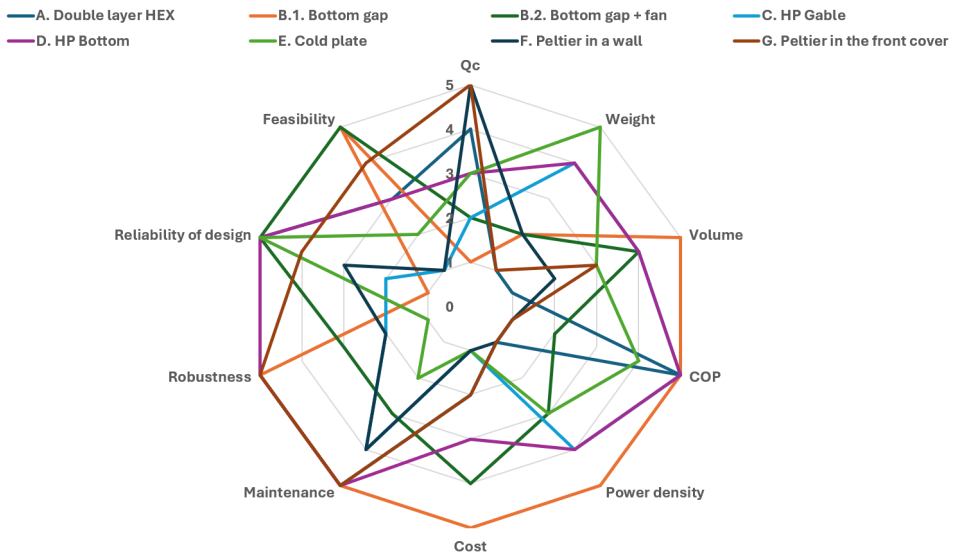

Figure 4.8: Evaluation of each feature for all the suggested designs.

Both of them have in common their bad feasibility, robustness, and cost. Two factors mainly affect here, on the one hand, the mechanical disadvantage of transmitting stress between the gable and the converter box and on the other hand the need to add an external heat dissipation system, as the free convection in the gable is not enough to dissipate even 15% of the heat transmitted by the heat pipes or 6% from the Peltier cells. The main differences between both, apart from the heat power, which is far above average for Design F and below the average for Design C, are the so-called non-monetary costs, which in this case include both physical and energy costs. On the one side, although both technologies isolated are light and small, the volume and weight involved in the heat pipe design is much smaller than that of the Peltier cells. This is because Peltier cells need a heat spreader to operate according to the desired requirements, which results in a considerable increase in volume and weight. Furthermore, the coefficient of performance also makes a difference. This lies in the nature of each technology, both operate by transferring heat from one end to the other, but heat pipes do so passively, by capillary action, whereas Peltier cells require a considerable amount of electric power to operate. These differences compensate for the difference in the heat power extracted from the internal air flow by each of the technologies, which explains why the final score of both designs is so close to each other.

It is worth noting that the two designs at the top of the ranking also involve the use of heat pipes, the first one, and Peltier cells, in the second.

Table 4.16: Ranking of designs based on the weighted average calculation.

Design	Description	Score
D	Heat pipes in the bottom gap	4.02
G	Front cover heat exchanger enhanced with Peltier cells	3.54
B.1	Heat exchanger in the bottom gap without extra fan	3.53
B.2	Heat exchanger in the bottom gap with extra fan	3.34
A	Modified front cover heat exchanger	3.24
E	Cold plate in compartment zero using the bottom gap	2.94
C	Heat pipes coupled to the gable	2.76
F	Peltier cells in compartment zero coupled to the gable	2.60

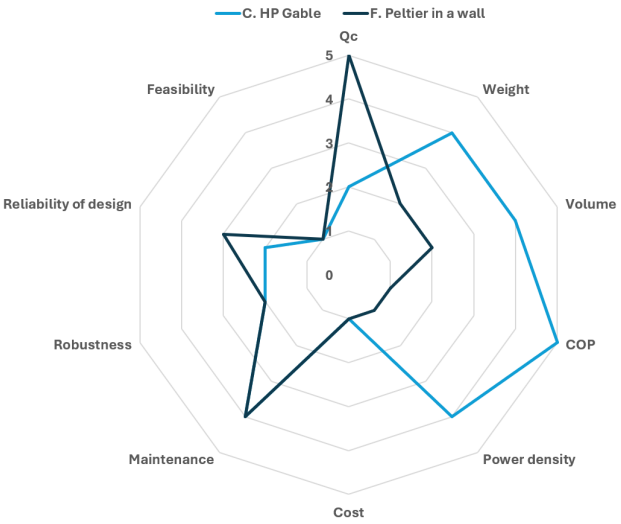

Figure 4.9: Evaluation of each feature for the two worst-ranked designs (Designs C and F).

The design that is positioned first in the ranking is D, the heat pipes in compartment six that use the bottom gap as a heatsink, with a weighted average score of 4.02 points out of 5. Despite the dissimilar heat power value for this option, which is below the average of all the designs studied, 165 versus 228. In the spiderweb graph in Figure 4.8, it can be seen that this design occupies a large surface area, which is also centered and does not have many peaks. It presents very good results in terms of quality and service offered during the operation, *i.e.,* robustness and maintenance, as well as in non-monetary costs, weight, volume, and coefficient of performance. All this, together with the great reliability of the design developed and the moderate values of costs and feasibility explains why this option has turned out to be the best valued among

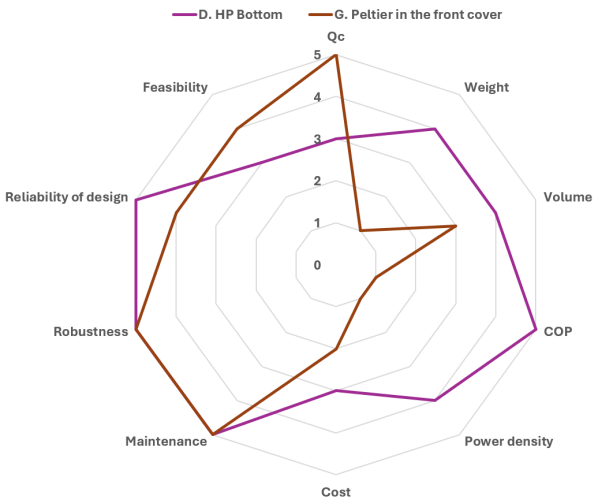

Figure 4.10: Evaluation of each feature for the two best-ranked designs (Designs D and G).

those considered.

When comparing this design with the second best rated, Design G, which consists of enhancing the heat exchanger on the front cover with Peltier cells, a similar effect is observed to what occurred between the C and F designs compared previously. The design involving Peltier cells is shifted to the upper left corner of the graph in Figure 4.10. This demonstrates good service delivery and reliability of the system but at the cost of high costs, both economically and in terms of space, weight, and energy. It is, therefore, an option with good results but expensive in every way.

Although it may seem striking that the same technologies are located at the beginning and at the bottom of Table 4.16, this can be interpreted as the final result depends not only on the cooling technology used but also on how it is implemented in the traction converter. If the two heat pipe designs are compared, as in Figure 4.11, it is evident that one has obtained the highest score and the other the least, since they only have similar characteristics when it comes to weight, volume and coefficient of performance, characteristics intimately linked to the nature of heat pipes. However, it can be seen how the curve of option C is noticeably shrunken in the rest of the graph compared to that of Design D, presenting worse results not only in heat power but also in cost and quality of operation such as feasibility and robustness. The reliability of the design is also much lower due to the need for heat dissipation in the gable. These last features are linked to the overall design and the extra

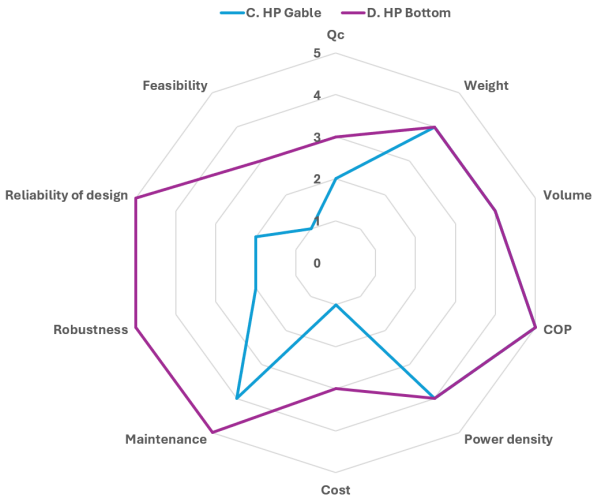

Figure 4.11: Evaluation of each feature for the two designs including Heat Pipes (Designs C and D).

components that need to be added to use the technology, in this case, heat pipes, in the desired way. This explains the difference in the overall result of these two designs.

A similar phenomenon can be seen when comparing the F and G designs, both of which use Peltier cells (see Figure 4.12). In both cases, the heat transfer is high, and they are expensive options with a high consumption of electrical energy, factors closely related to the principle of operation of Peltier cells. The volume and weight also present poor results, which is indirectly linked to the choice of cooling technology, since its use involves having large plates of heat spreaders to avoid overheating. The differences are observed, again, in the left area of the graph, factors related to the general design, especially in robustness and feasibility, where the curve of option F is significantly more retracted than that of design G.

Moving towards the central area of Table 4.16, Design B, which involves the use of the bottom gap as a forced convection heat exchanger, is the simplest option, with intermediate results. In the graph in Figure 4.8, it is on the opposite side of the Peltier cell on the front cover, with modest but low-cost results. Figure 4.13, shows that adding a fan shifts the curve to the center of the graph. Although the overall result is slightly worse, 3.34 points versus 3.53, if this option is implemented, one could consider adding an extra fan to get a better balance of the different factors, without any being excessively low.

If one wants to prioritize weight limitation, the best option would be the

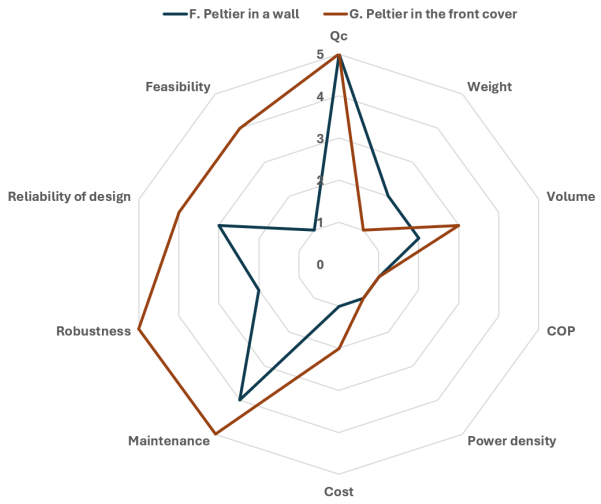

Figure 4.12: Evaluation of each feature for the two designs including Peltier Cells (Designs F and G).

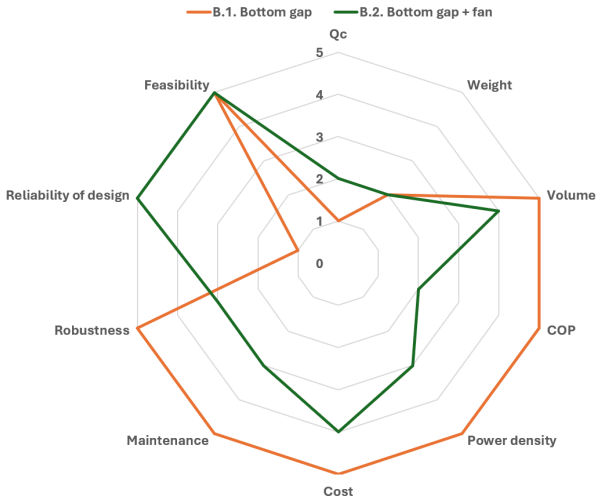

Figure 4.13: Evaluation of each feature for the two options of Design B.

cold plate design (Design E). As seen in Figure 4.14, its curve is in the upper right side, meaning modest results with good conditions when it comes to volume, weight, and power consumption, but complex operation. The most relevant feature of this design is the use of liquid coolant, as opposed to only air, which explains the low score in robustness and maintenance. It is a lightweight design, with which good thermal results are obtained, but which requires attention and monitoring to guarantee a quality service, with a low

failure rate.

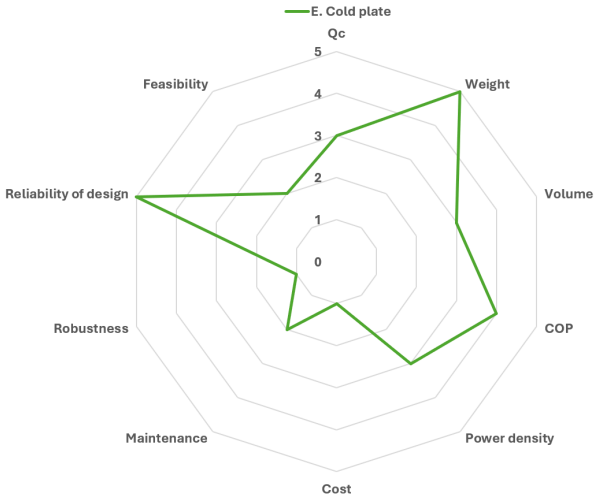

Figure 4.14: Evaluation of each feature for Design E.

Another interesting comparison is that of Designs A and B, both involve using only forced convection as a cooling technology and the total score obtained in both cases is very similar, especially if the case with an extra fan is considered for Design B. If both cases are compared in Figure 4.15, it can be seen that Design B with an extra fan is more stable, in the sense that it does not stand out for better or worse in almost any aspect, maintaining intermediate positions in practically all features. On the other hand, the area covered by the curve of Design A, despite being of practically equal length, is star-shaped and presents many more peaks. This means that it stands out for good in some of the features, such as the coefficient of performance, something that, as already explained in previous comparisons, is expected as it is a passive design, but also for worse in others, especially volume or power density, two features that are strongly related to each other. Other areas in which Design A is clearly better than B with an extra fan are those related to robustness and maintenance. The common factor between these features is that they are direct results of fan use.

On the other hand, the modification of the heat exchanger in the front cover presented in Design A is overshadowed by Design G, which, as already mentioned, tries to improve this heat exchanger using Peltier cells. The graph in Figure 4.16 shows that both designs follow a very similar curve in most of the features studied, with the main difference being the volume occupied. As can be seen, at the same weight, the increase in the width of the front cover

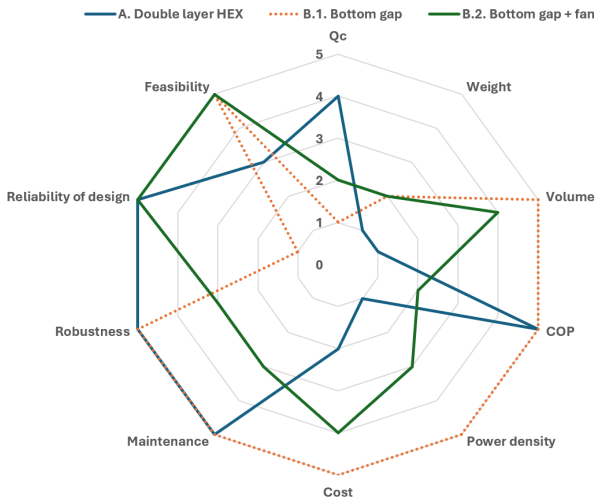

Figure 4.15: Evaluation of each feature for designs with pure forced air cooling (Designs A and B).

in the case of Peltier cells is 12.5% of that of Design A. In addition, as it refers to the width of the front cover, this is a particularly critical feature. If the converter is wider than necessary, it can cause collisions with the rails or other elements of the track system, damaging the converter or even preventing the train from running.

The other fundamental difference is the coefficient of performance, which is logical since the first option implies a passive modification, that is, it does not involve a power supply of any kind, which is its main advantage. The similarity in power density despite the large difference in volume is because the heat power that Design G is able to absorb from the internal air flow is considerably greater than that of option A, specifically 42% more. Therefore, the difference in volume is compensated by this difference in the heat extracted when the thermal power density quotient is calculated.

So far, the value of heat extracted from the internal air has been used as a reference to compare the efficiency of the different designs. However, the heat transfer through the different technologies depends on the temperature gradient between the hot and cold medium. In this project the temperature difference is always 10°C, based on the assumptions stated in the Section 3.3, therefore comparisons within the limits of this project can be made only in terms of heat output.

However, in order to extract the results of this project and compare them with those of similar or future projects, it is necessary to calculate the thermal

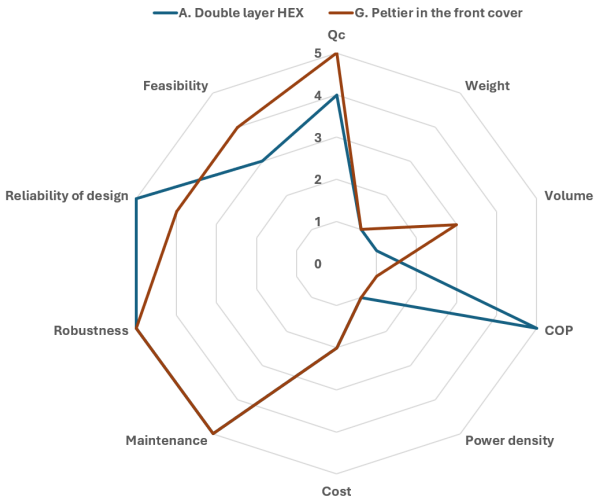

Figure 4.16: Evaluation of each feature for the two designs that modify the front cover (Designs A and G).

resistance of the different options. The thermal resistance represents the heat transfer per degree of temperature difference, based on Equation (3.9).

Table 4.17 shows the thermal resistance of the different designs proposed in Section 4.1.

Table 4.17: Thermal resistance of Designs A to G.

	Design A	**Design B.1**	**Design B.2**	**Design C**	**Design D**	**Design E**	**Design F**	**Design G**
$\mathbf{R_{th}}$	23.7 W/ºC	7.9 W/ºC	13.6 W/ºC	15.8 W/ºC	16.5 W/ºC	21.6 W/ºC	33.6 W/ºC	44.5 W/ºC

Chapter 5

Conclusions and Future Work

In conclusion, the thesis project is focused on the expansion of electric mobility, and specifically railways, towards new horizons and broadening its range of application. The evolution of electric traction has highlighted the need to develop new thermal management systems for critical equipment in this industry, such as traction converters. The increasing demand for more compact and powerful converters in this field underlines the importance of addressing thermal challenges effectively to ensure optimal performance, reliability and safety of electrical systems in various transport systems, such as trains. This project provides a basis for research and development of innovative thermal management solutions in traction converters.

The project addresses the state-of-the-art of electric cooling technologies. Subsequently, some of these technologies are selected to develop up to seven different designs, specifically adapted to the MITRAC/TC1500^{TM} traction converter developed by Alstom. Among the technologies chosen are forced air convection, heat pipes, Peltier cells and cold plates. Each of these technologies is evaluated in terms of its suitability for the particular needs of the traction converter considering up to ten different features.

From the analysis of the results obtained, it can be concluded that the option of using cold plates is not optimal for the converter in question. However, its potential use in converters subject to weight restrictions, for instance in other industries, is highlighted due to its lightweight nature. On the other hand, the modification of the heat exchanger layout is also discarded, as it is evident that this option has critical disadvantages compared to similar alternatives, especially in terms of volume. Although its main advantage lies in its passivity, there are other passive designs with superior results. Finally, the use of the external gable as a heatsink, despite its considerable surface area, is

strongly discouraged because its orientation, perpendicular to the direction of the train speed, results in poor convection and, therefore, poor heat dissipaton capacity.

Therefore, the recommendations after the analysis of the results are as follows. If a more basic and simple solution is sought, the use of the bottom gap with pure forced convection and an extra fan is suggested, even though this may result in worse results in terms of heat removal. However, if an investment in more sophisticated and innovative technologies is contemplated, it is suggested to consider alternatives such as the use of heat pipes or Peltier cells. These technologies offer greater potential to improve heat removal.

The choice between these two options depends on the specific priorities of the project and the market approach that wants to be taken. Unlike Peltier cells, heat pipes are passive so they operate continuously and do not require a control cycle or other expensive system add-ons so they can be added as general equipment across the range of converters. In contrast, Peltier cells require controllers and power supply. In addition, they are an expensive technology, so it is a technology that could be implemented in a specific range of converters for hot climates, paying a higher price for a service with a wider range of operating temperatures.

It is important to note that the implementation of these technologies in the converter can lead to significant variations in the results, which could not be satisfactory if a wrong decision is made. For example, the two worst ranked designs proposed in Chapter 4 are based on heat pipes and Peltier cells. However, alternative designs have been proposed for both technologies that consider different approaches in the application of the same technology, resulting in options that offer improvements in most of the features analyzed. This shows that it is not the technology itself that is insufficient to improve the thermal management system of electric propulsion systems, but that the design of the cooling system as a whole, taking into account the boundary conditions and constraints specific to each system, plays a key role in the search for solutions or improvements. Therefore, it is not enough to know the principle of operation of technologies, but it is also necessary to understand the system in which they are going to be implemented and the associated possibilities or difficulties.

Another relevant conclusion derived from the results is that, while the overall score provides a useful guide, it should not be considered as the sole determining criterion. For instance, in the case of the bottom gap, it is observed that the balance between various factors is more crucial than simply the overall score. This highlights the importance of thoroughly evaluating each

option against a range of criteria, thus ensuring an informed and balanced decision in selecting the best thermal management solution for the traction converter, without compromising any critical feature.

Finally, the possible future lines of work derived from this project offer a wide range of opportunities for the improvement of the thermal management of electric traction converters.

On the one hand, the designs proposed in this document are mainly conceptual and each of them can be optimized and divided into several different models, changing the distribution of components or the way they are attached to the converter box, which would lead to slight variations in the results. An example of this, taking Design D which is the best rated, would be to attach the heat pipes to the base plate of the heat sink. This would improve heat dissipation, but may reduce the efficiency of the heat pipes due to flattening. In this line, one option for future work is to select a specific market case and, based on one of the designs proposed in this study, develop a detailed and definitive design of the additional cooling system tailored to the specific case. This approach involves performing mechanical and stress calculations, carrying out experimental tests, producing a full economic analysis, and performing more detailed thermal simulations to ensure the feasibility and effectiveness of the proposed system.

On the other hand, aiming for a broader project, the second option involves scaling the designs and technologies used in this project to apply them to other electric converters in various fields of industry. It can be analyzed which technologies and lines of implementation are the most suitable for each application, considering the specific boundary conditions and constraints of each case. The third option is to divert the line of research to other forms of cooling the front section. This includes exploring methods such as transferring heat directly from components before dissipation to the internal air, or cooling external air used as a refrigerant before it enters the converter box. These alternatives represent a promising field for research and could offer more efficient and effective solutions in terms of thermal management for electric converters in the future.

References

[1] D. P. O. T. Hiren Lakhani, Jan Agren, "Technical description of traction system," Jan. 2023, Alstom. Internal REF: VARoQ6102IR100R01. [Pages xiii, xv, 2, and 112.]

[2] M. D. B. S. Hiren Lakhani, Benny Redholm, "Traction converter. technical description," *Indian Railways. Rail Coach Factory (RCF)*, Aug. 2023, Alstom. Internal REF: 100622067. [Pages xiii, xvii, 4, 12, and 13.]

[3] Y. Y. Zhihao Zhang, Xuehui Wang, "A review of the state-of-the-art in electronic cooling," 2021, e-Prime. Advances in Electrical Engineering, Electronics and Energy. [Online]. Available: https://doi.org/10.1016/j.prime.2021.100009 [Pages 17, 20, and 21.]

[4] V. H. S.V.J. Narumanchi and D. Bharathan, "Modeling single-phase and boiling liquid jet impingement cooling in power electronics," 2005, National Renewable Energy Laboratory. [Online]. Available: https://www.nrel.gov/docs/fy06osti/38787.pdf [Page 20.]

[5] Q.-W. W. W.-X. C. Yi-Gao Lv, Gao-Peng Zhang, "Thermal management technologies used for high heat flux automobiles and aircraft: A review," 2022, Energies. [Online]. Available: https://doi.org/10.3390/en15218316 [Pages 20 and 21.]

[6] K. C. P. Paik, Vamsee K. Pamula, "Droplet-based hot spot cooling using topless digital microfluidics on a printed circuit board," 2005, THERMINIC. [Online]. Available: https://hal.science/hal-00189486 [Page 21.]

[7] "Calculating the loads for liquid cooling systems," June 2009, Qpedia. [Pages xiii, 22, and 99.]

[8] X. Y. L. Q. S. L.-L. M. Zhao K, Sun X, "Cold plate performance enhancement based on parametric modeling of multiple structures,"

2023, Front. Energy Res. [Online]. Available: 10.3389/fenrg.2022.1087682 [Page 21.]

[9] Wordpress, "Thermoelectric cooler (tec)," 2024. [Online]. Available: https://thermalbook.wordpress.com/thermoelectric-module-tem/ [Pages xiii and 23.]

[10] J. W. K. J. Biela, "Thermoelectric cooling for power density maximisation of power electronic converters," ETH Zurich, Power Electronic Systems Laboratory. [Page 23.]

[11] R. N. H. Shankara Murthy H. M., Niranjana Rai, "Electronic cooling," 2023, Sahyadri College of Engineering and Management, India. [Online]. Available: https://orcid.org/0000-0003-3491-4356 [Pages xiii and 24.]

[12] P. S. G. P. P. R. More Amol, Kore S.S., "A review: Advances in heat sink cooling systems," 2020, International Journal of Innovative Studies in Sciences and Engineering Technology (IJISSET). [Page 24.]

[13] MyHeatSinks, "Heat pipe solutions," 2024. [Online]. Available: https://myheatsinks.com/heat-pipe-solutions/ [Page 25.]

[14] F. Z. E. M. D.-S. V. G. S. Sudhakar, J. A. Weibel, "Electronic cooling," 2019, CTRC Research Publications. Paper 347. [Online]. Available: http://dx.doi.org/doi.org/10.1016/j.ijheatmasstransfer.2019.02.075 [Page 25.]

[15] "Phase change material heat exchanger (pcm hx)." [Online]. Available: https://www.nasa.gov/image-article/phase-change-material-heat-exchanger-pcm-hx/ [Page 26.]

[16] "Pcm products." [Online]. Available: https://www.pcmproducts.net/Encapsulated_PCMs.htm [Page 26.]

[17] A. Benallou, "Heat exchangers for electronic equipment cooling," 2021, IntechOpen. [Page 26.]

[18] U. P. M. Department of Thermodynamics of the School of Industrial Engineering, "Transferencia de calor - formulario oficial, curso 19/20 (rev 2)," 2019, (tr. Heat Transfer. Official formula sheet, year 2019/2020 (rev 2)). [Page 30.]

[19] "Ventiladores para electrónica." [Online]. Available: https://solectroshop.com/es/1473-ventiladores-para-electronica [Pages 45 and 86.]

[20] G. Thomas, "Pump and compressor solutions for oems worldwide, 3003-series." [Online]. Available: www.gd-thomas.com [Page 53.]

[21] A. I. Documentation, "Varoq6067tc15r05 converter 200504." [Page 88.]

[22] Y. A. V. K. R.S. Melnyk, Yu.E. Nikolaenko, "Heatr trasnfer limitations od heat pipes for a cooling systems of electronic components," 2017, National Technical University of Ukraine. [Page 98.]

[23] Celsia, "Heat pipe design guide." [Online]. Available: https://celsiainc.com/heat-sink-blog/heat-pipe-design-guide/ [Pages 105 and 107.]

[24] ——, "Heat pipe calculator." [Online]. Available: https://celsiainc.com/resources/calculators/heat-pipe-calculator/ [Page 105.]

[25] A. C. Technologies, "Heat pipe calculator." [Online]. Available: https://www.1-act.com/resources/tools/heat-pipe-calculator/ [Pages 105 and 106.]

[26] BodyCorp, "Heat pipe calculator." [Online]. Available: https://calculator.boydcorp.com/ [Page 105.]

[27] L. T. Systems, "Etx15-24-f2-5252-ta-w6." [Online]. Available: https://lairdthermal.com/products/thermoelectric-cooler-modules/peltier-hitemp-etx-series/ETX15-24-F2-5252-TA-W6 [Page 108.]

Appendix A

Air Flow Characterisation

This appendix exposes and justifies the selection of inputs values to characterize the air flows for the different designs in the simulations. These values applies to both mathematical and CFD simulations.

A.1 Design A. Modified Front Cover Heat Exchanger

As shown in Figure 4.1, there are three different air paths considered in the design: Internal air flows inside the tubes, and external air flows around the tubes and along the first layer, parallel to the filter.

- Internal air
  - The volume flow rate is set to 0.105 m^3/s, as it is the total flow going through the internal fan.
  - The flow is modelled as a flow going inside tubes. The hydraulic diameter of teh flow inside the tubes is 0.034 m, based on Equation (3.1).

  The measured average speed of the flow and the obtained values for the Reynolds and Prandtl numbers after applying Equations (3.2) and (3.3) are summarized in Table A.1.

v	Re	Pr
9.7 m/s	$1.67 \cdot 10^4$	0.708

Table A.1: Parameters for internal air flow in Design A.

The expression for calculating the Nusselt number for the application of forced convection inside tubes with the flow characteristics obtained is Equation (A.1).

$$Nu = 0.023 \cdot Re^{0.8} \cdot Pr^{0.3} \quad \text{s.t.} \begin{cases} T_f - T_w < 60^o C \\ 0.7 < Pr < 160 \\ 10^4 < Re < 10^6 \\ 2300 < Re < 10^6 \text{ (less precision*)} \end{cases} \tag{A.1}$$

where T_f and T_w are the air and the wall temperatures respectively.

The Nusselt number and the heat convection coefficient obtained from Equation (3.4) are shown in Table A.2.

Nu	***h***
49.56	41.92 W/m^{2}K

Table A.2: Heat convection coefficient for internal air flow in Design A.

- External air around tubes
  - The volume flow rate is set to 0.051 m^3/s, being 15% of the total air flow going through the external fan.
  - The flow is modelled as a flow around tubes, with an hydraulic diameter of 0.034 m, based on Equation (3.1).

The measured average speed of the flow and the obtained values for the Reynolds and Prandtl numbers after applying Equations (3.2) and (3.3) are summarized in Table A.3.

v	***Re***	***Pr***
2.5 m/s	$4.45 \cdot 10^3$	0.727

Table A.3: Parameters for the external air flow around tubes in Design A.

The expression for calculating the Nusselt number for the application of forced convection around staggered tube bundles with the flow

characteristics obtained is Equation (A.2).

$$Nu = 0.76 \cdot (0.35 \cdot Re^{0.6} \cdot Pr^{0.36}) \quad \text{s.t.} \begin{cases} S_V/S_H < 2 \\ N_L = 2 \\ Pr_{\text{inf}} \approx Pr_w \\ 0.7 < Pr < 500 \\ 10^3 < Re < 2 \cdot 10^5 \end{cases} \tag{A.2}$$

where S_V and S_H are the vertical and horizontal distances between tubes respectively (see Figure A.1), N_L the number of bundles, and Pr_{inf} and Pr_w the Prandtl number for the air far away and close to the tubes surface respectively.

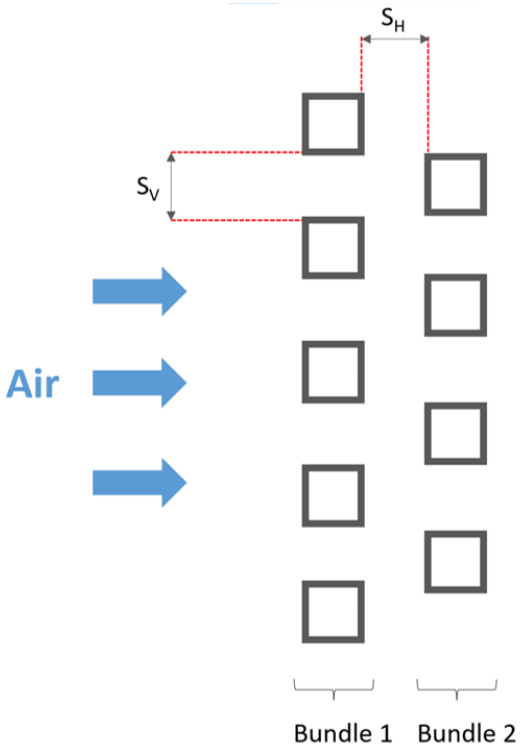

Figure A.1: Definition of parameters in Equation (A.2).

The Nusselt number and the heat convection coefficient obtained from Equation (3.4) are shown in Table A.4.

- External air in the path parallel to the filter (first layer in Figure 4.1)

Nu	***h***
36.64	28.85 W/m^{2}K

Table A.4: Heat convection coefficient for external air flow around tubes in Design A.

- The volume flow rate is set to 0.287 m^3/s, being 85% of the total external air flow.
- The flow is modelled as a flow inside tubes, with an hydraulic diameter of 0.040 m, based on Equation (3.1).

The measured average speed of the flow and the obtained values for the Reynolds and Prandtl numbers after applying Equations (3.2) and (3.3) are summarized in Table A.5.

v	***Re***	***Pr***
3.6 m/s	$7.9 \cdot 10^3$	0.727

Table A.5: Parameters for the external air flow parallel to the filter in Design A.

The expression for calculating the Nusselt number for the appliacion of forced convection inside tubes with the flow characteristics obtained is Equation (A.3).

$$Nu = 0.023 \cdot Re^{0.8} \cdot Pr^{0.4} \quad \text{s.t.} \begin{cases} T_w - T_f < 60^o C \\ 0.7 < Pr < 160 \\ 10^4 < Re < 10^6 \\ 2300 < Re < 10^6 \text{ (less precision } ^\dagger) \end{cases} \tag{A.3}$$

The Nusselt number and the heat convection coefficient obtained from Equation (3.4) are shown in Table A.6.

Nu	***h***
26.57	18.05 W/m^{2}K

Table A.6: Heat convection coefficient for external air flow parallel to the filter in Design A.

A.2 Design B. Heat Exchanger in the Bottom Gap

As in the previous case, there are three air flows involved in the heat exchange in this design: The internal air flow flowing through the bottom gap, the external air flow flowing through the heat sink and the ambient air flow underneath the base plate. Each of this air flows can be easily identified in Figure 4.2.

- Internal air
  - The volume flow rate if the extra fan IS NOT considered is set to 0.021 m^3/s, being 20% of the total hot air flow.
  - The volume flow rate if the extra fan IS considered is set to 0.037 m^3/s, being 20% of the total hot air flow with increased velocity due to the effect of the fan.
  - The flow is modelled as a flow going inside tubes, with an hydraulic diameter of 0.029 m, based on Equation 3.1. This value decreases if the distance between two consecutive fins decreases.

  The measured average speed of the flow and the obtained values for the Reynolds and Prandtl numbers after applying Equations (3.3) and (3.2) are summarized in Table A.7.

	v	***Re***	***Pr***
No extra fan	1.7 m/s	$2.55 \cdot 10^3$	0.708
Extra Fan	3.4 m/s	$9.27 \cdot 10^3$	0.708

Table A.7: Parameters for internal air flow in Design B.

  The expression for calculating the Nusselt number for the application of forced convection inside tubes with the flow characteristics obtained is Equation A.1.

  The Nusselt number and the heat convection coefficient obtained from Equation 3.4 are shown in Table A.8.

- External air flowing in the heat sink
  - The volume flow rate is set to 0.338 m^3/s, as it is the total air flow going through the fan in the middle section.

	Nu	***h***
No extra fan	11.01	10.83 W/m^{2}K
Extra Fan	30.92	16.50 W/m^{2}K

Table A.8: Heat convection coefficient for internal air flow in Design B.

  - The flow is modelled as a flow inside tubes. The hydraulic diameter is 0.07 m, based on Equation 3.1.

The measured average speed of the flow and the obtained values for the Reynolds and Prandtl numbers after applying Equations (3.3) and (3.2) are summarized in Table A.9. The values do not vary if the extra fan is considered as it does not affect this air flow.

v	***Re***	***Pr***
13 m/s	$5.22 \cdot 10^4$	0.727

Table A.9: Parameters for the external air flow in the heat sink in Design B.

The expression for calculating the Nusselt number for the application of forced convection inside tubes with the flow characteristics obtained is Equation A.3.

The Nusselt number and the heat convection coefficient obtained from Equation 3.4 are shown in Table A.10.

Nu	***h***
124.20	43.33 W/m^{2}K

Table A.10: Heat convection coefficient for external air flow in the heat sink in Design B.

- Ambient air underneath the base plate
  - The average speed of the external air flow is set to 7 m/s in this case, being approximately 20% of the train speed (see Table A.11).
  - The flow is modelled as a flow parallel to a flat plate, with a characteristic length of 1 m.

The obtained values for the Reynolds and Prandtl numbers after applying Equations (3.3) and (3.2) are summarized in Table A.11. The values do not vary with the extra fan, as it does not affect this air flow.

v_{train}	v_{air}	Re	Pr
125 km/h (34.7 m/s)	$0.2 \cdot v_{train}$ (m/s)	$3.9 \cdot 10^5$	0.727

Table A.11: Parameters for the ambient air flow underneath the base plate in Design B.

The expression for calculating the Nusselt number for the application of forced convection on flat plates with mixed flow and the obtained characteristics is Equation A.4.

$$Nu = (0.037 \cdot Re^{0.8} - 872) \cdot Pr^{1/3} \quad \text{s.t.} \begin{cases} 0.6 < Pr < 60 \\ 5 \cdot 10^5 < Re < 10^7 \end{cases} \tag{A.4}$$

The Nusselt number and the heat convection coefficient obtained from Equation 3.4 are shown in Table A.12.

Nu	h
203.76	5.50 W/m^{2}K

Table A.12: Heat convection coefficient for ambient air flow underneath the base plate in Design B.

A.3 Design C. Heat Pipes Coupled to the Gable

As shown in Figure 4.3, there are two air flows that play a role in this case: The internal air flow around the evaporator side of the heat pipes, and the external air flow parallel to the gable.

- Internal air
  - The volume flow rate is set to 0.021 m^3/s, being 20% of the total air flow going through the internal fan.
  - The flow is modelled as a flow going around tubes, where the characteristic length is the diameter of the heat pipes, 4.76 mm.

The measured average speed of the flow and the obtained values for the Reynolds and Prandtl numbers after applying Equations (3.3) and (3.2) are summarized in Table A.13.

v	*Re*	*Pr*
1.5 m/s	358.04	0.708

Table A.13: Parameters for internal air flow in Design C.

The expression for calculating the Nusselt number for the application of forced convection around tubes with the flow characteristics obtained is Equation A.5.

$$Nu = 0.9 \cdot 0.51 \cdot Re^{0.5} \cdot Pr^{0.37} \quad \text{s.t.} \begin{cases} N_L = 8 \\ Pr \leq 10 \\ 40 < Re < 1000 \end{cases} \tag{A.5}$$

where N_L represents the number of tubes, in this case, of heat pipes.

The Nusselt number and the heat convection coefficient obtained from Equation 3.4 are shown in Table A.14.

Nu	*h*
7.64	46.56 W/m^{2}K

Table A.14: Heat convection coefficient for internal air flow in Design C.

- External air parallel to the gable
  - The average speed of the flow is 8 m/s. The air speed is predicted by the CFD simulation as a function of the fan curve. A generic fan curved based on the information given in Ref. [19] is used. *
  - The flow is modelled as a flow on a flat plate, with a characteristic length of 2.314 m.

  The measured average speed of the flow and the obtained values for the Reynolds and Prandtl numbers after applying Equations (3.3) and (3.2) are summarized in Table A.15.

  The expression for calculating the Nusselt number for the application of forced convection on a flat plate with pure turbulent flow and the flow

*The use of any other fan curve would lead to a different average value of the air speed. However, unless the air speed is very low, this does not influence the results because the heat dissipation capacity of the gabble with a fan is much higher than the heat transferred by the heat pipes.

Re	***Pr***
$1.191 \cdot 10^6$	0.685

Table A.15: Parameters for the external air flow parallel to the gable in Design C.

characteristics obtained is Equation A.6.

$$Nu = 0.0296 \cdot Re^{0.8} \cdot Pr^{1/3} \quad \text{s.t.} \begin{cases} 0.6 < Pr < 60 \\ 5 \cdot 10^5 < Re < 10^7 \end{cases} \tag{A.6}$$

The Nusselt number and the heat convection coefficient obtained from Equation 3.4 are shown in Table A.16.

Nu	***h***
$1.894 \cdot 10^3$	22.10 W/m^{2}K

Table A.16: Heat convection coefficient for external air flow parallel to the gable in Design C.

A.4 Design D. Heat Pipes in the Bottom Gap

As shown in Figure 4.4, there are two air flows that play a role in this case: The internal air flow around the evaporator side of the heat pipes, and the cold air that flows in the bottom gap. In this case the cold air is assumed to be a spillage from the main heat sink, but it can also be external air that is drawn into the bottom gap through the base plate.

- Internal air
  - The volume flow rate is set to 0.105 m^3/s, being the total internal air flow.
  - The flow is modelled as a flow going around tubes, where the characteristic length is the diameter of the heat pipes, 8 mm.

  The measured average speed of the flow and the obtained values for the Reynolds and Prandtl numbers after applying Equations (3.3) and (3.2) are summarized in Table A.17.

v	Re	Pr
3.9 m/s	$1.604 \cdot 10^3$	0.708

Table A.17: Parameters for internal air flow in Design D.

The expression for calculating the Nusselt number for the application of forced convection around tubes with the flow characteristics obtained is Equation A.5.

The Nusselt number and the heat convection coefficient obtained from Equation 3.4 are shown in Table A.18.

Nu	h
16.18	58.65 W/m^{2}K

Table A.18: Heat convection coefficient for internal air flow in Design D.

- Cold air in the bottom gap
  - From Ref. [21], the air speed in the heat sink is 13.5 m/s, therefore the total air volume flow is 0.8 m^3/s, *i.e.,* approximately 0.2 m^3/s underneath each compartment (compartments one, two, three and four). The air volume flow rate is set to 0.02 m^3/s, being the 10% of the total air flow going below one of the compartments.
  - The flow is modelled as a flow around tubes, with the characteristic length being the diameter of the heat pipes, 8 mm.

The measured average speed of the flow and the obtained values for the Reynolds and Prandtl numbers after applying Equations (3.3) and (3.2) are summarized in Table A.19.

v	Re	Pr
8.1 m/s	$3.563 \cdot 10^3$	0.727

Table A.19: Parameters for the cold air in the bottom gap flow in Design D.

The expression for calculating the Nusselt number for the application of forced convection on a flat plate with pure turbulent flow and the flow

characteristics obtained is Equation A.7.

$$Nu = 0.9 \cdot 0.26 \cdot Re^{0.6} \cdot Pr^{0.37} \quad \text{s.t.} \begin{cases} N_L = 10 \\ Pr \leq 10 \\ 1000 < Re < 2 \cdot 10^5 \end{cases} \tag{A.7}$$

The Nusselt number and the heat convection coefficient obtained from Equation 3.4 are shown in Table A.20.

Nu	***h***
28.13	94.93 W/m^{2}K

Table A.20: Heat convection coefficient for cold air flow in the bottom gap in Design D.

A.5 Design E. Cold Plate in Compartment Zero Using the Bottom Gap

As shown in Figure 4.5, there are two air flows and one water flow that play a role in this case: The internal air flow inside compartment zero, the cold air that flows in the bottom gap and the mixture of water with glycol that flows inside the pipes. As well as in Design D, the cold air flowing in the bottom gap is assumed to be a spillage from the main heat sink, but it can also be external air that is drawn into the bottom gap through the base plate.

- Internal air
  - The volume flow rate is set to 0.105 m^3/s, being the total internal air flow.
  - The flow is modelled as a flow parallel to a flat plate, with a characteristic length of 0.13 m.

  The measured average speed of the flow and the obtained values for the Reynolds and Prandtl numbers after applying Equations (3.3) and (3.2) are summarized in Table A.21.

  The expression for calculating the Nusselt number for the application of forced convection on a flat plate with laminar flow and the characteristics

v	*Re*	*Pr*
5.8 m/s	$3.911 \cdot 10^4$	0.708

Table A.21: Parameters for internal air flow in Design E.

obtained is Equation A.8.

$$Nu = 0.664 \cdot Re^{0.5} \cdot Pr^{1/3} \quad \text{s.t.} \begin{cases} 0.6 < Pr < 50 \\ Re < 5 \cdot 10^5 \end{cases} \tag{A.8}$$

The Nusselt number and the heat convection coefficient obtained from Equation 3.4 are shown in Table A.22.

Nu	*h*
117.02	26.10 W/m^{2}K

Table A.22: Heat convection coefficient for internal air flow in Design E.

- Cold air in the bottom gap
  - The air volume flow rate is set to 0.02 m^3/s. This choice is explained in section A.4.
  - The flow is modelled as a flow around tubes, with the characteristic length being the diameter of the pipes, 11 mm.

The measured average speed of the flow and the obtained values for the Reynolds and Prandtl numbers after applying Equations (3.3) and (3.2) are summarized in Table A.23.

v	*Re*	*Pr*
8.1 m/s	$4.90 \cdot 10^3$	0.727

Table A.23: Parameters for the cold air flow in the bottom gap in Design E.

The expression for calculating the Nusselt number for the application of forced convection around tubes with the flow characteristics obtained is Equation A.7.

The Nusselt number and the heat convection coefficient obtained from Equation 3.4 are shown in Table A.24.

Nu	***h***
34.05	83.57 W/m^{2}K

Table A.24: Heat convection coefficient for cold air flow in the bottom gap in Design E.

- Water flow
  - The volume flow rate is the nominal flow of the selected cold plate, 4 L/min, it is $6.67 \cdot 10^{-5}$ m^3/s.
  - The flow is modelled as a flow inside tubes, with the characteristic length being the diameter of the pipes, 11 mm.
  - The properties of the fluid considered are the ones in Table A.25.

Temperature (T)	**Density** (ρ)	**Specific Heat** (c_p)	**Viscosity** (μ)	**Thermal conductivity** (k)
64ºC	983.21 kg/m^3	4186 J/kgºC	10^{-3} kg/ms	0.058 W/mºC

Table A.25: Properties for water flow in Design E.

The measured average speed of the flow and the obtained values for the Reynolds and Prandtl numbers after applying Equations (3.3) and (3.2) are summarized in Table A.26.

v	***Re***	***Pr***
0.7 m/s	$5.288 \cdot 10^3$	72.17

Table A.26: Parameters for water flow in Design E.

The expression for calculating the Nusselt number for the application of forced convection inside tubes with the characteristics obtained is Equation A.3.

The Nusselt number and the heat convection coefficient obtained from Equation 3.4 are shown in Table A.27.

A.6 Design F. Peltier Cells in Compartment Zero Coupled to the Gable

As shown in Figure 4.6, there are two air flows involved in the heat transfer in this case: The internal air flow inside compartment zero, and the external air

Nu	***h***
161.86	853.43 W/m^{2}K

Table A.27: Heat convection coefficient for the water flow in Design E.

that flows parallel to the gable.

- Internal air
  - The volume flow rate is set to 0.105 m^3/s, being the total internal air flow.
  - The flow is modelled as a flow parallel to a flat plate, with a characteristic length of 0.2 m, which is the length of the thermal interface material added between the Peltier cell and the wall. It is also the length of the fins coupled to the wall.

  The measured average speed of the flow and the obtained values for the Reynolds and Prandtl numbers after applying Equations (3.3) and (3.2) are summarized in Table A.28.

v	***Re***	***Pr***
5.7 m/s	$6.018 \cdot 10^4$	0.708

Table A.28: Parameters for internal air flow in Design F.

The expression for calculating the Nusselt number for the application of forced convection on a flat plate with laminar flow and the characteristics obtained is Equation A.8.

The Nusselt number and the heat convection coefficient obtained from Equation 3.4 are shown in Table A.22.

Nu	***h***
145.15	21.05 W/m^{2}K

Table A.29: Heat convection coefficient for internal air flow in Design F.

- External air flowing parallel to the gable

  This flow is exactly the same as the one modelled in Design C (section A.3).

A.7 Design G. Front Cover Heat Exchanger Enhanced with Peltier Cells

The schematics of this design is shown in Figure 4.7. There are two air flows that affect the heat transfer capacity in this case: The internal air flow inside the tubes, and the external air flowing parallel to the filter.

- Internal air

  The modelling of this air flow is exactly the same as the model for the internal air flow in Design A (Section A.1).

- External air flowing parallel to the filter.

  - The volume flow rate is set to 0.338 m^3/s, the total air flow going through the external fan.
  - The flow is modelled as a flow inside tubes. The hydraulic diameter of 0.040 m, based on Equation 3.1.

  The measured average speed of the flow and the obtained values for the Reynolds and Prandtl numbers after applying Equations (3.3) and (3.2) are summarized in Table A.30.

v	Re	Pr
4 m/s	$9 \cdot 10^3$	0.727

Table A.30: Parameters for the external air flow in Design G.

The expression for calculating the Nusselt number for the application of forced convection inside tubes with the flow characteristics obtained is Equation A.3.

The Nusselt number and the heat convection coefficient obtained from Equation 3.4 are shown in Table A.31.

Nu	h
29.48	20.02 W/m^2K

Table A.31: Heat convection coefficient for external air flow in Design G.

Appendix B

Heat Power Calculation for Mathematical Models

This section provides the input values used to calculate the cooling capacity of each of the proposed designs by applying the methodology exposed in Section 3.2.

The input values complies with the heat convection coefficient (h), the area of the contact wall or surface (A), and the temperature difference between the convective air flow and the contact surface ($T_{air} - T_{surface}$ if internal air flow is used, or $T_{surface} - T_{air}$ for external air flow).

B.1 Design A. Modified Front Cover Heat Exchanger

The input parameters for Design B can be seen in Table B.1, and are justified below.

- Heat convection coefficient (h): The heat transfer modelled in this case is the forced convection of the internal air flowing inside the tubes. Therefore, the heat convection coefficient to be used is that of the internal air flow calculated in Appendix A.

  The choice of the internal air flow as the limiting one is because it is not scalable, *i.e.,* the amount of internal air going through the front cover cannot be modified by adding extra components.

- Area of the contact surface (A): It computes the side of the tubes that are in contact with the cold air. As seen in Figure 4.1, four of the tubes

are in contact with the air flow in the first layer by one of their faces ($A_{first} = 0.127m^2$). In addition, the rest of the faces of the tubes that are in contact with the air flowing around them are nine vertical faces and seventeen horizontal faces ($A_{around} = 1m^2$).

$$A = A_{first} + A_{around} \tag{B.1}$$

- Temperature difference ($T_{air} - T_{surface}$): The internal air is at 70ºC, as it is the worst-case scenario. The aluminum in the external plate is assumed to be at the same temperature than the external air flowing parallel to the filter in the first layer, 60ºC, whereas the temperature of the aluminum in the other walls of the tubes is assumed to be slightly higher due to the lower airflow, 62ºC. These assumptions are validated based on the simulation results.

  Therefore the average temperature difference is estimated as follows.

$$T_{air} - T_{surface} = \frac{(70-60)\cdot A_{first} + (70-62)\cdot A_{around}}{A_{first} + A_{around}} = 8.22^oC \tag{B.2}$$

h	A	$T_{air} - T_{surface}$
41.92 W/m^2 ºC	1.13 m^2	8.22 ºC

Table B.1: Input parameters for mathematical calculation of the cooling capacity of Design A.

It is important to remember that the value of heat transferred in this case includes all the heat that is extracted through the front converter and, therefore, the performance improvement of the cooling system should not take into account this value in full but the difference between this value and that transferred under the same temperature conditions if the design were unchanged.

B.2 Design B. Heat Exchanger in the Bottom Gap

The input parameters for Design B can be seen in Table B.2, and are justified below.

- Heat convection coefficient (h): The heat transfer modelled in this case is the forced convection of the internal air flowing inside the bottom channel on the surrounding aluminum plates. Therefore, the heat convection coefficient to be used is that of the internal air flow calculated in Appendix A.

  The choice of the internal air flow as the limiting one is because it is not scalable, *i.e.,* the amount of internal air going through the channel cannot be modified by adding extra components.

- Area of the contact surface (A): It computes the bottom plate of the converter box and the base plate of the heat sink ($A_{plate} = 0.391m^2$, per plate), and the fins ($A_{fin} = 0.026m^2$, per fin). For the case of study, ten fins are considered:

$$A = 2 \cdot A_{plate} + 10 \cdot A_{fin} \tag{B.3}$$

- Temperature difference ($T_{air} - T_{surface}$): The internal air is at 70ºC, as it is the worst-case scenario. The aluminum of both the upper and the bottom plate is assumed to be at the same temperature than the external air, 60ºC, whereas the temperature of the aluminum in the fins is assumed to be at the mean temperature between cold and hot mediums, 65ºC. Therefore the average temperature difference is estimated as follows.

$$T_{air} - T_{surface} = \frac{(70-60) \cdot 2A_{plate} + (70-65) \cdot 10A_{fin}}{2 \cdot A_{plate} + 10 \cdot A_{fin}} = 8.78^oC \tag{B.4}$$

	h	A	$T_{air} - T_{surface}$
No extra fan	10.83 W/m^2 ºC	1.035 m^2	8.78 ºC
Extra fan	16.50 W/m^2 ºC	1.035 m^2	8.78 ºC

Table B.2: Input parameters for mathematical calculation of the cooling capacity of Design B.

B.3 Design C. Heat Pipes Coupled to the Gable

The input parameters for Design C can be seen in Table B.3, and are justified below.

- Heat convection coefficient (h): The heat transfer modelled in this case is the forced convection of the external air flowing parallel to the gable. Therefore, the heat convection coefficient to be used is that of the external air flow calculated in Appendix A.

  The choice of the external air flow as the limiting one is because it is a scalable technology, *i.e.,* the amount of heat that can be removed from the internal air increases if more heat pipes are added. Thus, heat pipes can be added as long as there is heat dissipation capacity in the gable.

- Area of the contact surface (A): It computes both the external and internal area of the gable, as the external air pushed by the external fan is assumed to be flowing in both sides.

- Temperature difference ($T_{surface} - T_{air}$): The gable is assumed to be at 68ºC, as it is the worst-case scenario based on CFD simulation results. and the external air at the reference temperature of 60ºC.

h	A	$T_{surface} - T_{air}$
22.10 W/m^2 ºC	2.31 m^2	8 ºC

Table B.3: Input parameters for mathematical calculation of the cooling capacity of Design C.

B.4 Design D. Heat Pipes in the Bottom Gap

The input parameters for Design D can be seen in Table B.4, and are justified below.

- Heat convection coefficient (h): The heat transfer modelled in this case is the forced convection of the cold air flowing inside the bottom gap.

Therefore, the heat convection coefficient to be used is that of the cold air flow calculated in Appendix A.

The choice of the cold air flow as the limiting one is because it is a scalable technology, *i.e.,* the amount of heat that can be removed from the internal air increases if more heat pipes are added. Thus, heat pipes can be added as long as there is heat dissipation capacity in the bottom gap.

- Area of the contact surface (A): It computes the external area of the condenser ends of the heat pipes ($A_{cond} = 0.028m^2$, per heat pipe), and the fins in the condenser end ($A_{fin} = 0.019m^2$, per fin). In the case of study, there are ten heat pipes and each of them has ten fins in the condenser end, thus

$$A = 10(\cdot A_{cond} + 10 \cdot A_{fin}) \tag{B.5}$$

- Temperature difference ($T_{surface} - T_{air}$): The cold air coming from the heat sink is assumed to be at the same temperature than the external air, 60ºC, and the external surface of the heat pipes at 70ºC, as it is the temperature of the internal air and, based on documentation in Ref. [22], the external temperature of the heat pipes is almost constant all along its external surface. Fins are assumed to have very high thermal conductivity, therefore their temperature is that of the heat pipes.

h	A	$T_{surface} - T_{air}$
94.93 W/m^2 ºC	0.124 m^2	10 ºC

Table B.4: Input parameters for mathematical calculation of the cooling capacity of Design D.

B.5 Design E. Cold Plate in Compartment Zero Using the Bottom Gap

The input parameters for Design E can be seen in Table B.5, and are justified below.

- Heat convection coefficient (h): The heat transfer modelled in this case is the forced convection of the water flowing inside the pipes and the

cold air in the bottom gap around them. Therefore, the heat convection coefficient to be used is that of the water flow calculated in Appendix A.

The choice of the water flow as the limiting one is because it is a scalable technology, *i.e.,* the amount of heat that can be removed from the internal air increases if a bigger cold plate or more than one is used. However, if that heat is not rejected from the water flow, the temperature of the water at the inlet of the cold plate would be higher and the cooling capacity would be reduced.

- Area of the contact surface (A): It computes the external area of the water pipes sitting in the bottom gap. The diameter of the pipe is 0.011 m^2, and the total length taking into accounts the loops goes up to 2.75 m.

- Temperature difference ($T_{water} - T_{surface}$): The water flowing in the pipes is assumed to be at 64°C, based on Ref. [7] given that the cold air coming from the heat sink is at the same temperature than the external air, 60°C, and the internal air in compartment zero at 70°C. The surface of the water pipes are assumed to have high thermal conductivity, therefore its temperature is set to 60°C.

h	A	$T_{water} - T_{surface}$
853.43 W/m^2 °C	0.095 m^2	4 °C

Table B.5: Input parameters for mathematical calculation of the cooling capacity of Design E.

B.6 Design F. Peltier Cells in Compartment Zero Coupled to the Gable

The input parameters for Design F can be seen in Table B.6, and are justified below.

- Heat convection coefficient (h): The heat transfer modelled in this case is the forced convection of the external air flowing parallel to the gable. Therefore, the heat convection coefficient to be used is that of the external air flow calculated in Appendix A.

The choice of the external air flow as the limiting one is because it is a scalable technology, *i.e.,* the amount of heat that can be removed from the internal air increases if a higher voltage is fed to the Peltier cells to induce a higher temperature difference between the hot and cold sides of the cell. Thus, heat can be pumped towards the gable as long as there is enough heat dissipation capacity.

- Area of the contact surface (A): It computes both the external and internal area of the gable, as the external air pushed by the external fan is assumed to be flowing in both sides.
- Temperature difference ($T_{surface} - T_{air}$): The gable is assumed to be at 70ºC, as it is the temperature of the hot side of the Peltier cells for the case of study.

h	A	$T_{surface} - T_{air}$
22.01 W/m^2 ºC	2.31 m^2	10 ºC

Table B.6: Input parameters for mathematical calculation of the cooling capacity of Design F.

B.7 Design G. Front Cover Heat Exchanger Enhanced with Peltier Cells

The input parameters for Design G can be seen in Table B.7, and are justified below.

- Heat convection coefficient (h): The heat transfer modelled in this case is the forced convection of the internal air flowing inside the tubes. Therefore, the heat convection coefficient to be used is that of the internal air flow calculated in Appendix A.

  The choice of the internal air flow as the limiting one is because it is not scalable, *i.e.,* the amount of internal air going through the front cover cannot be modified by adding extra components.

- Area of the contact surface (A): It computes the vertical plate that separates the internal and external air flows ($A_{plate} = 0.44m^2$). In addition, the plates perpendicular to it that make up the top and bottom

sides of the tubes are counted as fins. However, only half of their area is counted, since in the area closest to the inside of the front section the temperature of the aluminium is almost equal to that of the internal air, so it does not count as a heat exchange area ($A_{tubes} = 0.59m^2$).

$$A = A_{plate} + A_{tubes} \tag{B.6}$$

- Temperature difference ($T_{air} - T_{surface}$): The internal air is at 70ºC, as it is the worst-case scenario. The aluminum of the plate is assumed to be at the control temperature of the Peltier cell, 50ºC, whereas the temperature of the aluminum that forms the tubes is assumed to be at the mean temperature between the Peltier cell and internal air flow, 60ºC. Therefore the average temperature difference is estimated as follows.

$$T_{air} - T_{surface} = \frac{(70-50)\cdot A_{plate} + (70-60)\cdot A_{tubes}}{A_{plate} + A_{tubes}} = 14.29^oC \tag{B.7}$$

h	A	$T_{air} - T_{surface}$
35.70 W/m^2 ºC	1.03 m^2	14.29 ºC

Table B.7: Input parameters for mathematical calculation of the cooling capacity of Design G.

It is important to remember that the value of heat transferred in this case includes all the heat that is extracted through the front converter and, therefore, the performance improvement of the cooling system should not take into account this value in full but the difference between this value and that transferred under the same temperature conditions if the design were unchanged.

Appendix C

Heat Power Calculation for CFD Models

This section provides the input values used to calculate the cooling capacity of each of the proposed designs by applying the methodology exposed in Section 3.3, specifically in Equation (3.7).

The input values complies with the mass flow rate ($\dot{m}$), the specific heat of the internal air ($c_p = 1009 J/kg^oC$), and the temperature difference in the internal air before and after going through the add-on cooling system (ΔT).

Values for the mass flow rate are calculated by multiplying the volume flow rate ($\dot{v}$) justified in Appendix A and the air density ($\rho = 1.029 m^3/kg$), *i.e.*, $\dot{m} = \dot{v}\rho$. The values for the temperature difference are those predicted in the simulation software StarCMM+®. These values are summarized in Table C.1.

	$\dot{v}$	Δ ***T***
Design A	0.105 m^3/s	2.2 °C
Design B.1	0.021 m^3/s	3.6 °C
Design B.2	0.037 m^3/s	3.6 °C
Design C	0.021 m^3/s	7.2 °C
Design D	0.105 m^3/s	1.5 °C
Design E	0.105 m^3/s	1.2 °C
Design F	0.105 m^3/s	3.1 °C
Design G	0.105 m^3/s	4.1 °C

Table C.1: Input parameters for heat transfer calculation based on the simulation results.

It is important to note that for Designs A and G the heat transfer through the original front cover heat exchanger must be subtracted in order to obtain

the heat transfer capacity for the new design, as it is simulated as a whole. For the rest of the designs the change in heat transfer through the heat exchanger in the front cover does not vary substantially despite the add-on components, and can be rejected based on the simulation results.

Appendix D

Selection and Dimensioning of Heat Pipes

This section outlines the dimensioning of the heat pipes used in Designs C and D. The parameters to be selected in each case are the length of both condenser and evaporator sides, the diameter of the pipe, the bending angle, and the height after flattening, if required.

The heat transfer capacity of each heat pipe, and the required temperature difference between both ends are derived from these parameters together with the orientation of the pipe, *i.e.,* the relative height between the condenser and the evaporator.

In general terms, the heat transfer capacity of heat pipes increases with the diameter and decreases with the total length. Moreover, if the condenser end is above the evaporator the heat transfer capacity is higher owing to the gravity effect, which pushes water back to the evaporator. The contrary effect occurs when the heat pipe is upside down, *i.e.,* the condenser is below the evaporator. Finally, bending and flattening the heat pipes decrease their capacity, as it reduces the capillary effect.

D.1 Design C. Heat Pipes Coupled to the Gable

Design C complies with heat pipes bent 90º, where the condenser is above the evaporator. Moreover, heat pipes are flattened in order to make it easier to couple them with the gable.

The limiting parameter in this design is the height of the pipe after

flattening, as it needs to fit the narrow gap between the converter box and the gable, which is 4 mm. The condenser end must be coupled to the gable but not in touch with the converter box since this would reduce the temperature difference between the two ends of the heat pipe, reducing its heat transfer capacity.

To satisfy this limiting condition, the height of the pipe once it is flattened is chosen to be 2 mm. The diameter of the heat pipe is derived from this constraint according to Table *Flat Heat Pipe Power Carrying Capacity* in Ref. [23], it is 4.76 mm.

Finally, the length of the condenser and the evaporator ends are chosen to be 330 and 180 mm respectively. This selection aims to maximize the power capacity subject to the available space for each of the ends. The available space is the height of the gable, 590 mm, for the condenser part, and the empty room in the bottom part of compartment six, 220 mm, for the evaporator side. The total length of the heat pipe is 550 mm. The online calculators in Ref. [24], Ref. [25], and Ref. [26] are used to determine these parameters.

When it comes to the heat transfer capacity, the average output of the online calculators from Ref. [24], Ref. [25], and Ref. [26] with the selected dimensions is 34.8 W. However, this value does not take into account the bending angle and the flattening of the heat pipes. According to Ref. [23], the heat transfer capacity of the heat pipe is reduced by 15% owing to the flattening up to 2 mm, and 5% due to the bending angle (2.5% for each 45°). Therefore, the heat transfer capacity is estimated to be 28 W.

This value represents the maximum heat power that can be transferred through the heat pipe. Nevertheless, this value is subject to a minimum temperature difference between the two ends, if the temperature difference between the hot and cold ends of the heat pipe is lower, the heat transfer will be lower as well.

The required temperature difference for this specific design of heat pipes is calculated by linear interpolation from the available data in Ref. [23] for 4 and 5 mm diameter heat pipes, keeping the rest of the parameters the same (see Table D.1).

	ϕ **= 4mm**	ϕ **= 5 mm**	ϕ **= 4.76 mm**
Min. Δ **T**	9.5°C	5.2 °C	6.2°C

Table D.1: Minimum temperature difference between the condenser and evaporator ends of the heat pipes to operate at maximum capacity in Design C (ΔT is the temperature difference between condenser and evaporator ends, and ϕ the diameter of the heat pipes).

Therefore, the minimum temperature difference between the cold and hot mediums must be at least 6.2ºC for the heat pipes to operate at maximum capacity. The heat transfer in the heat pipe decreases linearly with the temperature difference, according to Equation D.1.

$$Q_{hp} = \frac{kA\Delta T}{L_{eff}} \tag{D.1}$$

Where Q_{hp} is the heat power transferred by the heat pipe, k the thermal conductivity of the heat pipe, A the cross-sectional area of the pipe, L_{eff} the effective length of the heat pipe defined in Equation (D.2), and ΔT the temperature difference between the cold and hot ends.

$$L_{eff} = \frac{L_{ev} + L_{cond}}{2} + L_{ad} \tag{D.2}$$

L_{ev}, L_{cond}, L_{ad} being the lengths of the evaporator end, condenser end, and the adiabatic region, respectively.

The thermal conductivity of the heat pipe in the specific case of application is calculated based on Equation (D.1), it is $65.6 \cdot 10^3$ W/mºC.

D.2 Design D. Heat Pipes in the Bottom Gap

In Design D the most important factor concerning the heat pipes is that they act against gravity, *i.e.,* the evaporator is above the condenser. This affects the heat transfer capacity significantly, so the selection of all the parameters is subject to compensate for this effect.

First, the height against gravity is minimised by selecting a shorter heat pipe compared to the previous design (Appendix D.1), and the bending angle is chosen to be 70°, being the minimum possible to avoid collision with other components sitting in compartment six. The condenser and evaporator are 110 and 65 mm long, respectively. As in Appendix D.1, these parameters are calculated with the aim of maximising the heat transfer capacity based on the results of the online calculator in Ref. [25]. The resulting total length of the heat pipe is 296 mm.

As for the diameter, heat pipes with a diameter of 8 mm are used, selected as a trade off between a larger diameter and therefore a greater heat transfer capacity and a smaller diameter and therefore a better placement and adaptation to the available space. In this case the decision is also based on the outputs from the online calculator in Ref. [25].

The capacity of the heat pipe according to Ref. [25] is 27.45 W, taking into

consideration the height against gravity. The capacity loss due to the bending angle is 3.75%, thus the heat transfer capacity of the heat pipe is estimated to be 26 W.

The temperature difference required for the heat pipe to operate at full output is 3°C. This value is calculated based on the data provided in Ref. [23] for heat pipes with similar sizing, but with capacity of 18 and 36 W. Similarly to Appendix D.1, linear interpolation is used (see Table D.2).

	$\mathbf{Q_{max}}$ **= 18 W**	**Q = 36 W**	$\mathbf{Q_{max}}$ **= 26 W**
Min. Δ **T**	2.8°C	5.6 °C	3°C

Table D.2: Minimum temperature difference between the condenser and evaporator ends of the heat pipes to operate at maximum capacity in Design D (ΔT is the temperature difference between condenser and evaporator ends, and Q_{max} the heat transfer capacity of the heat pipe).

Heat transfer decreases if the temperature difference decreases according to Equation D.1.

The thermal conductivity of the heat pipes for this specific case of application is $13.6 \cdot 10^3$ W/m°C, based on Equation (D.1).

Appendix E

Selection and Dimensioning of Peltier Cells

The selection and calculations relating to Peltier cells in this document are based on the data provided in Ref. [27].

The same Peltier cell model can be used to transfer more or less heat from one side to the other depending on the voltage level at which it is supplied. The greater the difference in voltage between the hot and cold sides, the more heat is transferred between the two sides. In addition, several cells can be connected in parallel to obtain higher heat transfer with lower electric power supply. Therefore the same result can be obtained with many different configurations.

The model provided in Ref. [27] is used to size the Peltier cells in Designs F and G. In all cases a difference of 20°C is applied between the hot and cold sides of the cell.

E.1 Design F. Peltier Cells in Compartment Zero Coupled to the Gable

The results in Section 4.1.4.1 show that the cooling capacity of Design F is 336 W. Therefore, the sizing of the Peltier cells for this design is rounded up to 400 W.

The number of Peltier cells to be used determines the heat dissipation capacity external to the converter, as well as the electrical power to be supplied for the cells to operate at the desired point. Figure E.1 shows how each of these factors evolves, as well as the coefficient of performance, as the number of cells used to extract 400 W from the internal airflow increases.

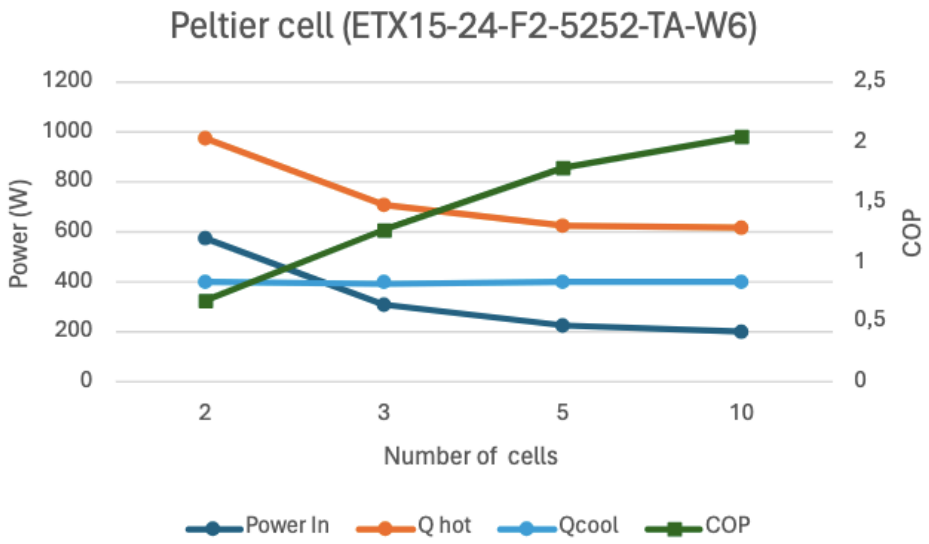

Figure E.1: Impact of the number of Peltier cells on the need of heat dissipation and on the electric power supply to remove 400 W of heat (*Power In* represents the electric power supply to the cells, Q_{hot} the required heat dissipation in the external side, Q_{cool} the total cooling capacity, and *COP* the coefficient of performance of the whole system).

As justified in Section 4.1.4.1, only two cells are used in Design F, which is the worst-case scenario as the external heat dissipation requirement is maximum.

E.2 Design G. Front Cover Heat Exchanger Enhanced with Peltier Cells

The results in Section 4.1.4.2 show that in Design G the cooling power is 445 W. Therefore the sizing is designed for 500 W. As in the previous case, the design requirements vary according to the number of cells used, as shown in Figure E.2.

In this case, the number of cells used in the Design G is three, being the worst case-scenario feasible, as it is justified in Section 4.1.4.2. The case of two cell is discarded in this case due to the huge requirement concerning external heat dissipation, which would compromise the air temperature entering the main heat sink and, therefore, the cooling of the IGBTs.

It can be seen that the design requirements, *i.e.,* external heat dissipation

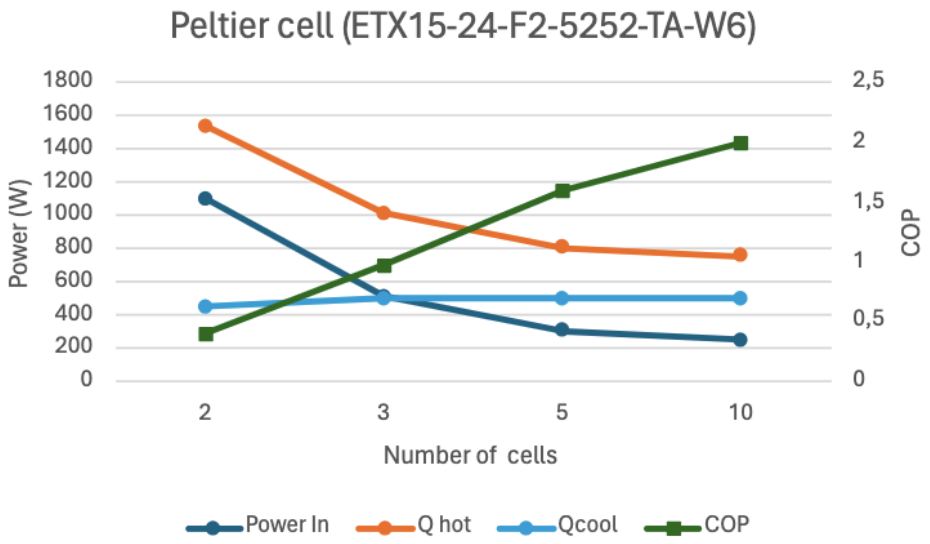

Figure E.2: Impact of the number of Peltier cells on the need of heat dissipation and on the electric power supply to remove 500 W of heat (*Power In* represents the electric power supply to the cells, Q_{hot} the required heat dissipation in the external side, Q_{cool} the total cooling capacity, and *COP* the coefficient of performance of the whole system).

and electric power supply, become less demanding as the number of cells used increases. However, a larger number of cells implies a more complex system, as well as a considerable increase in the cost of implementation and procurement.

Appendix F

Resumen en Español

F.1 Introducción

F.1.1 Tracción Eléctrica Ferroviaria

El proyecto utiliza uno de los diseños de Alstom para explicar las bases de la tracción eléctrica en la industria ferroviaria. El sistema elegido se muestra en la Figura F.1, en él, el 50% de los ejes de cada coche están motorizados.

El proceso para transformar la corriente eléctrica que circula por la catenaria a energía mecánica para mover el tren consta de varios pasos. En primer lugar, la tensión de corriente alterna de la línea de alimentación se absorbe a través del pantógrafo y se reduce a un nivel menor de tensión en el transformador principal. Todo ello compone el denominado sistema de alta tensión. A continuación, esta corriente alimenta el sistema de propulsión. Este consta de un convertidor de tracción eléctrica que a su vez se compone de un convertidor de línea y un convertidor de motor. El convertidor de línea transforma la tensión alterna procedente del lado de baja tensión del transformador principal en corriente continua con valores de tensión controlables y, posteriormente, esta corriente continua se utiliza como alimentación del convertidor de motor, que es un inversor trifásico que la transforma en corriente alterna trifásica con valores de módulo y frecuencia controlables. Finalmente, la corriente trifásica alimenta los motores eléctricos que transforman la energía eléctrica en mecánica y mueven el tren.

Además de los sistemas de alta tensión y de propulsión, en la Figura F.1 se muestra el sistema auxiliar. Este último se utiliza para la alimentación eléctrica de otros sistemas, como por ejemplo los sistemas de iluminación en el interior del tren.

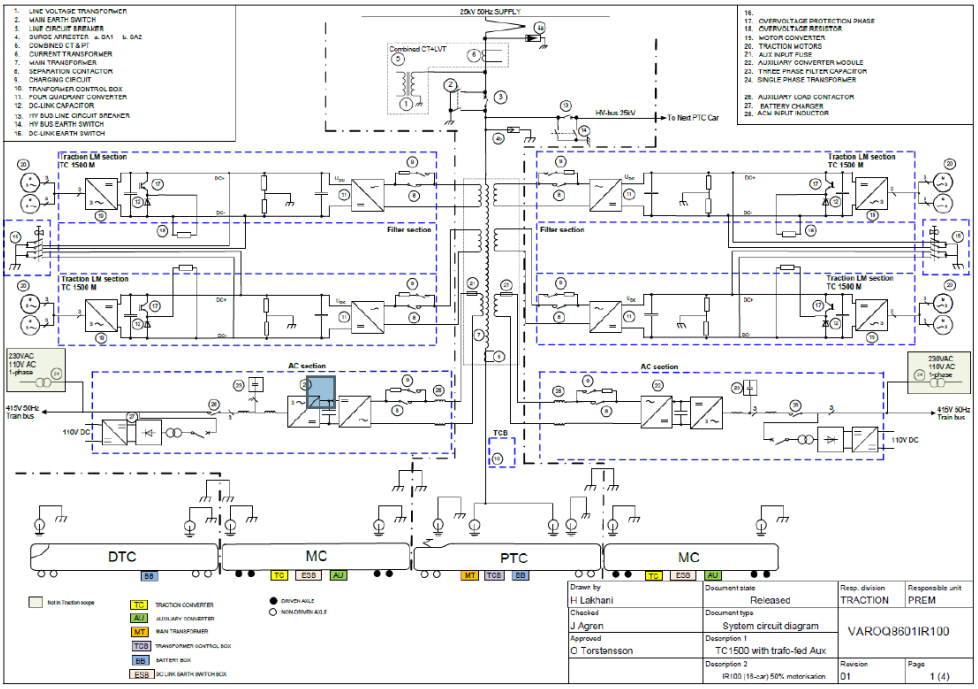

Figure F.1: Vista general del circuito principal de una unidad de cuatro coches para motorización del 50%. **Fuente:** [1].

F.1.2 Formulación del Problema

El proyecto aborda la gestión térmica de los convertidores de tracción eléctrica en la industria ferroviaria, especialmente la refrigeración del aire interno en la sección delantera del convertidor MITRAC/TC1500^{TM} desarrollado por Alstom.

El convertidor en cuestión está compuesto por tres secciones o partes diferenciadas, dos secciones delanteras o secciones del convertidor, y una sección central entre ellas. A diferencia de la sección central, las secciones delanteras están cerradas y aisladas del aire exterior.

La refrigeración del aire encerrado en el interior de las secciones delanteras se realiza de forma indirecta a través de las paredes del convertidor, así como a través de un intercambiador de calor que utiliza aire externo a temperatura ambiente como fluido refrigerante y que está localizado en una de las paredes laterales del convertidor, denominada de ahora en adelante cubierta delantera en este documento.

Para garantizar el correcto funcionamiento de los componentes que se alojan en la sección delantera, la temperatura del aire interno de dicha sección no debe superar los 70^{o}C. Por tanto, en zonas con climas cálidos, donde la

temperatura del aire exterior utilizado como refrigerante puede llegar a ser extremadamente elevada, en torno a 50ºC o 60ºC, la diferencia de temperatura entre los medios frío y caliente en el intercambiador de calor es muy pequeña, lo que limita la transferencia de calor entre ambos y, por tanto, la temperatura del aire interior aumenta.

Por otro lado, el desarrollo de convertidores eléctricos tiende al diseño de convertidores de mayor potencia y más compactos, lo que aumenta las pérdidas en forma de calor y reduce el volumen de aire disponible para absorberlas. Esto pone en evidencia la necesidad de desarrollar nuevos sistemas de gestión térmica con mayor capacidad de transmisión de calor para los convertidores de tracción.

F.2 Información Previa

F.2.1 Convertidor MITRAC/TC1500^{TM}

El convertidor MITRAC/TC1500 es un convertidor de tracción destinado a la industria ferroviaria diseñado y desarrollado por Alstom. Se trata de un convertidor flexible y escalable, que puede encontrarse en diferentes tamaños y con diferentes configuraciones según la aplicación.

Como ya se ha explicado en la sección F.1.2, la caja del convertidor está dividida en tres secciones, dos secciones delanteras o secciones principales y una sección central entre ellas. Este proyecto se centra en las secciones delanteras.

En el modelo de convertidor utilizado a lo largo de este proyecto, el MITRAC/TC1500^{TM} de tamaño medio y con una configuración LMM (un covertidor de línea y dos convertidores de motor), la sección delantera está compuesta por seis compartimentos diferentes, denominados compartimentos cero, uno, dos, tres, cuatro y seis. El compartimento cero aloja los sistemas de control y el ventilador interno, responsable de marcar el flujo de aire en el interior de esta sección, los compartimentos dos al cuatro los componentes activos y componentes electrónicos que forman los convertidores de línea y motores, así como los sistemas de protección por sobretensión. Finalmente, en el compartimento seis se encuentran otros componentes como sensores de corriente e interruptores.

El sistema de refrigeración de la sección delantera se muestra en la Figura F.2. Por un lado, la mayor parte del calor de las IGBTs se derivan al disipador de calor principal, localizado bajo ellas, evitando así el sobrecaliento del aire interno, que solo absorbe las pérdidas de calor del resto de los componentes,

sensiblemente menores que las de las IGBTs. Por otro lado, el ventilador mueve el aire interno desde el compartimento cero hacia el compartimento seis, fluyendo alrededor de los diferentes componentes activos y absorbiendo las pérdidas en forma de calor de los mismos. Una vez el flujo de aire interno llega al compartimento seis, la temperatura del mismo es máxima, ya que se han absorbido todas las pérdidas de los componentes activos, y retorna al compartimento cero a través del intercambiador de calor situado en la cubierta delantera. El ventilador externo, situado en la sección central, absorbe un flujo de aire procedente del exterior que, una vez filtrado, atraviesa primero el intercambiador de calor de la cubierta delantera absorbiendo el calor del aire flujo de aire interno y, posteriormente, el disipador de calor principal para disipar las pérdidas de las IGBTs hasta, finalmente, llegar a la sección central antes de ser expulsado al exterior de nuevo.

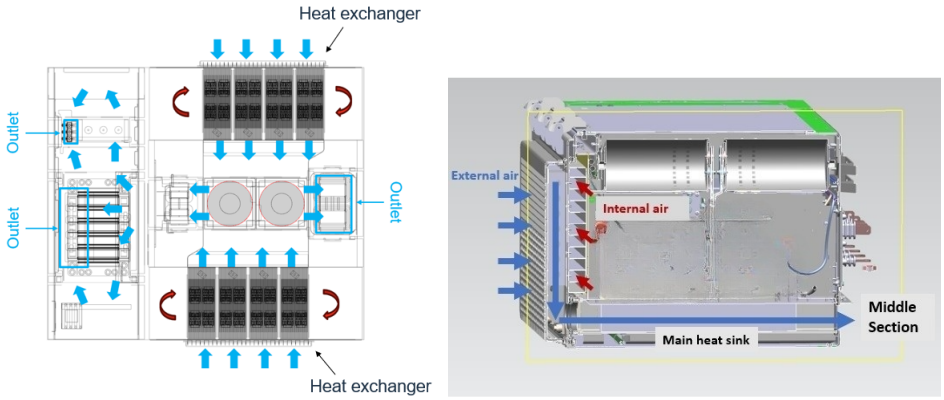

(a) Vista superior (b) Vista lateral

Figure F.2: Esquema del sistema de refrigeración del MITRAC/TC1500^{TM}. **Fuente:** Adaptado de la documentación interna de Alstom.

Pese a que la mayor parte del calor del aire interno se disipa durante su paso por el intercambiador de calor, es importante mencionar que este no es el único punto de transferencia de calor entre el aire interno y el ambiente exterior, ya que toda la carcasa del convertidor también permite la disipación térmica, transmitiendo parte del calor del aire interno al exterior por convección natural. Las pérdidas totales que han de ser absorbidas por el flujo de aire interno ascienden a, aproximadamente, 613 W.

En lo que respecta a las restricciones físicas o mecánicas presentes a la hora de añadir nuevos componentes al sistema de refrigeración, cabe destacar la necesidad de mantener la sección delantera cerrada y aislada del aire exterior, minimizar la relocalización de objetos o componentes ya existentes, añadir el

menor peso y volumen posible, especialmente si se trata de modificaciones en la cubierta delantera, así como mantener una baja caída de presión en el flujo de aire externo y limitar la velocidad de entrada del mismo para evitar la obstrucción del filtro.

Finalmente, existen algunos espacios y superficies que pueden resultar de utilidad a la hora de implementar nuevos componentes o tecnologías de refrigeración. Por un lado, los compartimentos cero y seis son especialmente interesantes ya que en el primero la velocidad del aire es máxima y en el segundo lo es su temperatura y ambas propiedades aumentan la capacidad de transferencia de calor. Por otro lado, existe un hueco inferior situado entre el disipador de calor principal y la placa base del convertidor que no se utiliza y podría ser aprovechado. Finalmente, existe una superficie metálica lateral paralela a las paredes laterales del convertidor que cuenta con una gran superficie vacía y en contacto con el aire exterior que se puede utilizar como elemento de disipación.

F.2.2 Estado del Arte de la Refrigeración Eléctrica y Electrónica

La refrigeración de componentes electrónicos es un requisito crucial, no solo en la industria ferroviaria, sino también en todas aquellas industrias que utilizan componentes eléctricos y electrónicos de alta potencia. Además, los requisitos de refrigeración son cada vez más estrictos debido a la tendencia de utilizar equipos compactos, con alta densidad de potencia, que utilizan valores de corriente eléctrica cada vez más elevados, resultando en mayores pérdidas.

Existen numerosas tecnologías, tanto convencionales como emergentes, cuyo objetivo es o bien disipar el calor producido por los componentes electrónicos o transferirlo a otros lugares o superficies del equipo en cuestión donde su disipación sea más sencilla. Estas tecnologías se pueden clasificar en tecnologías de contacto directo e indirecto, dependiendo de si el medio refrigerante toca al componente que se quiere refrigerar o no, y en tecnologías activas y pasivas. Las tecnologías activas son aquellas que necesitan suministro de energía para funcionar, mientras que las pasivas las que no.

Entre las categorías activas estudiadas en este proyecto se encuentran la convección de aire forzado, el sistema de aire acondicionado con compresor tradicional, la refrigeración por pulverización (*spray cooling*), la refrigeración por chorro de impacto (*jet impingement cooling*), la electrodeposición de gotas (*droplet electrowetting*), las placas frías (*cold plate*) y los refrigeradores termoeléctricos o células de Peltier (*Peltier cells*). Por su parte, en las

tecnologías pasivas cabe destacar las correas térmicas (*termal straps*), los tubos de calor (*heat pipes*), el termosifón (*thermosiphon*), las cámaras de vapor (*vapor chamber*), los materiales de cambio de fase (*phase changing materials*) y los microcanales (*microchannels*).

De todas ellas las que mejor se adaptan a las condiciones de operación del convertidor ferroviario son la convección forzada de aire, los refrigeradores termoeléctricos, la placa fría y los tubos de calor.

La convección forzada de aire consiste en forzar el flujo de aire alrededor del componente que se quiere enfriar. La temperatura del flujo de aire debe ser menor a la del componente que se quiere enfriar, de forma que la potencia térmica disipada por pérdidas en el componente electrónico sea absorbida por el flujo de aire.

Los refrigeradores termoeléctricos o células de Peltier consisten en dos placas de metal separadas por semiconductores de tipo P y N. Las placas están conectadas eléctricamente en serie y térmicamente en paralelo, de forma que cuando se aplica tensión a una de las dos, empieza a circular corriente eléctrica a través de los semiconductores, induciendo una diferencia de temperatura entre las dos placas debido al efecto Peltier. Por tanto, actúan como bombas de calor, transfiriendo calor de un lado de la célula al otro, es decir de una placa a la otra.

Las placas frías, por su parte, son placas metálicas de muy baja resistencia térmica por las que circulan tuberías con un fluido refrigerante, normalmente una mezcla de agua y glicol. Forman parte de circuitos cerrados de refrigeración por líquido, de forma que el líquido absorbe el calor del componente a su paso por la placa fría y lo transporta a otro intercambiador de calor en contacto con el aire exterior, donde el calor se transfiere del líquido al ambiente. A continuación, el líquido enfriado se bombea de nuevo a la placa fría para repetir el ciclo.

Un tubo de calor es un conductor térmico muy eficiente que transfiere calor a temperatura casi constante. Consiste en un tubo metálico sellado con una estructura mallada en su superficie interior. En su interior hay una pequeña cantidad de fluido de trabajo, generalmente agua, en su punto de saturación. En un lado del tubo – el llamado evaporador – se absorbe calor que provoca la evaporación del fluido. El resultado es un aumento de presión que empuja el vapor hacia el otro lado del tubo, el condensador. Este lado puede acoplarse a un disipador de calor para que el calor se transfiera al entorno exterior y el fluido se condense. A continuación, el líquido es absorbido por la estructura mallada, que lo bombea de nuevo hacia el lado del evaporador por capilaridad. El resultado es un funcionamiento continuo.

F.3 Metodología

Las diferentes tecnologías seleccionadas se evalúan en base a simulaciones matemáticas con modelos analíticos y a simulaciones térmicas basadas en programas de dinámica de fluidos computacional aplicadas al convertidor MITRAC/TC1500™.

El primer paso consiste en desarrollar diseños para implementar la tecnología de refrigeración seleccionada en el convertidor tratando de maximizar la capacidad de transferencia de calor y cumplir con las restricciones estipuladas en la Sección F.2.1. Para estudiar la viabilidad de cada uno de los diseños se estiman los parámetros que afectan a la transmisión de calor, especialmente las características de los flujos de aire implicados y sus coeficientes de convección. Estos últimos se calculan en base a modelos analíticos. Todos estos parámetros se utilizan posteriormente para desarrollar un modelo de simulación matemática en MATLAB®. Este modelo tiene por objeto estimar la capacidad de disipación térmica de los nuevos componentes añadidos al sistema de refrigeración. En caso de resultados satisfactorios, se procede al modelado y simulación del diseño en el programa StarCMM+®, basado en dinámica de fluidos computacional y que utiliza los mismos parámetros y datos de entrada que se calcularon para el modelo matemático. Los resultados obtenidos de esta simulación se validan mediante comparación con los obtenidos en el modelo matemático y son los utilizados para la evaluación y el análisis de resultados, ya que se trata de un modelo más completo y con menor número de hipótesis.

Cada uno de los diseños desarrollados incluye una tecnología de las seleccionadas y se evalúa en base a las siguientes características:

i. Potencia térmica (W): Cantidad de calor extraída del flujo de aire interno gracias a los nuevos componentes añadidos al sistema de refrigeración.

ii. Volumen (cm^3): Volumen ocupado en la sección delantera por los nuevos componentes del sistema de refrigeración.

iii. Masa (kg): Masa añadida a la sección delantera debido a los nuevos componentes del sistema de refrigeración.

iv. Coeficiente de rendimiento: Cociente entre la potencia térmica extraída del flujo de aire interno por los nuevos componentes añadidos al sistema de refrigeración y la potencia eléctrica suministrada a los mismos para operar.

v. Densidad de potencia térmica (W/cm^3): Relación entre la potencia térmica extraída del flujo de aire interno y el volumen ocupado por los componentes añadidos al sistema de refrigeración en la sección delantera.

vi. Fiabilidad del diseño: Cómo de realista es el comportamiento del modelo, es decir, cómo de similar sería el comportamiento real del nuevo sistema de refrigeración y los flujos de aire implicados a las predicciones, expectativas y suposiciones utilizadas para crear el diseño y a los resultados obtenidos en el programa de simulación.

vii. Viabilidad: Cómo de fácil es implementar el nuevo sistema de refrigeración al convertidor y cómo de bien se adapta a los requisitos expuestos en la Sección F.2.1.

viii. Robustez: Habilidad del nuevo sistema de refrigeración para operar de forma continua sin que se produzcan fallos en ninguno de los componentes añadidos ni en el resto del convertidor. La resistencia a vibraciones y colisiones con objetos externos también se incluyen.

ix. Coste: Cómo de caro, en término económicos, sería implementar el nuevo sistema de refrigeración.

x. Mantenimiento: Con qué frecuencia deben revisarse los componentes añadidos al sistema de refrigeración. Dificultad en el proceso de revisión y la accesibilidad de los mismos en comparación al actual.

Las características *i*-*v* son cuantitativas y se miden en unidades indicadas, salvo el coeficiente de rendimiento que es adimensional. El resto, *v*-*x*, son cualitativas y se evalúan como *muy bien*, *bien*, *neutro*, *mal* y *muy mal*, de acuerdo a los criterios establecidos.

Para facilitar la comparación de resultados y prestaciones de los diferentes diseños, se aplica el método de media ponderada. Para ello se puntúan, en cada uno de los diseños, las características explicadas anteriormente del uno al cinco, siendo uno la peor valoración y el cinco la mejor en cada caso, según los criterios establecidos en las Tablas F.1 y F.2. Posteriormente, se calcula la media ponderada para cada diseño con los coeficientes de ponderación mostrados en la Figura F.3.

De cara a poder comparar los resultados del proyecto con otros proyectos del mismo área, se calcula la resistencia térmica de cada uno de los diseños.

Table F.1: Criterio para la evaluación de media ponderada. Características cuantitativas.

Puntuación	Potencia térmica (W)	Masa (kg)	Volumen (cm^3)	Rendimiento	Densidad de potencia (W/cm^3)
1	< 100	> 2.2	> 1500	< 60	< 0.4
2	[100, 160]	[1.65, 2.2]	[1000, 1500]	[60, 120]	[0.4, 0.8]
3	[160, 220]	[1.1, 1.65]	[500, 1000]	[120, 180]	[0.8, 1.2]
4	[220, 300]	[0.55, 1.1]	(0, 500]	[180, 240]	[1.2, 1.6]
5	> 300	< 0.55	0	> 240	> 1.6

Table F.2: Criterio para la evaluación de media ponderada. Características cualitativas.

Puntuación	Categoría
1	*Muy mal*
2	*Mal*
3	*Neutro*
4	*Bien*
5	*Muy bien*

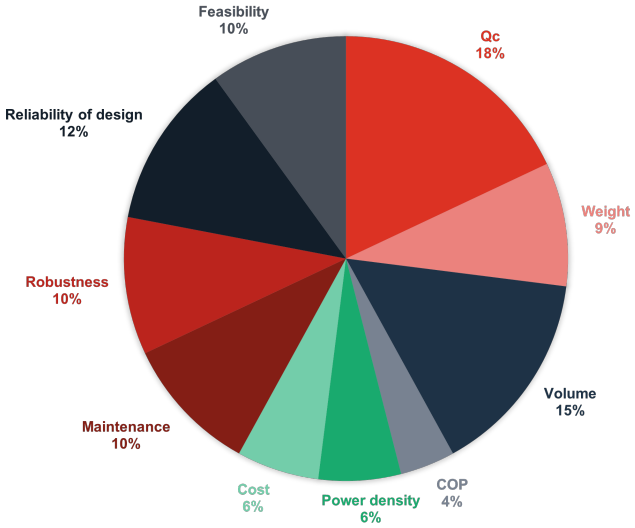

Figure F.3: Distribución de los coeficientes de peso para la evaluación de media ponderada (*Qc* es la potencia térmica, *Weight* la masa, *Volume* el volumen, *COP* el coeficiente de rendmiento, *Power density* la densidad de potencia, *Cost* el coste, *Maintenance* el mantenimiento, *Robustness* la robustez, *Reliability of Design* la fiabilidad del diseño y *Feasibility* la viabilidad).

F.4 Implementación de las Tecnologías de Refrigeración en el MITRAC/TC1500^{TM}

En total se desarrollan siete diseños diferentes, dos de ellos utilizan únicamente convección forzada de aire como tecnología de refrigeración, otros dos tubos de calor, otro una placa fría y, finalmente, los dos últimos células de Peltier.

Los valores de potencia térmica que figuran en esta sección son los obtenidos en la simulación basada en dinámica de fluidos computacional cuando la temperatura del flujo de aire interno es de 70ºC y la del aire externo 60ºC.

F.4.1 Diseño A. Modificación del Intercambiador de Calor de la Cubierta Delantera

Este diseño consiste en modificar la disposición física y la estructura mecánica del intercambiador de calor de la cubierta delantera para aumentar la superficie de contacto entre las corrientes de aire caliente y frío y mejorar la transferencia de calor entre ambos medios. La disposición propuesta se muestra en la Figura F.4, y consiste en alternar los tubos a través de los que circula el aire interno, de forma que estén en contacto con aire frío a través de la mayor parte de sus paredes. Además, se mantiene una primera capa de aire frío justo tras la entrada del aire exterior a través del filtro, manteniendo los canales aleteados del diseño original, para evitar una gran caída de presión en el flujo de aire exterior. Si la caída de presión en el flujo de aire exterior es demasiado grande, la velocidad del aire en el disipador de calor principal sería menor y, por tanto, se reduciría su capacidad de refrigeración.

La Tabla F.3 muestra los resultados obtenidos y la evaluación de características para este diseño.

Table F.3: Evaluación del Diseño A.

Potencia Térmica (Q)	**Masa**	**Volumen**	**Rend.**	**Densidad Potencia**
237 W	2.4 kg	1 559 cm^3	*Pasivo*	0.15 W/cm^3

Fiabilidad de Diseño	**Viabilidad**	**Robustez**	**Coste**	**Mantenimiento**
Muy bien	*Neutro*	*Muy bien*	*Mal*	*Muy bien*

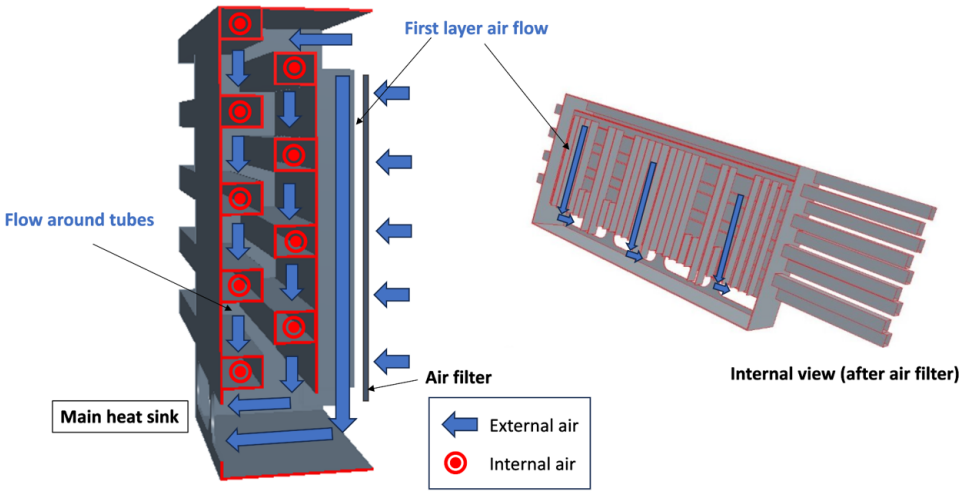

Figure F.4: Diseño A. Modificación del intercambiador de calor de la cubierta delantera.

F.4.2 Diseño B. Intercambiador de Calor en el Hueco Inferior

El hueco inferior situado entre el disipador de calor principal y la placa base del convertidor se utiliza como intercambiador de calor en esta opción, forzando a parte del aire interno a fluir a través de este nuevo canal. Tanto la superficie superior como la inferior del canal están en contacto con aire externo (frío). La Figura F.5 muestra un esquema del diseño propuesto.

Esta opción se divide en dos posibles diseños:

- Uno en el que no se considera ningún ventilador adicional, es decir, en el compartimento cero solo está el ventilador ya existente. Se supone que, o bien la caída de presión entre los compartimentos seis y cero es suficiente para mover el aire de forma natural, o bien que el ventilador actual puede reubicarse de forma que aspire ambos flujos de aire: El de la cubierta delantera y el del hueco inferior.

- Otra en la que se considera un ventilador adicional, es decir, se modifica el compartimento cero para alojar dos ventiladores. El ventilador añadido obliga a que el aire fluya a través del canal inferior. Esto aumenta el caudal másico en comparación con el diseño anterior.

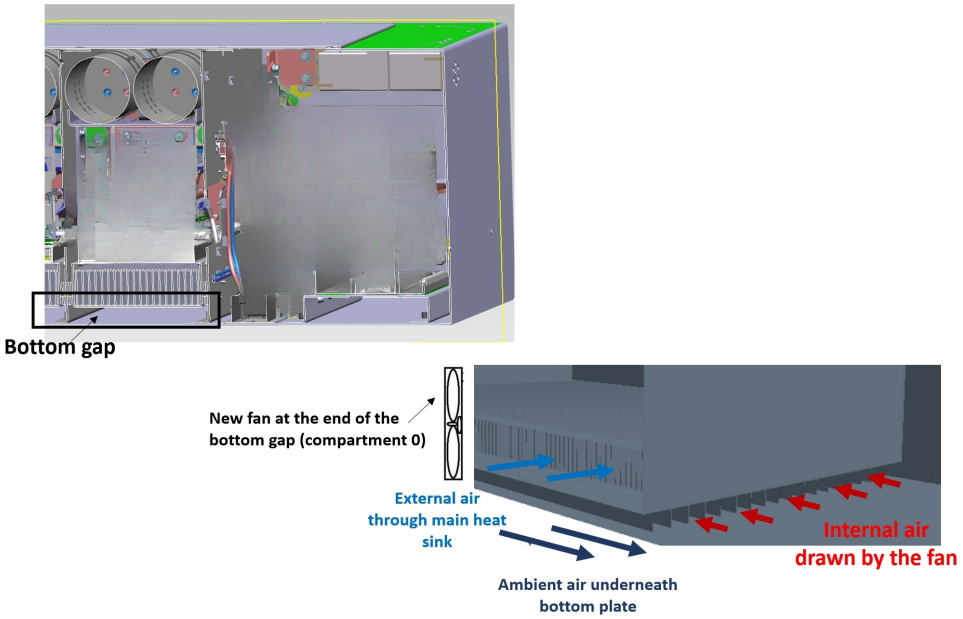

Figure F.5: Diseño B. Intercambiador de calor en el hueco inferior.

La Tabla F.4 muestra los resultados obtenidos y la evaluación de características para este diseño.

Table F.4: Evaluación del Diseño B.

	Potencia Térmica (Q)	**Masa**	**Volumen**	**Rend.**	**Densidad Potencia**
Sin ventilador extra	79 W	1.9 kg	0 cm^3	*Pasivo*	-
Ventilador extra	136 W	2.1 kg	160 cm^3	90.93	0.85 W/cm^3

	Fiabilidad de Diseño	**Viabilidad**	**Robustez**	**Coste**	**Mantenimiento**
Sin ventilador extra	*Muy mal*	*Muy bien*	*Muy bien*	*Muy bien*	*Muy bien*
Ventilador extra	*Muy bien*	*Muy bien*	*Neutro*	*Bien*	*Neutro*

F.4.3 Diseño C. Tubos de Calor Acoplados a la Placa Lateral

El Diseño C consiste en utilizar tubos de calor para transferir calor del aire interior del compartimento seis, donde la temperatura del aire interior es máxima, a la placa lateral que es paralela a la pared del convertidor (ver Figura F.6).

La disipación de calor de la placa al entorno no puede realizarse por convección natural, ya que esta es perpendicular a la velocidad del tren, lo

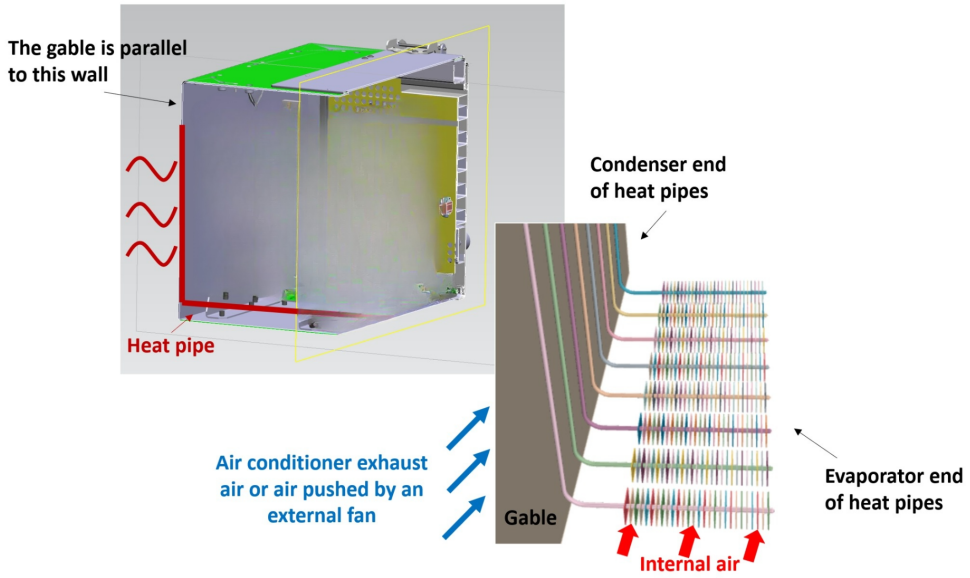

Figure F.6: Diseño C. Tubos de calor acoplados a la placa lateral.

que significa que, en el mejor de los casos, si está orientada hacia la parte delantera del tren, el flujo de aire exterior incide perpendicularmente sobre la placa y, en el peor, cuando está orientada hacia la parte trasera del tren, el flujo incidente es muy pequeño porque está protegido del aire incidente por la propia caja del convertidor.

Por lo tanto, en este diseño se consideran dos opciones diferentes para disipar el calor de la placa lateral. Puede hacerse redirigiendo el aire de escape procedente del sistema de aire acondicionado de los coches de pasajeros, o mediante un ventilador adicional colocado fuera de la caja del convertidor. En ambos casos, se utiliza la convección forzada con el flujo de aire paralelo a la placa.

La Tabla F.5 muestra los resultados obtenidos y la evaluación de características para este diseño. En la simulación se ha utilizado un ventilador exterior para disipar el calor de la placa lateral.

F.4.4 Diseño D. Tubos de Calor en el Hueco Inferior

En este diseño, el canal vacío situado debajo del disipador de calor principal de las IGBTs se utiliza para enfriar los tubos de calor. Los tubos de calor están situados como se muestra en la Figura F.7, con los extremos del evaporador

Table F.5: Evaluación del Diseño C.

Potencia Térmica (Q)	**Masa**	**Volumen**	**Rend.**	**Densidad Potencia**
158 W	0.7 kg	112 cm^3	*Passive*	1.41 W/cm^3

Fiabilidad de Diseño	**Viabilidad**	**Robustnez**	**Coste**	**Mantenimiento**
Mal	*Muy mal*	*Mal*	*Muy mal*	*Bien*

hacia la entrada del flujo de aire interno en el compartimento seis, para reducir la temperatura del aire interno antes de entrar en el intercambiador de calor en la cubierta delantera, y el lado del condensador en el hueco inferior. Para enfriar los extremos del condensador, se utiliza aire externo (frío), por lo que el hueco inferior debe sellarse para evitar que se mezclen los flujos de aire interno y externo.

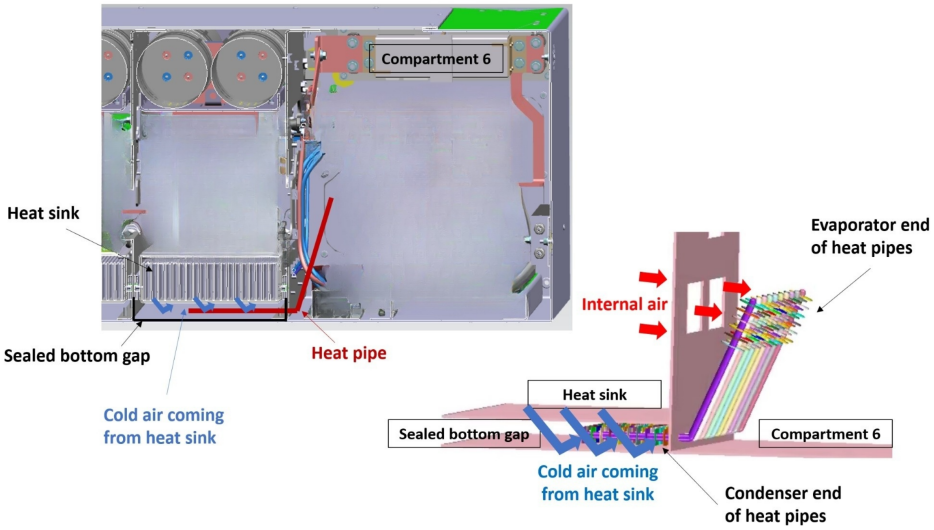

Figure F.7: Diseño D. Tubos de calor en el hueco inferior.

Hay dos opciones para introducir aire frío en el hueco inferior, o bien se hacen aperturas en la placa inferior y se deja entrar y salir el aire ambiente que fluye por debajo de la placa, o bien se extrae una parte del aire que fluye por el disipador de calor a través de unos orificios situados al principio del disipador. En este documento, es esta última opción la que se utiliza y, por tanto, la que se muestra en la Figura F.7. La razón es que el aire que fluye a través del disipador de calor ya está filtrado y reduce la probabilidad de deterioro de los tubos de calor debido a impurezas o colisiones.

La Tabla F.6 muestra los resultados obtenidos y la evaluación de características para este diseño.

Table F.6: Evaluación del Diseño D.

Potencia Térmica (Q)	**Masa**	**Volumen**	**Rend.**	**Densidad Potencia**
165 W	0.8 kg	120 cm^3	*Pasivo*	1.38 W/cm^3

Fiabilidad del Diseño	**Viabilidad**	**Robustez**	**Coste**	**Mantenimiento**
Muy bien	*Neutro*	*Muy bien*	*Neutro*	*Muy bien*

F.4.5 Diseño E. Placa fría en el compartimento cero

Se trata de una aplicación de refrigeración líquida. Una mezcla de agua y glicol circula por un circuito cerrado de tuberías desde una placa fría en el compartimento cero, donde se absorbe el calor del aire interior y aumenta la temperatura del agua, hasta el hueco inferior, donde se utiliza una corriente de aire frío para disipar el calor y reducir de nuevo la temperatura del agua. A continuación, el agua se bombea de nuevo a la placa fría para iniciar un nuevo ciclo. En la Figura F.8 se muestra un esquema de este diseño.

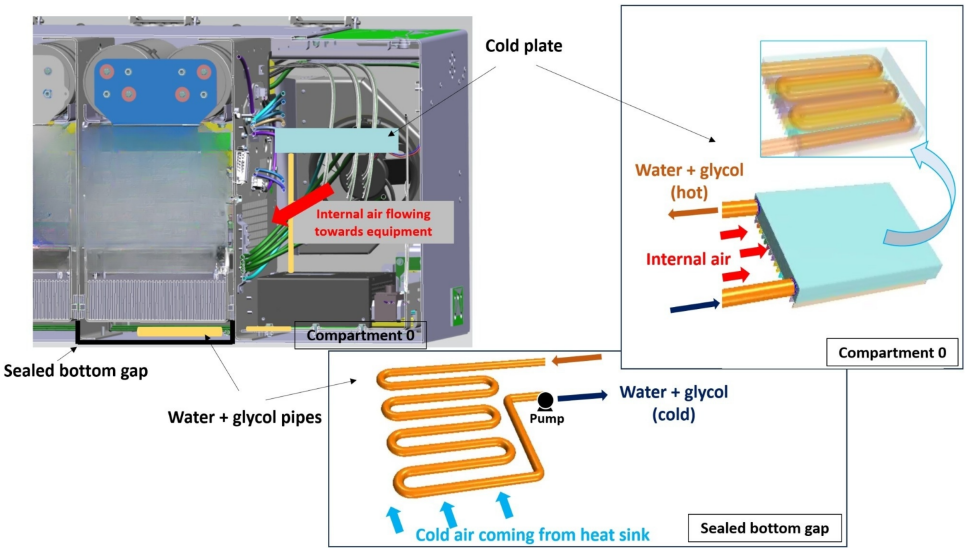

Figure F.8: Diseño E. Placa fría en el compartimento cero.

En el compartimento cero, el ventilador interno empuja el aire hacia la placa fría, que tiene aletas para mejorar la absorción del calor. Por lo tanto,

el aire interno que sale del compartimento cero tiene una temperatura más baja en comparación con el diseño original y, como consecuencia, tiene una mayor capacidad para absorber calor cuando fluye alrededor de los distintos elementos.

Por otro lado, de forma análoga al Diseño D, en el hueco inferior el flujo de aire que enfría la mezcla de agua en las tuberías puede proceder del exterior, entrando por la placa base, o del disipador de calor, entrando por la parte superior del hueco inferior como una pequeña desviación del flujo de aire que enfría las IGBTs. En este caso, al igual que en el Diseño D, se utiliza esta última opción.

Tuberías adiabáticas conectan la placa fría del compartimento cero y el bucle de refrigeración del hueco inferior. El circuito de tuberías debe incluir, además de la bomba, un pequeño depósito de agua y sensores y válvulas que garanticen el correcto funcionamiento del sistema. Todos estos componentes pueden situarse en el interior de la sección delantera o trasladarse a la sección central para facilitar el acceso en caso necesario. Además, el hueco inferior debe sellarse para que no se mezclen los flujos de aire interior y exterior.

La Tabla F.7 muestra los resultados obtenidos y la evaluación de características para este diseño.

Table F.7: Evaluation of Design E.

Potencia Térmica (Q)	**Masa**	**Volumen**	**Rend.**	**Densidad Potencia**
216 W	0.25 kg	835 cm^3	237.8	0.14 W/cm^3

Fiabilidad de Diseño	**Viabilidad**	**Robustez**	**Coste**	**Mantenimiento**
Muy bien	*Mal*	*Muy mal*	*Muy mal*	*Mal*

F.4.6 Diseño F. Células de Peltier en el Compartimento Cero Acopladas a la Placa Lateral

Las células de Peltier pueden utilizarse como elementos de refrigeración, ya que mantienen una temperatura constante en uno de los lados, actuando como una bomba de calor y transfiriendo calor al otro lado.

La idea es colocar células de Peltier a lo largo de una pared o superficie vacía en la sección delantera, de modo que la temperatura de la pared se mantenga a una temperatura constante independientemente de la temperatura ambiente, y el aire interior se enfríe al entrar en contacto con ella. Este diseño propone acoplar células Peltier a la pared lateral del compartimento cero, y

añadir aletas en la zona central de dicha pared. La elección se debe a que el flujo volumétrico de aire es máximo en esta región gracias al ventilador interno. La Figura F.9 muestra este diseño.

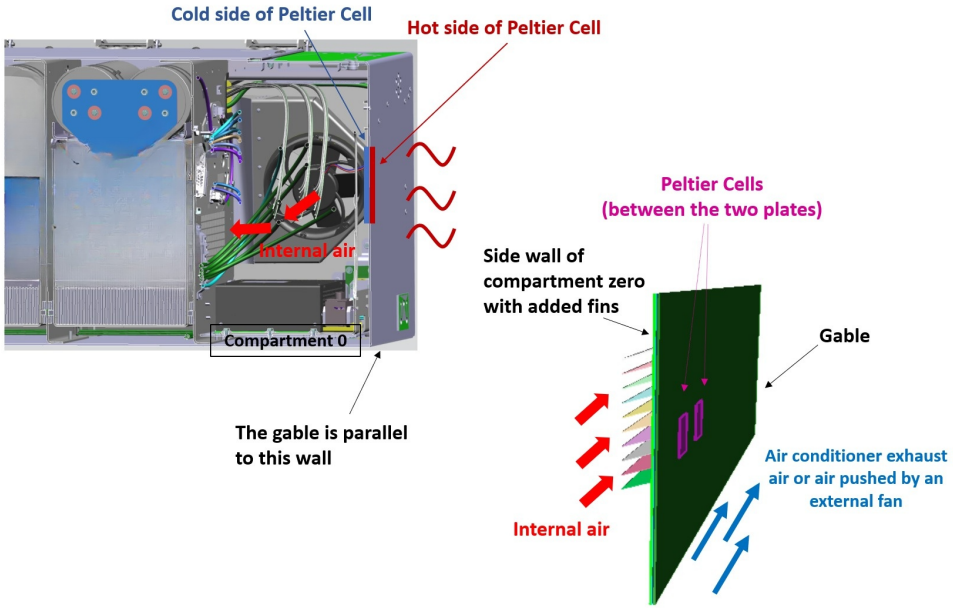

Figure F.9: Diseño F. Células de Peltier en el compartimento cero acopladas a la placa lateral.

En este caso, la placa lateral se utiliza como disipador de calor. La configuración es exactamente la misma que la explicada en Diseño C. Sin embargo, como la superficie de las células de Peltier es muy pequeña, es necesario disponer de una fina capa de material de disipación térmica o interfaz térmica en el acoplamiento, tanto entre éste y la placa lateral como entre éste y la pared del compartimento cero. Esta capa tiene una conductividad térmica muy alta, lo que garantiza una distribución uniforme de temperatura a lo largo de toda la superficie.

La Tabla F.8 muestra los resultados obtenidos y la evaluación de características para este diseño.

F.4.7 Diseño G. Células de Peltier en el Intercambiador de Calor

Este diseño pretende mejorar la capacidad de transferencia de calor en el intercambiador de la cubierta delantera aumentando la diferencia de

Table F.8: Evaluación del Diseño F.

Potencia Térmica (Q)	**Masa**	**Volumen**	**Rend.**	**Densidad Potencia**
336 W	2.1 kg	1 390 cm^3	2.55	0.24 W/cm^3

Fiabilidad de Diseño	**Viabilidad**	**Robustez**	**Coste**	**Mantenimiento**
Bien	*Muy mal*	*Mal*	*Muy mal*	*Bien*

temperatura entre los medios frío y caliente. Para ello, se añaden células de Peltier entre ambos medios.

De forma similar al Diseño F, las células se acoplan a través de materiales de interfaz térmica a las placas de aluminio donde se produce el intercambio de calor. El lado frío de la célula de Peltier se mantiene a temperatura constante y se utiliza para reducir la temperatura del aire interior. El calor del lado caliente de las células se disipa utilizando el flujo de aire exterior que entra a través del filtro de la cubierta delantera, tal como se muestra en la Figura F.10.

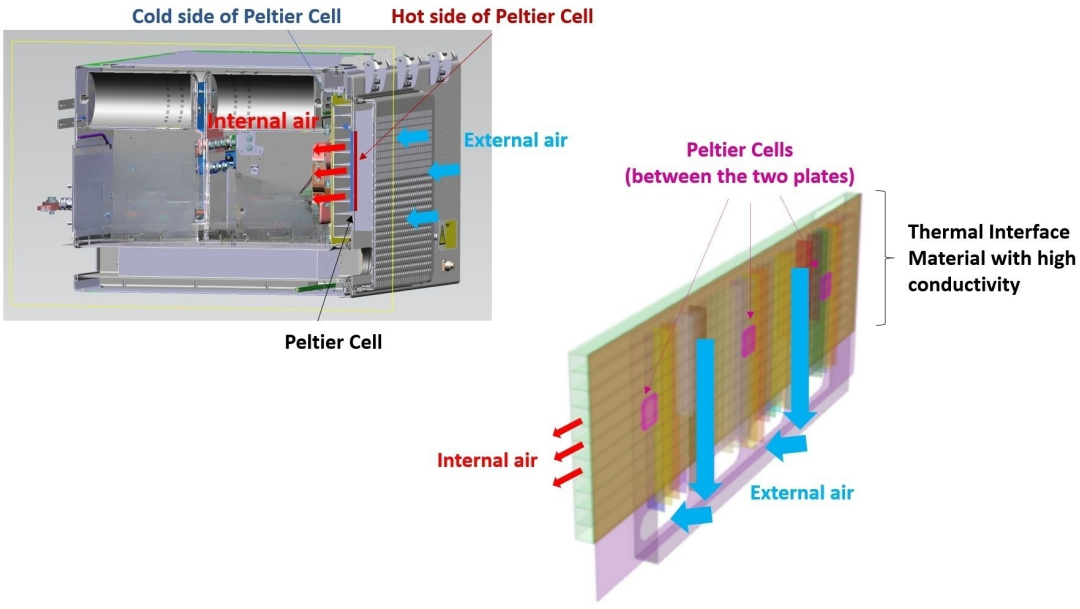

Figure F.10: Diseño G. Células de Peltier en el intercambiador de calor.

La Tabla F.9 muestra los resultados obtenidos y la evaluación de características para este diseño.

Table F.9: Evaluación del Diseño G.

Potencia Térmica (Q)	**Masa**	**Volumen**	**Rend.**	**Densidad Potencia**
445 W	2.35 kg	1 476 cm^3	2.28	0.3 W/cm^3

Fiabilidad de Diseño	**Viabilidad**	**Robustez**	**Coste**	**Mantenimiento**
Bien	*Bien*	*Muy bien*	*Mal*	*Muy bien*

F.5 Análisis de Resultados

Si se aplica el método de media ponderada explicado en la Sección F.3, los diseños se pueden clasificar de mejor a peor, en base a su puntuación global, según el orden mostrado en la Tabla F.10. Además, el gráfico de la Figura F.11 muestra una visión global de las diferentes características en los diseños.

Table F.10: Clasificación de los diseños basada en el cálculo de la media ponderada.

Diseño	**Descripción**	**Puntuación**
D	Tubos de calor en el hueco inferior	4.02
G	Células de Peltier en el intercambiador de calor	3.54
B.1	Intercambiador de calor en el hueco inferior sin ventilador extra	3.53
B.2	Intercambiador de calor en el hueco inferior con ventilador extra	3.34
A	Modificación del intercambiador de calor de la cubierta delantera	3.24
E	Placa fría en el compartimento cero	2.94
C	Tubos de calor acoplados a la placa lateral	2.76
F	Células de Peltier en el compartimento cero acopladas a la placa lateral	2.60

Mientras que la potencia térmica es el objetivo principal, la zona derecha de la gráfica representa los denominados costes no monetarios (volumen, masa, coeficiente de rendimiento y densidad de potencia térmica), ya que se mejora la refrigeración a expensas de empeorar una o varias de estas características, y el coste los costes monetarios. Por otro lado, la esquina inferior izquierda (mantenimiento y robustez) representa la calidad de servicio prestada a los clientes, es decir, cómo de bien opera el sistema, y la esquina superior izquierda evalúa el diseño conceptual en sí mismo.

Se puede observar que tanto los dos diseños mejor valorados como los dos peores incluyen las mismas tecnologías: tubos de calor y células de Peltier. Las gráficas de la Figura F.12 muestran una comparativa de los dos mejores diseños y los dos peores, respectivamente. En ambas gráficas las principales diferencias entre curvas se encuentran en la zona derecha, esto se debe a que estas propiedades depende de la tecnología utilizada y no de cómo son implementadas en el convertidor. Pese a que, a priori, ambas

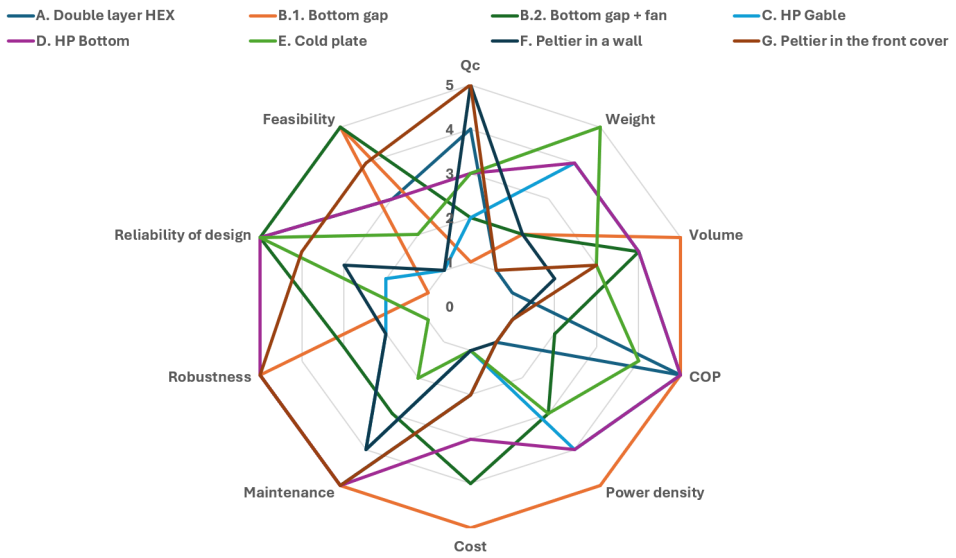

Figure F.11: Evaluación de cada característica para todos los diseños propuestos.

tecnologías son pequeñas y compactas, las células de Peltier necesitan grandes superficies de interfaz térmica para su implementación en el convertidor, lo que aumenta el volumen y la masa del diseño. Además, los tubos de calor son pasivos, mientras que las células de Peltier requieren de potencia eléctrica para funcionar.

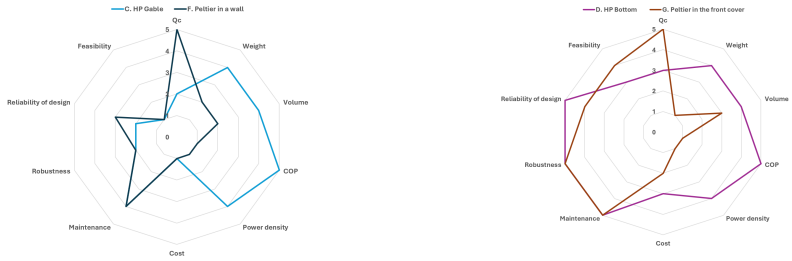

(a) Peor clasificados (F y C). (b) Mejor clasificados (D y G).

Figure F.12: Evaluación de características de los diseños peor y mejor clasificados.

La Figura F.13 compara los mismos cuatro diseños pero emparejándolos por tecnologías. En este caso se aprecia el efecto contrario, es decir, las diferencias aparecen en la zona izquierda de la gráfica, debido a las diferencias en la implementación de las tecnologías en el convertidor y de los espacios

utilizados como disipadores de calor. Este fenómeno explica la diferencia de resultados entre los dos diseños de la misma tecnología, ya que el uso de la placa lateral como disipador de calor presenta resultados malos en lo que respecta a calidad de servicio y desarrollo del diseño conceptual.

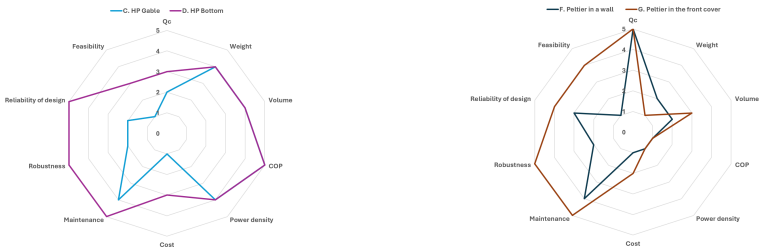

(a) Tubos de calor (C y D). (b) Células Peltier (F y G).

Figure F.13: Evaluación de características de los diseños con las mismas tecnologías (tubos de calor y células de Peltier).

Por su parte, la Figura F.14 muestra cómo la curva correspondiente a la placa fría está desplazada hacia la esquina superior derecha, demostrando bajos costes no monetarios, pero operación compleja. En cuanto a las soluciones del intercambiador de calor en el hueco inferior, se observa que las curvas son más extensas y que la que incluye un ventilador adicional está más centrada y presenta un mayor equilibrio entre las distintas características. Por este motivo, la opción con un ventilador adicional es más recomendable pese a tener una puntuación global menor.

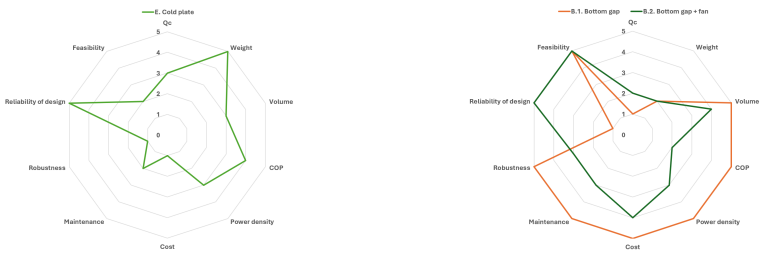

(a) Placa fría (E). (b) Hueco inferior (B.1 y B.2).

Figure F.14: Evaluación de características de los Diseños E y B.

Finalmente, la Figura F.15 compara el Diseño A (modificación del intercambiador de calor de la cubierta delantera) con el Diseño B, también basado en convección forzada de aire, y con el Diseño G, que también implica una modificación en la cubierta delantera. En la primera comparación se

observa que la curva correspondiente al Diseño A tiene una forma estrellada, lo que demuestra que los buenos resultados que se obtienen en algunas de las características se oponen a malos resultados en otros casos. Esto, junto con una menor puntuación global, muestra que el Diseño B es mejor si se opta por un diseño que implique únicamente convección forzada de aire. En lo que respecta a modificar la cubierta delantera, se puede ver que las dos curvas son muy parecidas, pero la curva del Diseño A queda eclipsada por la del Diseño G, ya que éste último presenta mejores resultados en términos de volumen, una característica crítica en la cubierta delantera.

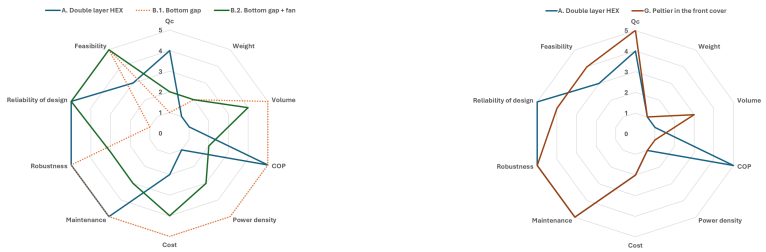

(a) Convección forzada (A y B). (b) Cubierta delantera (A y G).

Figure F.15: Evaluación de características de los diseños A, B y G.

F.6 Conclusiones y Trabajo Futuro

El análisis concluye que el uso de placas frías no es óptimo para el convertidor específico analizado, aunque podrían ser adecuadas para convertidores con restricciones de peso más estricas en otras industrias. Tampoco se considera adecuado modificar la disposición del intercambiador de calor de la cubierta delantera debido a sus desventajas críticas. En su lugar, se recomienda utilizar el hueco inferior con convección forzada y un ventilador adicional para una solución básica y con resultados modestos, mientras que se consideran opciones más sofisticadas como tubos de calor o células de Peltier para inversiones en tecnología innovadora.

La elección entre estas últimas depende de las prioridades del proyecto y del enfoque de mercado que se quiera dar. Los tubos de calor ofrecen un funcionamiento pasivo continuo, adecuado para uso general, mientras que las células de Peltier requieren controladores y son más caras, adecuadas para convertidores específicos de clima cálido. Además, es importante notar que la tecnología en sí no garantiza una solución eficiente, sino que hay que tener en cuenta toda el sistema de implementación en su conjunto. Por último,

pese a que la puntuación global que se obtiene al aplicar el método de media ponderada es un criterio útil, este no debe ser el único criterio a tener en cuenta, ya que en ocasiones prima el balance o equilibrio entre los resultados de las distintas características.

En lo que respecta a líneas futuras se plantean tres posibles direcciones de investigación. Por un lado se puede seleccionar y desarrollar uno de los diseños presentados hasta obtener un diseño optimizado y completamente desarrollado que aplique a un convertidor específico. Por el contrario, otra opción es ampliar el rango de aplicación del proyecto a otras industrias para analizar como afectas los diferentes factores en distintas industrias con diferentes condiciones de controno y, finalmente, se puede divergir la línea de investigación, tratando de eliminar el calor directamente de los componentes en lugar de utilizar el aire interno como medio intermedio entre los componentes y el exterior.